

Contribution no. 273

**NORSAR**

ROYAL NORWEGIAN COUNCIL FOR SCIENTIFIC AND INDUSTRIAL RESEARCH

Technical Report No. 2/80

**SEISMIC METHODS IN METAMORPHIC ROCK  
FINAL REPORT**

Håvar Gjøystdal  
NTNF/NORSAR, Kjeller, Norway

November 1979



0006

SEISMIC METHODS IN METAMORPHIC ROCK

FINAL REPORT

by

H. Gjøystdal

November 1979

NORSAR Contribution No .273.  
.....



## ACKNOWLEDGEMENTS

The work described in this report has mainly been sponsored by NTNF under the project 'Seismikk i metamorft bergartsmiljø', and by A/S Sulitjelma Gruber under the project 'Malmprospektering med seismikk' which has also been supported by NTNF.

NORSAR wants to thank all sponsors, also including Orkla Industrier A/S who freely carried out a considerable work during the field experiments.

Especially, we benefited directly from the close cooperation with A. Dahle, Geoteam, G. Grammeltvedt, Orkla Industrier, and T. Søyland-Hansen, Sulitjelma Gruber, and we hereby express our thanks for many valuable discussions.

TABLE OF CONTENTS

	<u>Page</u>
1. INTRODUCTION	1
1.1 Background	1
1.2 Financial Summary	3
2. SCRUTINY OF BACKGROUND MATERIAL	4
2.1 Inquiries to national geological surveys, etc.	4
2.2 Scrutiny of data collected in Sulitjelma/Løkken (Orkla) 1971-77	5
3. ESTIMATION OF EXPECTED SIGNAL-TO-NOISE RATIO OF REFLECTED PULSES FROM A GIVEN ORE BODY	9
3.1 General	9
3.2 Simple signal/noise model	9
3.3 Noise estimation	10
3.4 Signal estimation	11
3.5 An attempt to estimate reflected signal amplitude in the Løkken area	13
3.6 The 1978 Løkken experiment. Estimation of expected SNR	23
4. THE EFFECT OF SHOT DEPTH ON SOURCE GENERATED NOISE - THE HADELAND 78 EXPERIMENT	33
4.1 The Hadeland 78 experiment	33
4.2 The 'water pulse' effect	34
5. SIGNAL/NOISE CHARACTERISTICS AND CORRESPONDING CRITERIA FOR OPTIMUM DESIGN OF SHOT/RECEIVER GEOMETRY	37
5.1 Source generated noise - Løkken 78	37
5.2 Analysis of 'static corrections'	62
5.3 Simulation of reflectors to obtain criteria for design of shot/receiver lay-out	66
6. SUMMARY - CONCLUSION	84
6.1 Background	84
6.2 Pre-project	84
6.3 Scrutiny of earlier work	84
6.4 Theoretical estimates of the expected strength of pulses	85

TABLE OF CONTENTS (cont.)

	<u>Page</u>
6.5 The effect of shot depth on source generated noise	85
6.6 Source generated noise	86
6.7 Criteria for optimum design of shot/receiver lay-out	86
7. DISCUSSION - RECOMMENDATIONS FOR FUTURE RESEARCH	88
7.1 Status of the project - August 1979	88
7.2 Re-profiling of the known Løkken ore body	88
7.3 Recommendations for further developments	89
REFERENCES	95



## 1. INTRODUCTION

### 1.1 Background

As far back as in 1971 A/S Sulitjelma Gruber made their first attempts to apply the reflection seismic method for ore prospecting purposes. Experiments were continued throughout the next two years, however, the results from these early investigations (see Geoteam 1972, 1974) were not too promising. The data were considerably dominated by noise, and no reliable interpretation of the seismic sections was possible. At this stage it was concluded that the recording equipment was not up to the proper standard (too low sampling frequency, etc.) and that more efforts should be made in determining favorable values of field parameters, such as geophone coupling, charge type and size, shot/receiver configuration, etc.

In 1976, A/S Sulitjelma Gruber, in cooperation with Orkla Industrier A/S, established a research project, 'Seismic Ore Prospecting'. The project which was financially supported by NTNF, had the following aims:

- Test seismic instrumentation and make it suitable for ore prospecting in crystalline rocks
- Develop methods for data acquisition and the following data processing
- Apply the methods on data collected in Sulitjelma and Løkken (Orkla) in an attempt to detect known and unknown ore bodies by seismic means.

During summer and fall 1976, the seismic experiments continued in Sulitjelma and Løkken with a new instrumentation (Digital Recorder DHR-1632, 24 channels, up to 4000 Hz sampling frequency). In particular, an interesting profile was shot in an area with a known ore body in Løkken, having a reflection depth of about 750 meters (see Geoteam 1976). The seismic sections from this survey showed relatively prominent events at slightly shallower depth than should be expected from earlier knowledge of the area. The results were characterized as successful and very promising as to the future progress of the project.



In 1977 more systematic attempts were made at establishing proper field parameters, together with fundamental characteristics of the seismic wave pulses and their propagation in metamorphic rocks. A series of experiments were performed in the Løkken mine tunnels, where a sequence of charges was fired (down to depths of 930 meters), and the signals were recorded at the surface. Parameters such as charge type and size, geophone coupling, instrument gain setting, and source depth were systematically varied, and frequency spectra of the various seismic pulses were analyzed (Geoteam, 1978).

In 1978, NORSAR was engaged in this work through a separate NTNF-funded project 'Seismic Methods in Metamorphic Rocks'. This project - in the following referred to as 'the NORSAR project' - had been established in order to support the original Sulitjelma project on selected problems related to:

- signal-to-noise improvement
- seismic wave attenuation in metamorphic rocks
- signal and noise coherency
- attenuation of source-generated noise by use of shot and receiver arrays
- design of proper field and processing techniques.

This report is intended to give a description of the NORSAR project. It contains relevant information on data collected, data analysis, methods, and results obtained since the project was initiated in June 1978. However, some of the studies undertaken have been partly based on data collected prior to the NORSAR engagement. For example, the Løkken 1977 experiment referred to above has played an important role in parts of our study as to the estimation of rock attenuation parameters. Experiments and surveys not directly connected to the NORSAR project have not been included. Consequently, the report should not be considered as a documentation of the total seismic ore prospecting project. Very little documentation exists here, apart from various reports worked out by A/S Geoteam who has been the main consultant in data acquisition and routine processing. Brief summaries of the seismic prospecting activity have been given by Grammeltvedt (1978), and Søyland Hansen (1978).

The 'NORSAR project' did not receive any NTNF funds for 1979. However, the steering committee of the Sulitjelma/NTNF project decided to engage NORSAR as a consultant in order to let NORSAR carry out parts of their

planned research for 1979. Since this work was a direct continuation of the research activity initiated under the 'NORSAR project', we found it natural to include it in this report. Thus, the report covers the time period June 1978 - October 1979.

For readers not familiar with the standard seismic prospecting techniques, we refer to general textbooks, such as Parasnis (1972), Dobrin (1976), and Waters (1978).

### 1.2 Financial Summary

Table 1.1 gives a summary of the financial sources for the work covered in this report.

	1978 (Jun-Dec) 1000 kr	1979 (Jan-Sept) 1000 kr
NTNF	150	50*
NORSAR	0	20
Sulitjelma	0	70

\* Transferred from 1978.

Table 1.1  
Financial Sources.

## 2. SCRUTINY OF BACKGROUND MATERIAL

### 2.1 Inquiries to national geological surveys, etc.

In the initial planning stage of the NORSAR project aimed at detection of ore deposits in crystalline rocks, we attempted to check on on-going research efforts on this type of problems in order to assess the current state of the art in the field. We contacted colleagues in key national geological surveys or corresponding academic positions, and although most of the responses to our inquiries were negative, we got certain indications that there is an increasing interest in high resolution seismic reflection methods and their potential use in non-sedimentary rocks.

One of the main reasons for this is the last years' rapid development of digital high resolution recording equipment, operating with sampling frequencies of 4000 Hz and even higher. In addition, the continuous development of sophisticated data processing techniques, including wave equation migration, 2-D or 3-D seismic modeling, etc., enables seismic methods to be applied for more and more complex geological structures. In principle, such methods have been known for a long time, however, their ultimate need for extremely high speed computers has delayed their practical application until a few years ago. Unfortunately, we have to realize that some of the work done on seismic ore prospecting methods has been under the direction of private mining companies or prospecting companies which are rather restrictive as to the publishing of their developments. For example, in a reply to one of our inquiries (Prof. Toksöz, MIT, Cambridge, USA) it was reported that a subsidiary of Newmont Mining Corp., Arizona, has performed seismic reflection experiments in a mining area, but the final report on these investigations is classified and thus unavailable.

Nevertheless, the above communications with various colleagues, together with a scrutiny of different geophysical journals have given certain references to works that are in some way related to the problems that we are faced with. For general information, we list some of these references here: King and Falvey (1977), King (1979), Nojonen et al (1978), Nojonen et al (1979), Nunn and Boztas (1977), Ward et al (1978), and Ziolkowski and Lerwill (1979).

## 2.2 Scrutiny of data collected in Sulitjelma/Løkken (Orkla) 1971-77

On the basis of our scrutiny of the work done on the seismic ore prospecting project prior to the NORSTAR engagement (for references see Section 1), we decided to concentrate upon the seismic experiments that had been performed in Løkken in 1976 and 1977.

### Løkken-76 experiment

The Løkken-76 experiment was the first attempt to apply the reflection seismic method in an area with reasonably simple and well-known conditions: A well-mapped 'ruler-shaped' ore body extending to a depth of at least 1100 m. Furthermore, this investigation differs from the earlier ones in that it was undertaken exclusively in order to test a method rather than searching for unknown deposits. A seismic profile was located in such a way that the normal rays to the potential reflector (ore body) penetrated approximately 750 m into the earth. That is, in the plane of reflection, the reflector was expected to be found at a depth of 750 m (see Fig. 2.1). The experiment has been documented in a specific report (Geoteam, 1976), and we shall briefly list the main conclusions:

- Seismic velocity  $\sim$  5000-6000 m/s in the rock between surface and ore body
- The processed seismic section shows relatively distinct 'events' that have been interpreted as reflections from the ore body (see Fig. 2.2).
- The results were characterized as satisfactory and very promising for a future application of a seismic ore prospecting technique in the Løkken area.

We shall make further comments on this profiling experiment at a later stage (Section 5.1).

### Løkken-77 experiment

Initiated by the positive prospects of the Løkken-76 profile, a new experiment was designed in 1977, having the following aims:

- Determine the seismic P-wave velocity between different levels of the Løkken mine and the surface
- Determine the frequency content of a seismic signal recorded at the surface when firing charges at different levels in the Løkken mine. (Results should be given for different types and sizes of the charge.)

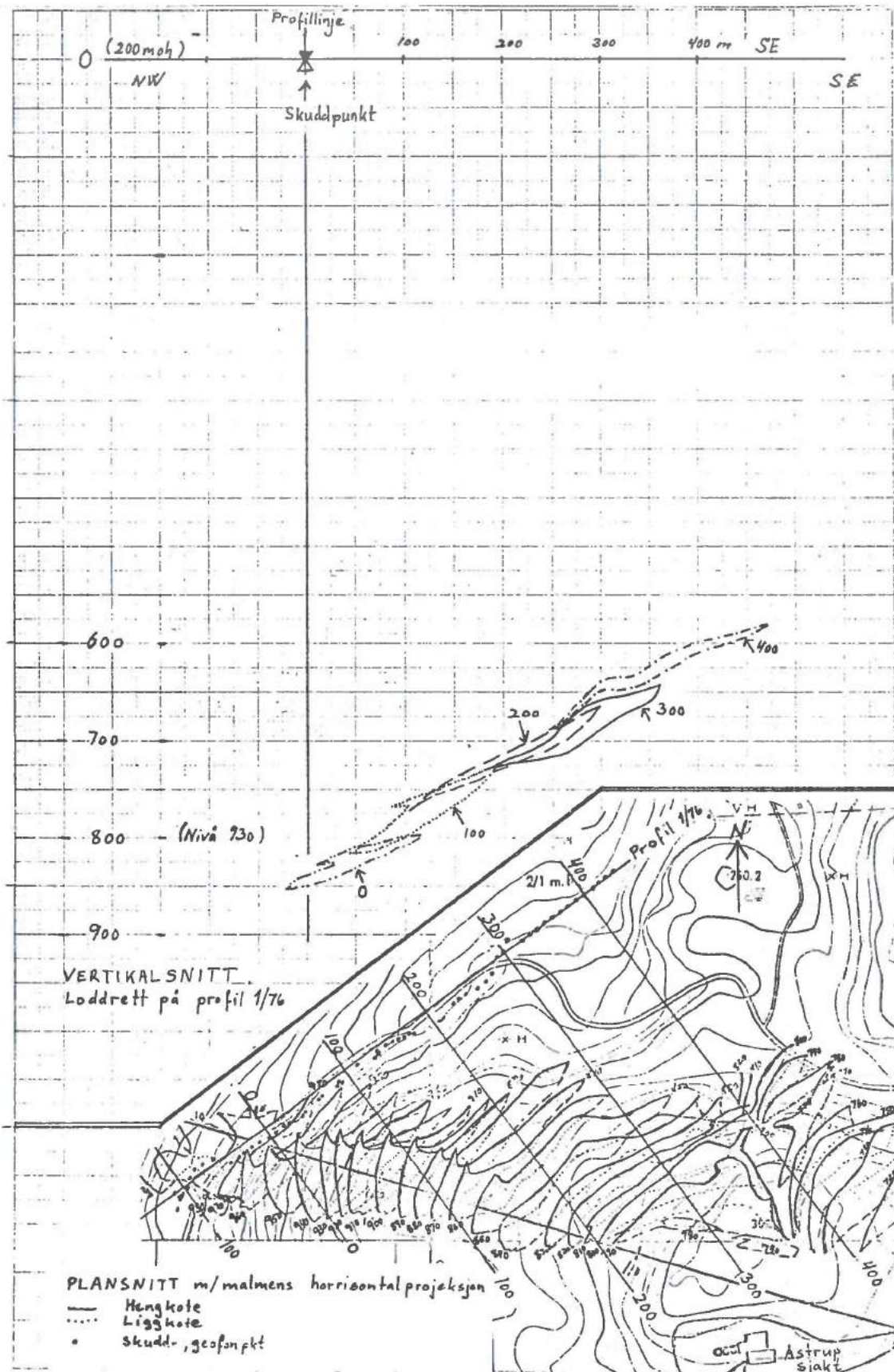


Fig. 2.1 Horizontal and vertical map of the 'Løkken ore body'. In the vertical cross-section, the profile runs perpendicular to the paper plane. (From Grammeltvedt, 1978.)

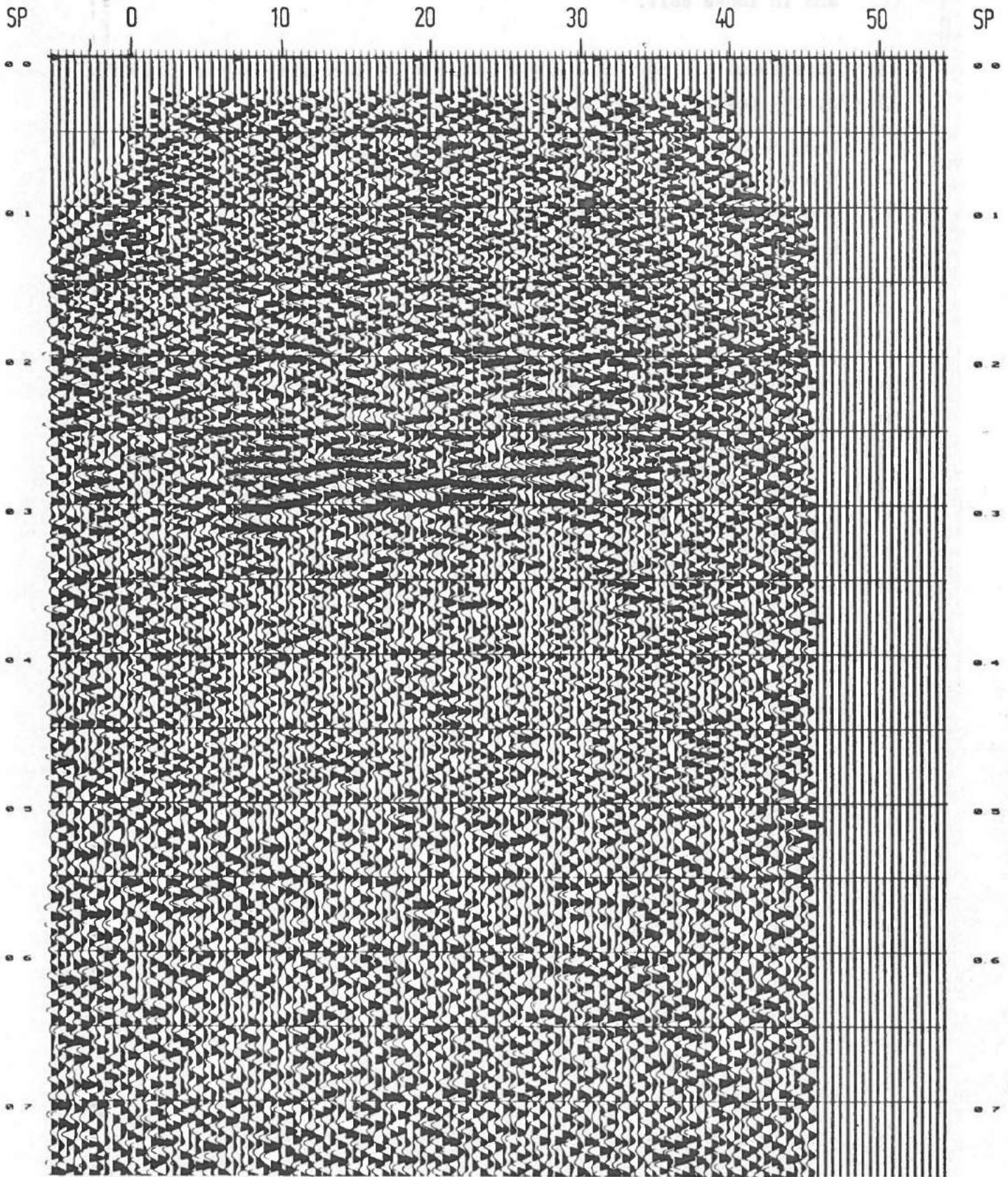


Fig. 2.2 Conventional stacked section (1200 % coverage) from the Løkken-76 profiling experiment. Note 'events' occurring between 250 and 300 ms. (From Geoteam, 1976.)

- Find an optimum way of mounting the geophones on solid rock and in loose soil.

This experiment has been described in a specific report (Geoteam, 1978), quoting the following main conclusions:

- P-velocities  $\sim 5900$  m/s, approximately constant down to at least 930 m depth
- Main frequency range 50-200 Hz, peak around 120-150 Hz
- Energy source 50-100 grams of C4 (military explosives)
- Geophone mounting, solid rock: on steel bolt
- Geophone mounting, loose soil: on small metal plate.

We have chosen to give this brief introduction to the activity in Løkken in 1976 and 1977, mainly because these experiments were - in our opinion - the first real attempts to systematically approach the problem of ore prospecting with the reflection seismic method. In consequence, the data collected during these two experiments can be regarded as the starting point of the NORSAR project, and will thus be frequently referred to in the following.

### 3. ESTIMATION OF EXPECTED SIGNAL-TO-NOISE RATIO OF REFLECTED PULSES FROM A GIVEN ORE BODY

#### 3.1 General

One of the major questions arising at the start of the NORSAR project was the following:

- On the bases of the relevant data at hand, what kind of reflectors can we actually expect to be able to detect?

In other words, what impedance contrasts would be expected to give detectable reflections at the surface, and at what depth?

In an attempt to give an answer to this question, we shall adopt a relatively simple model for signal and noise, characterized by a given number of parameters. The next steps will be to try to estimate as many as possible of these parameters on the basis of existing data, and, if necessary, design new experiments in order to solve the rest of the problem.

#### 3.2 Simple signal/noise model

The signal/noise model will be as follows:

The total wave-field recorded at time  $t$  at a distance  $x$  from the surface shot may be written as

$$u(x,t) = n_b(x,t) + n_i(x,t) + n_s(x,t) + p(x,t) \quad (3.1)$$

Here we have:

- $n_b$  = Background noise (cultural activity, wind, etc.) being always present, although at various levels (shot independent).
- $n_i$  = Electronic noise generated in the recording equipment (cables, amplifiers, etc.) (shot independent).
- $n_s$  = Shot-generated noise. This term contains all types of waves generated by the shot which are not the primary pulse reflected from a given reflector at a certain depth. These waves are direct P- or S- waves propagating from the source to the receiver along the surface, other types of surface waves (Rayleigh waves), scattered waves from various surface and buried sources, and so on. Expressed in a different way: This term constitutes waves associated with all other travelling paths than the direct path from the shot down to the reflector and back to the receiver point at the surface.



$p$  = Reflected wave pulse from the given reflector. This term constitutes the wave pulse associated with the ray paths from the shot, down to the reflector and back to the receiver point at the surface. The sum  $n_s + p$  includes the total seismic wave-field generated by the shot.

Now, the total noise field will be

$$n = n_b + n_i + n_s \quad (3.2)$$

The signal-to-noise ratio of the reflected pulse in a distance  $x$  from the shot can be defined as

$$\text{SNR}(x) = \left[ \frac{\frac{1}{\Delta t} \int_t^{t+\Delta t} p(x,t)^2 dt}{\frac{1}{\Delta t} \int_t^{t+\Delta t} n(x,t)^2 dt} \right]^{\frac{1}{2}} \quad (3.3)$$

Here,  $t$  is the arrival time of the reflected pulse and  $\Delta t$  is the duration of the pulse. The signal-to-noise ratio is then defined as the ratio between the rms-estimates of the reflected pulse and the total noise recorded.

### 3.3 Noise estimation

Obviously, estimates of the noise field can only be found by field experiments. For example, rms-estimates of  $n_i$  and  $n_b$  can be found by recording with unconnected and connected geophones, respectively, without firing surface shots. In addition, estimates of the total noise field  $n$  can be found by firing shots at the surface and recording the total wave field. Of course, such recordings could contain reflections from present reflectors, however such effects can be smoothed out by averaging over a number of surface shots fired at different places.

In conclusion, noise estimates may be found by relatively simple field experiments. We shall now turn to the problem of estimating the reflected signal pulse ( $p$ ).

### 3.4 Signal estimation

In order to be able to detect a reflected signal, it must be strong enough to rise over the noise level, or at least have certain characteristics which make possible an identification by signal-statistical means. For example, it may be possible to identify reflections on a seismic section even if the reflected pulse on each single trace is undetectable; in that the phase of the reflected pulse varies continuously from trace to trace. The reflections may then be identified by a simultaneous inspection of a number of adjacent traces.

Nevertheless, if the reflected signal shall have a chance to be detected, it must at least be of the same order of magnitude as the noise. For example, in earthquake seismology, one usually operates with a threshold signal-to-noise ratio of 3-4 in order to claim a detection.

As a somewhat optimistic working hypothesis, let us state the following requirement for a reflected signal to be identified on a seismic section:

- For a single trace in the seismic section we must have (see eq. (3.3)):

$$\text{SNR} \geq 1 \qquad (3.4)$$

Now, let us see what parameters must be known in order to estimate the size of a reflected signal recorded at the surface.

We shall adopt the following simple signal model:

- A charge of a given size fired at the surface gives a seismic pulse with zero-to-peak amplitude  $A_0$  at unit distance from the shot point.
- On its travelling down to a certain reflector and back to the surface, the pulse will be affected by the following three factors:
  - 1) Geometrical spreading, due to the fact that the source energy is continuously distributed over a larger and larger area.
  - 2) Attenuation loss due to imperfections of the medium, i.e., heat loss due to solid friction.
  - 3) Loss due to leakage of transmission energy through the reflector.

- The total effect of the three factors above can be expressed by the relation (see, f.ex., Jaeger and Cook, 1976)

$$A(z) = r \cdot \frac{A_0}{z} e^{-\alpha(z-1)} \quad (3.5)$$

Here we have used the following symbols:

- $z$  = travelling distance  
 $A(z)$  = amplitude of wave after travelling a distance  $z$   
 $r$  = reflection coefficient  
 $\alpha$  = attenuation constant.

As to the geometrical spreading, this factor is generally dependent upon the distribution of wave velocity in the medium between surface and reflector, producing a certain 'lens effect' on the travelling wave field. Assuming a constant wave velocity, the spreading becomes spherical, as expressed by the  $\frac{1}{z}$  term in eq. (3.5). Furthermore, it turns out that the attenuation constant  $\alpha$  depends on wave frequency, and can be written as

$$\alpha = \frac{\pi f}{Qv} \quad (3.6)$$

where

- $f$  = wave frequency  
 $Q$  = seismic 'quality factor'  
 $v$  = wave velocity.

Considering for the moment only frictional loss (and not transmission loss and geometrical spreading), we have

$$A(z) = A_0 e^{-\frac{\pi f}{Qv}(z-1)} \quad (3.7)$$

The relative loss in decibels due to internal friction over a travelling distance  $d$  can be expressed as

$$\text{Loss [dB]} = 8.69 \frac{\pi f d}{Qv} \quad (3.8)$$

The loss in dB is thus proportional to both frequency and travelling distance. Setting  $d$  equal to one wavelength  $\lambda$ , we get (since  $v=\lambda f$ )

$$\text{Loss [dB]/wavelength} = \frac{8.69 \pi}{Q} = \frac{27.3}{Q} \quad (3.9)$$

This means that the frictional loss in dB per wavelength is a material constant dependent only upon the seismic quality factor  $Q$ : The larger the 'rock quality', the smaller the loss per wavelength.

The effect of transmission loss can be expressed by the reflection coefficient

$$r = \frac{\rho_2 v_2 - \rho_1 v_1}{\rho_1 v_1 + \rho_2 v_2} \quad (3.10)$$

where

$v_1, \rho_1$  = velocity and density immediately above the reflecting interface (rock)

$v_2, \rho_2$  = velocity and density immediately below the reflecting interface (ore body).

The product  $\rho v$  is the so-called acoustic impedance. It is the jump in this factor that determines how much energy will be reflected from and transmitted through the reflector. The transmission coefficient is given by

$$t = 1-r = \frac{2\rho_1 v_1}{\rho_1 v_1 + \rho_2 v_2} \quad (3.11)$$

It should be noted that the expressions (3.10) and (3.11) are valid for waves propagating approximately normal to the reflector (for horizontal reflectors, close to the vertical direction).

### 3.5 An attempt to estimate reflected signal amplitude in the Løkken area

In section 3.4 we adopted a relatively simple model for the amplitude of a reflected signal, namely (eq. (3.5))

$$A(z) = r \frac{A_0}{z} e^{-\alpha(z-1)} \quad (3.12)$$

Now we shall try to obtain a rough estimate of the amplitude of a reflected signal pulse from a given reflector in the Løkken area. Having estimated this amplitude, we will also get a certain estimate of what signal-to-noise ratio we could possibly expect to observe in a reflection seismic survey. It must be stressed that the estimates will be rather uncertain, and the results should only be taken as an indication of what chance we actually have of ore detection in the area.

#### Attenuation

Very few data exist which are relevant to the calculation of attenuation constants in the metamorphic rocks of the Løkken or Sulitjelma area. However, the experiments performed at Løkken in 1977 (see Geoteam, 1978), may give certain rough estimates. By inspection of the numerous data from these experiments, we found three shots that had been fired at three different levels of the mine, namely, at 380 m, 720 m and 930 m, and recorded at the surface at geophones carefully screwed into the bedrock (see Fig. 3.1). In all cases, 100 grams of dynamite was fired under equal conditions, and these charges should ideally give the same seismic pulse towards the surface. Fig. 3.2 shows a number of records from this field experiment. Three geophones, G2, G4 and G8, which were all mounted in the same way on hard rock (steel bolt) are included.

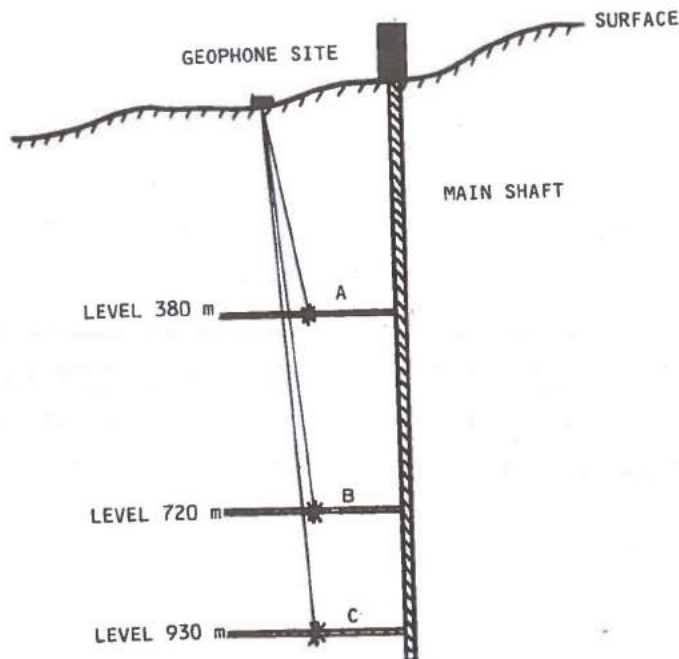


Fig. 3.1 Schematic view of the Løkken-77 experiment. Shots were fired at points A, B and C at levels 380 m, 720 m and 930 m, respectively.

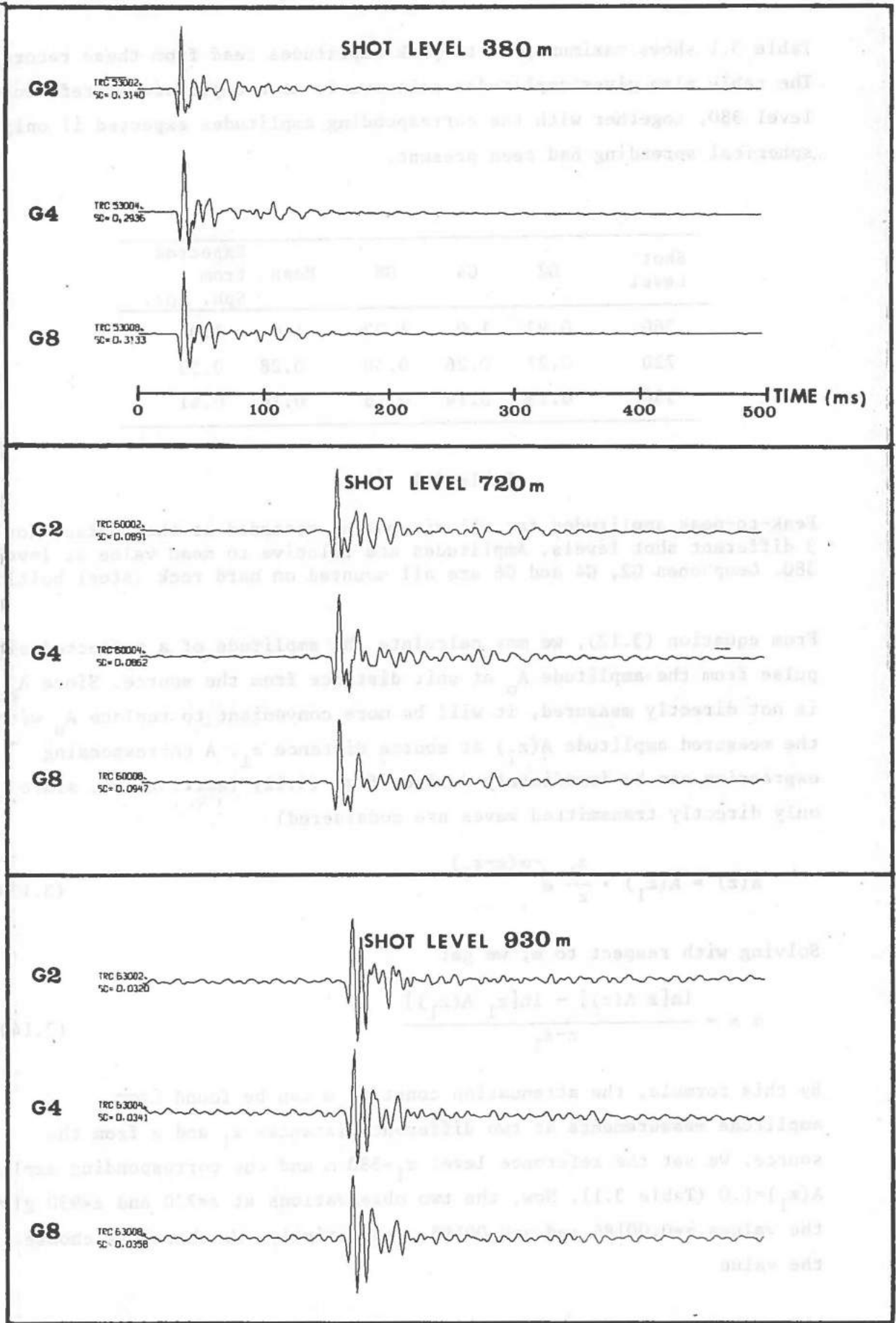


Fig. 3.2 Records for three different shot levels in the Løkken-77 experiment. All geophones G2, G4, and G8 are mounted on hard rock. Note that the scale factors are different for the different traces, and that zero time is not necessarily consistent with shot time.

Table 3.1 shows maximum peak-to-peak amplitudes read from these recordings. The table also gives amplitudes relative to mean amplitude at reference level 380, together with the corresponding amplitudes expected if only spherical spreading had been present.

Shot Level	G2	G4	G8	Mean	Expected from Sph. Spr.
380	0.97	1.0	1.02	1.0	1.0
720	0.27	0.26	0.30	0.28	0.53
930	0.13	0.14	0.15	0.14	0.41

Table 3.1

Peak-to-peak amplitudes for seismic pulses recorded at the surface for 3 different shot levels. Amplitudes are relative to mean value at level 380. Geophones G2, G4 and G8 are all mounted on hard rock (steel bolt).

From equation (3.12), we may calculate the amplitude of a reflected signal pulse from the amplitude  $A_0$  at unit distance from the source. Since  $A_0$  is not directly measured, it will be more convenient to replace  $A_0$  with the measured amplitude  $A(z_1)$  at source distance  $z_1$ . A corresponding expression can be immediately derived from (3.12) (setting  $r=1$ , since only directly transmitted waves are considered)

$$A(z) = A(z_1) \cdot \frac{z_1}{z} e^{-\alpha(z-z_1)} \quad (3.13)$$

Solving with respect to  $\alpha$ , we get

$$\alpha = - \frac{\ln[z A(z)] - \ln[z_1 A(z_1)]}{z-z_1} \quad (3.14)$$

By this formula, the attenuation constant  $\alpha$  can be found from amplitude measurements at two different distances  $z_1$  and  $z$  from the source. We set the reference level  $z_1=380$  m and the corresponding amplitude  $A(z_1)=1.0$  (Table 3.1). Now, the two observations at  $z=720$  and  $z=930$  give the values  $\alpha=0.00186$  and  $\alpha=0.00195$ , respectively. We therefore choose the value

$$\alpha = 0.0019 \quad (3.15)$$

as a reasonable estimate of the attenuation factor. For a dominant signal frequency of 150 Hz (see Fig. 3.3), and wave velocity around 5900 m/s we obtain from eq. (3.6) a value of the seismic quality factor

$$Q = 42 \quad (3.16)$$

This value is in good agreement with values published for similar rock types (see Table 3.2). From eq. (3.9) we can now compute the loss [dB] per wavelength:

$$\text{Loss [dB]/wavelength} = 0.6 \quad (3.17)$$

Fig. 3.4 shows attenuation curves for the Løkken granitic rock, showing both simple spherical spreading and the combined effect of spherical spreading and frictional loss calculated from eq. (3.13), setting  $\alpha=0.0019$ . The figure also shows the amplitude observations at the three different levels of the mine.

To avoid confusion we would like to comment on a result obtained in an earlier attempt on estimating the attenuation in the Løkken bedrock (Geoteam, 1978, p. 6). This result is based on the same data as we have applied and it says as follows: 'For the frequency range 100-200 Hz, the total attenuation (included geometric spreading) seems to be about 1.5 dB per wavelength'.

Here we would like to remark that only the frictional loss may be characterized in terms of 'loss [dB]/wavelength', since this value is independent of distance from source. An attempt at including also the geometrical spreading effect in this parameter makes little sense, since its value would then be a function of distance from source and no longer a material constant.

#### Reflection coefficients

Measurements of rock densities and seismic velocities in the Løkken mine in 1974 show that expected values of reflection coefficients towards the ore deposits are in the range 0.1-0.25 (see Table 3.3, Grammeltvedt, 1978).



Typical velocities of propagation and the dissipation constants for seismic waves in common materials\*

Material	$C_p$ (ft/millisecond)	$C_s$ (ft/millisecond)	Q (approx)
Water (room temp.)	4.9	0	10 <sup>5</sup>
Steel	19.5	10.6	3,000
Glass	22.3	10.7	600
Taconite, Minnesota	17.5	—	300
Sandstone, Pennsylvania	9.5	—	50
Chalk, Texas	9.2	3.6	80
Granite, Westerly	19.0	10.6	40
Quincy	19.3	9.7	70
Limestone, Solenhöten	19.6	9.5	150
Norite, Sudbury	20.4	1.1	125

\* Based on data from Memoir 97 of the Geological Society of America Clark (1966).

Table 3.2

Typical velocities and Q-factors for seismic waves in various materials.  
(From Jaeger and Cook, 1976.)

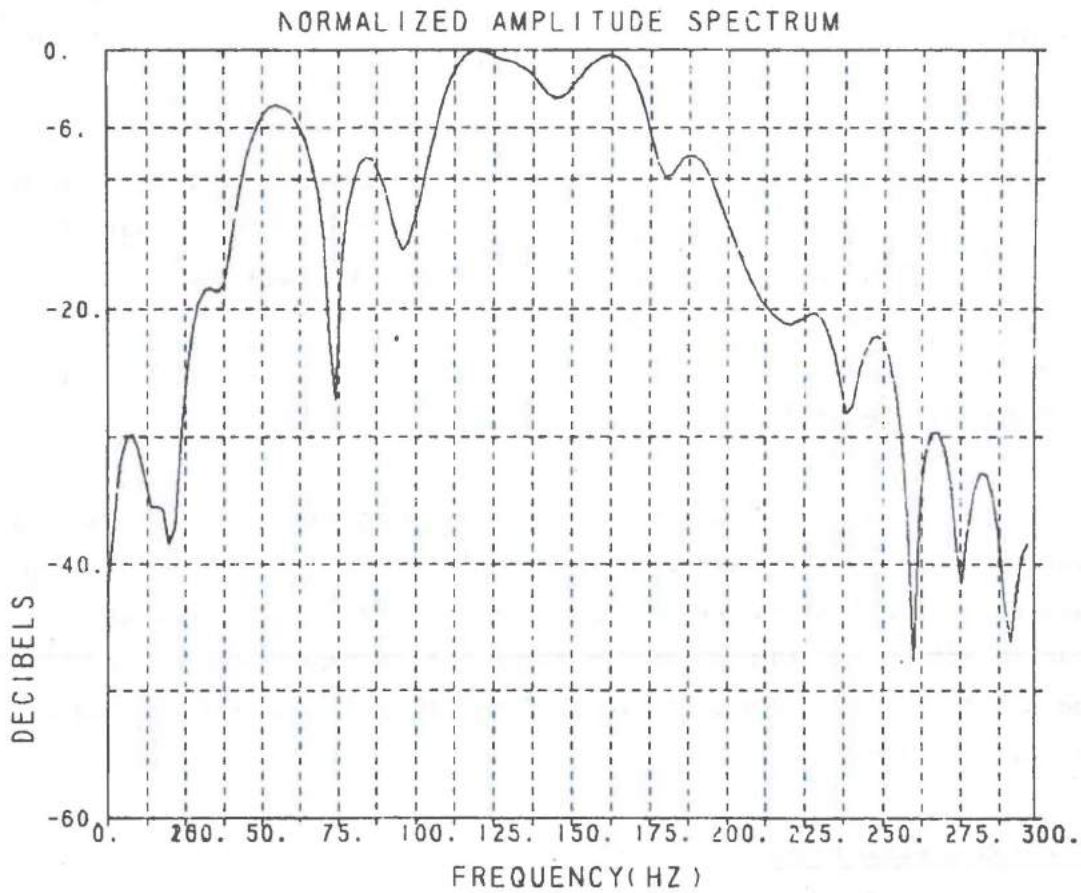


Fig. 3.3 Typical amplitude spectrum for signals recorded from shot level 930. (Ref. to trace G2 in Fig. 3.2.) Peak frequency is around 150 Hz, which can also be immediately measured from the time trace (period ~ 6-7 ms). (From Geoteam, 1978.)

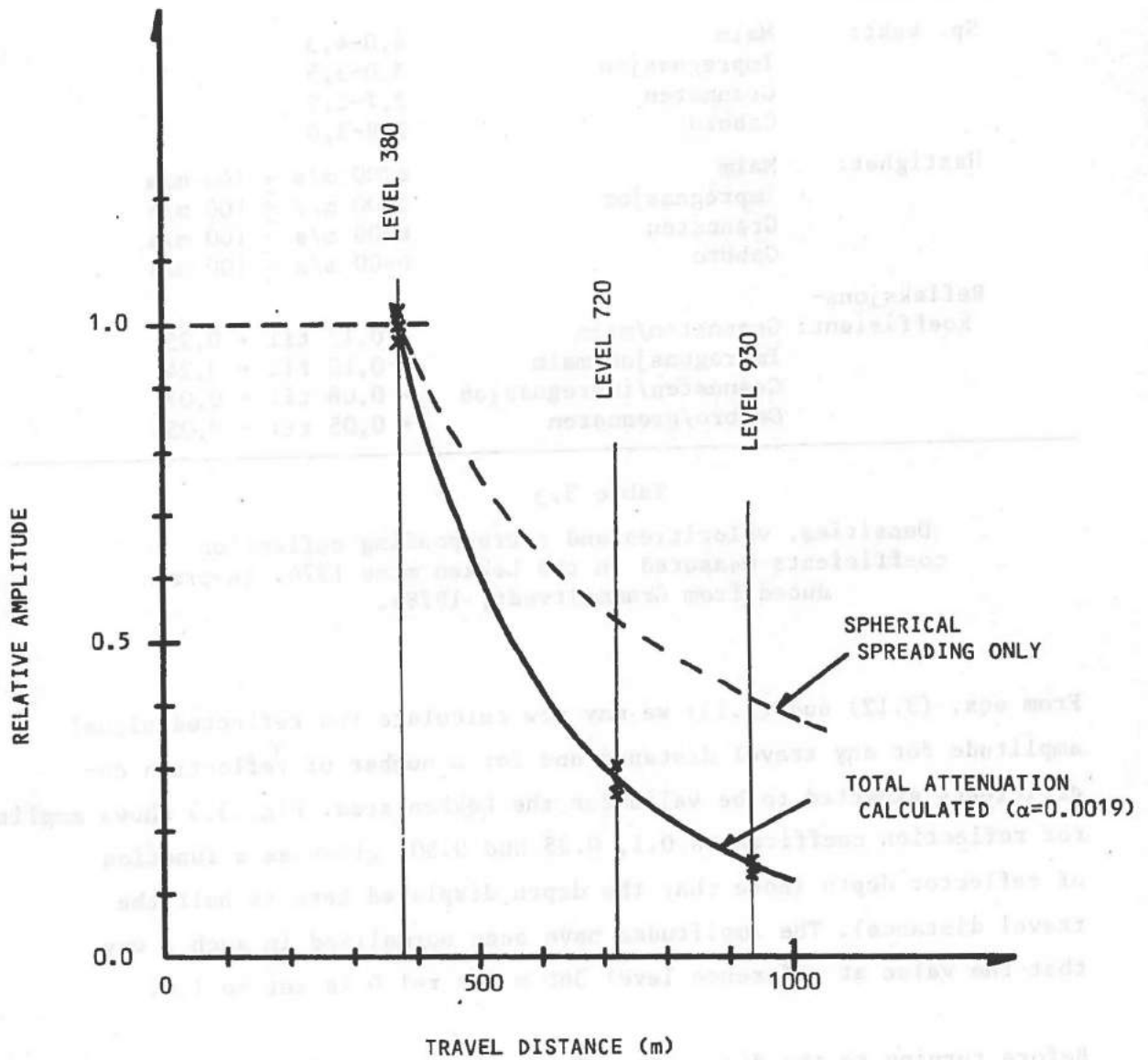


Fig. 3.4 Attenuation curve for the Løkken granitic rock, showing simple spherical spreading, and the total attenuation calculated for  $\alpha=0.0019$ . Observed values are also given (crosses).

---

Hastigheter i malm og fjellgrunn ble målt i gruben april 1974 med utrustning TRIO ABEM.

Nøkkeltall:

Sp. vekt:	Malm	4,0-4,3
	Impregnasjon	3,0-3,5
	Grønnsten	2,7-2,9
	Gabbro	2,8-3,0
Hastighet:	Malm	6200 m/s $\pm$ 100 m/s
	Impregnasjon	5600 m/s $\pm$ 100 m/s
	Grønnsten	6400 m/s $\pm$ 100 m/s
	Gabbro	6400 m/s $\pm$ 100 m/s
Refleksjons- koeffisient:	Grønnsten/malm	+ 0,13 til + 0,25
	Impregnasjon/malm	+ 0,10 til + 0,24
	Grønnsten/impregnasjon	+ 0,08 til - 0,07
	Gabbro/grønnsten	+ 0,05 til - 0,05

---

Table 3.3

Densities, velocities and corresponding reflection coefficients measured in the Løkken mine 1974. (Reproduced from Grammelvedt, 1978).

From eqs. (3.12) and (3.13) we may now calculate the reflected signal amplitude for any travel distance and for a number of reflection coefficients expected to be valid for the Løkken area. Fig. 3.5 shows amplitudes for reflection coefficients 0.1, 0.25 and 0.50, given as a function of reflector depth (note that the depth displayed here is half the travel distance). The amplitudes have been normalized in such a way that the value at reference level 360 m for  $r=1.0$  is set to 1.0.

Before turning to the discussion of the signal-to-noise ratio, we would like to make one further comment. Using the expression for the reflection coefficient in eq. (3.10) we have in fact assumed that the layer beneath the reflecting interface (that is, the ore body) is not so thin that reflected signals from the upper and lower side of this layer will overlap. Theoretical analyses show that if the thickness of the 'reflecting layer' becomes less than 1/8 of a wavelength, the reflected pulses from the

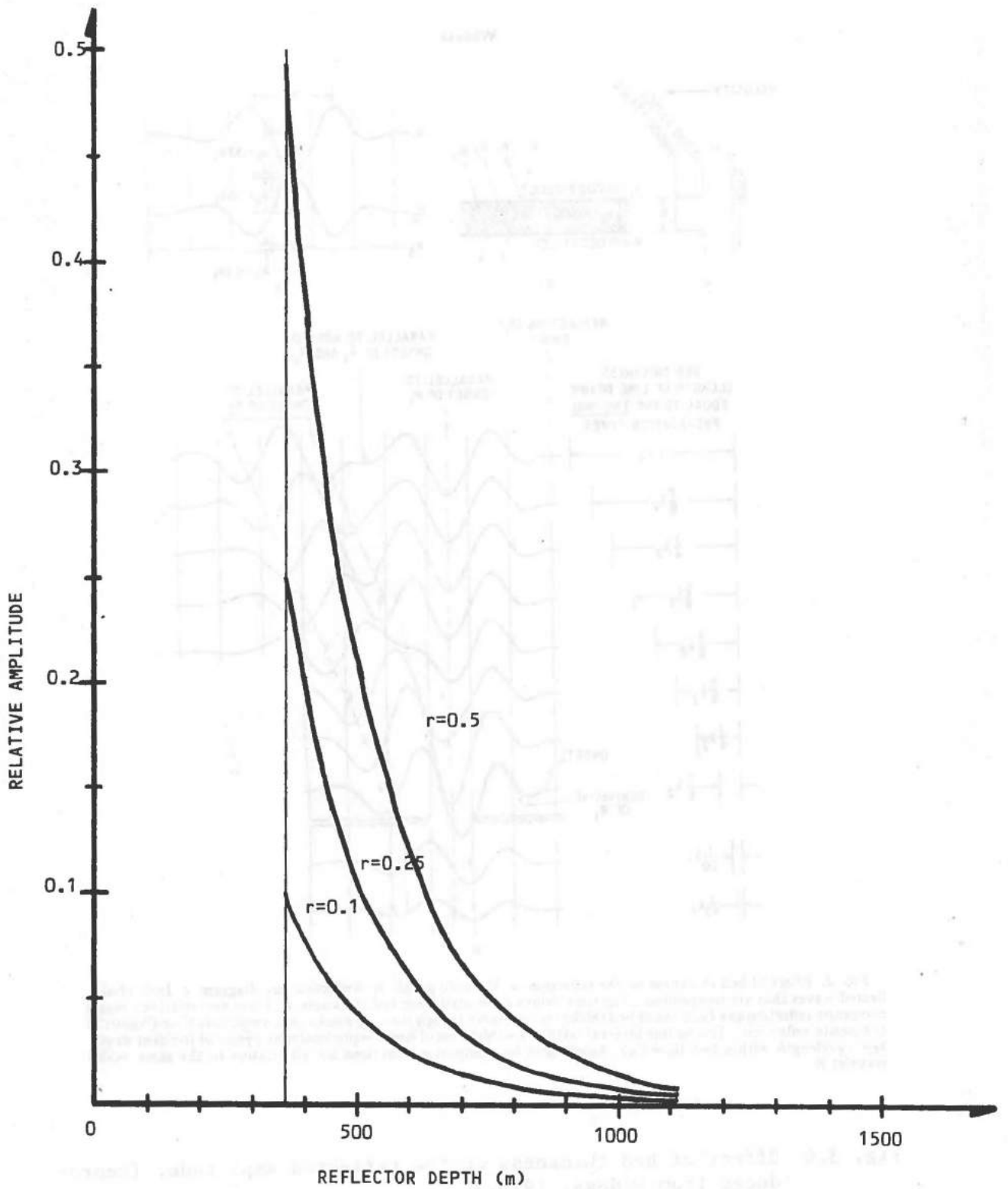


Fig. 3.5 Amplitude curves for reflected signals to be applied in the Løkken area. The amplitude has been normalized in such a way that a reflector at 360 m depth (i.e., total travel distance=720 m) with reflection coefficient=1.0 gives the amplitude 1.0. This means that the reflection coefficient corresponding to a given curve is equal to the amplitude value at level 360.

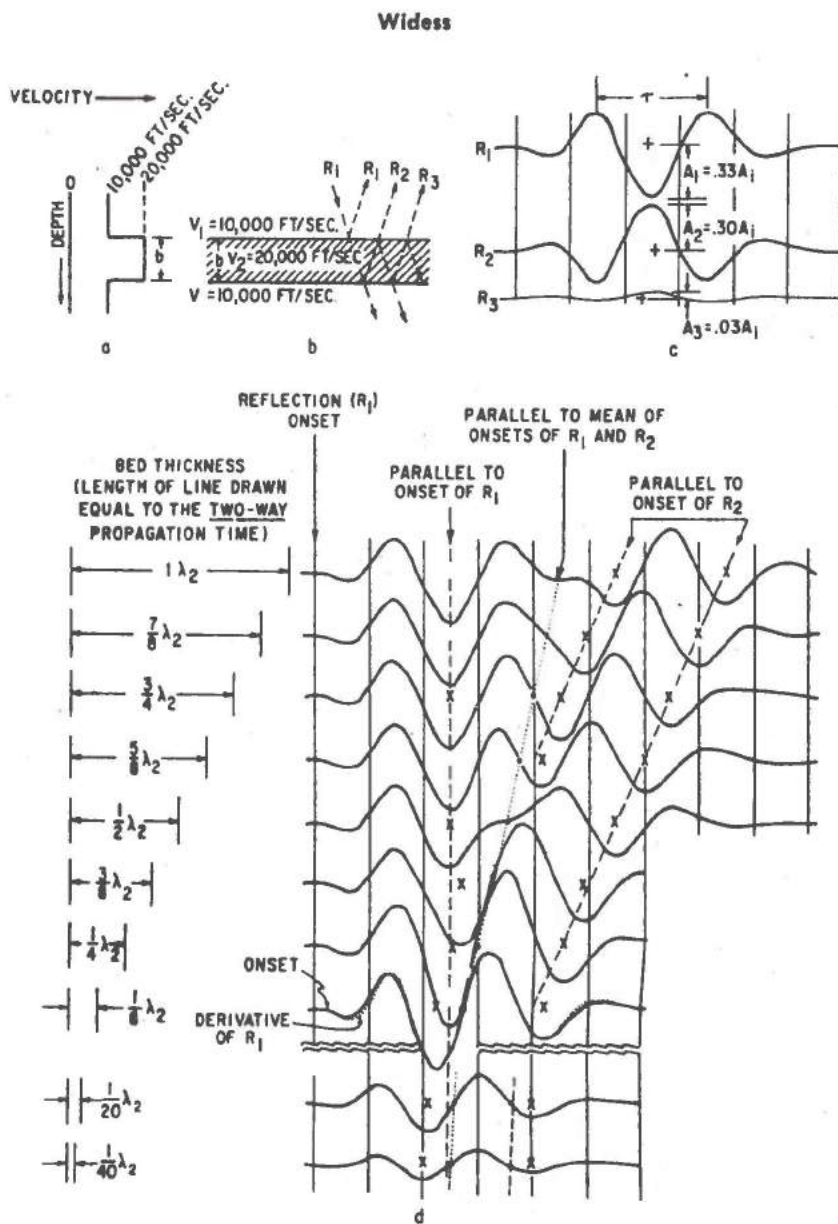


FIG. 2. Effect of bed thickness on the reflection. a. Velocity graph. b. Reflection ray diagram. c. Individual reflected waves that are composited using time delays computed from bed thickness. d. Form and relative timing of composite reflection as a function of bed thickness. X marks trough time. O marks zero-amplitude time ("center" of composite reflection). Timing line interval is  $0.5\tau$ .  $b$  = thickness of bed.  $\tau$  = predominant period of incident wavelet  $\lambda_2$  = wavelength within bed ( $\lambda_2 = V_2\tau$ ). Amplitudes for composite reflections are all relative to the same incident wavelet  $R_i$ .

Fig. 3.6 Effect of bed thickness on the reflected amplitude. (Reproduced from Widess, 1973.)

upper and lower discontinuity will effectively cancel each other. A demonstration of this effect is given in Fig. 3.6. (for reference, see Widess, 1973) which shows that a layer thicker than  $1/8$  of a wavelength roughly maintains the reflected signal amplitude, although the layer itself only can be resolved if the thickness exceeds one wavelength. In our case this means that the ore deposits should be thicker than 5-10 meters in order to give effective reflections. In the Løkken area ore bodies of 20-30 m thickness are commonly observed.

### 3.6 The 1978 Løkken Experiment. Estimation of expected SNR

In order to find expected signal-to-noise ratios of reflected signals in the Løkken area, we decided to perform additional field experiments during the summer 1978. These experiments were designed in such a way that signal pulses from shots deep in the mine should be recorded under realistic noise conditions. In earlier experiments, such signals had been recorded only in presence of instrument and background noise (i.e., the terms  $n_i$  and  $n_b$  in eq. (3.1)). However, in an actual profiling case, reflections will also be affected by the source-generated noise ( $n_s$ ) introduced by the surface shot.

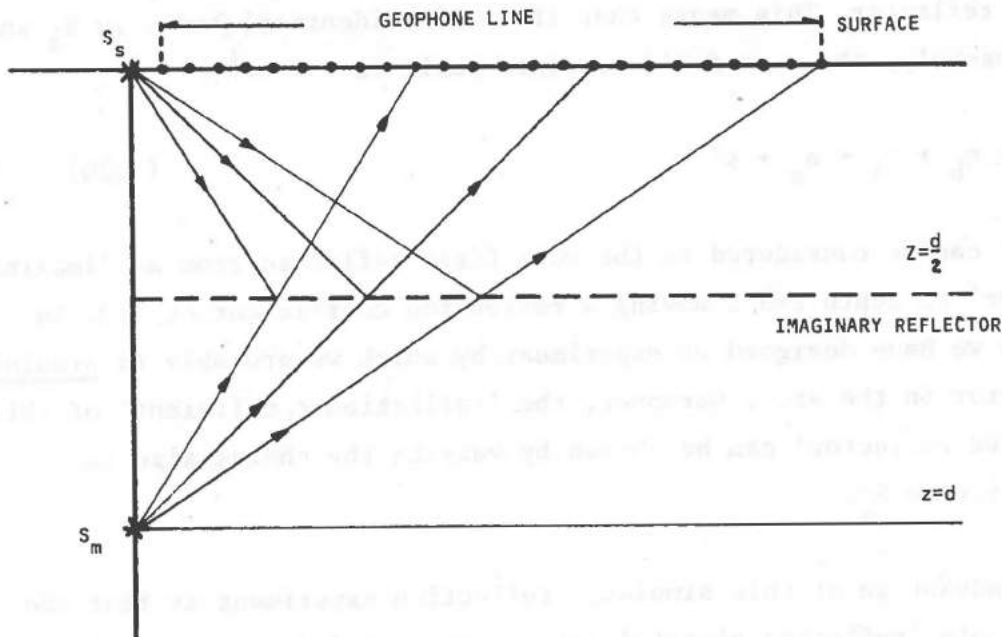


Fig. 3.7 Schematic illustration of the Løkken-78 reflector simulation experiment.

Fig. 3.7 explains the idea behind the experiments. Assume that we have an area composed of relatively homogeneous rock, which is the case in Løkken where measurements have shown approximately constant seismic velocities at least down to depths of 1000 m. Assume further that a shot is fired at a point  $S_s$  at the surface. If there is no reflector in the area, the wave field recorded by the geophones will be the sum

$$u = n_b + n_i + n_s \quad (3.18)$$

(Even if there are weak reflectors in the area, we are not interested in these for the moment, so that the corresponding reflected signals can be included in the term  $n_s$ .)

Assume that a second shot is fired in the mine at the point  $S_m$  having a depth  $z=d$ . The wave field recorded from this shot will be

$$u = n_b + n_i + s' \quad (3.19)$$

We now observe the fact that the wave field  $s'$  is equivalent to a wave field which would have been reflected from a plane horizontal reflector located at depth  $z = d/2$ , since  $S_m$  is the 'image point' of  $S_s$  relative to this reflector. This means that if we fire identical shots in  $S_s$  and  $S_m$  simultaneously, the wave field recorded would be

$$u = n_b + n_i + n_s + s' \quad (3.20)$$

where  $s'$  can be considered as the wave field reflected from an 'imaginary reflector' at depth  $z=d/2$  having a reflection coefficient of 1.0. In this way we have designed an experiment by which we are able to simulate a reflector in the area. Moreover, the 'reflection coefficient' of this 'simulated reflector' can be chosen by varying the charge size in  $S_m$  relative to  $S_s$ .

A great advantage of this simulated reflection experiment is that the controllable 'reflected signals' can now be recorded under exactly the same conditions as would reflections from a real reflector. The surface shot provides the same complicated noise field as we would observe in a real profiling survey, and the various field parameters can be systematically varied in order to obtain optimal results. In combination

with values of reflection coefficients and attenuation constant derived in the previous section, results from this experiment can also give estimates of the expected signal-to-noise ratios in the area.

Figs. 3.8-3.10 show displays of field records from three different charges (50, 100 and 200 grams) fired at depth level 720 m in the Løkken mine and recorded at the surface. In these cases, no shot is fired at the surface and we have the situation described in eq. (3.19). From these records, we have obtained rms-estimates of  $(n_b + n_i)$  and  $s'$ . Results for a 100 g charge are given in Table 3.3, which shows expected SNR of the 'reflected' signal in absence of source-generated noise.

Reflector Depth (m)	SNR r=0.1	SNR r=0.2	SNR r=0.3
400	0.22	1.54	2.31
500	0.42	0.84	1.26
600	0.24	0.48	0.72
700	0.14	0.28	0.42
800	0.09	0.17	0.27
900	0.05	0.10	0.15
1000	0.03	0.06	0.09

Table 3.3

Expected signal-to-noise ratio (SNR) of a 'reflected' signal in absence of source-generated noise, given for different reflector depths and reflection coefficients. (Calculated on basis of signals from a 100 g charge, recorded with the DHR 1632 instrument.)



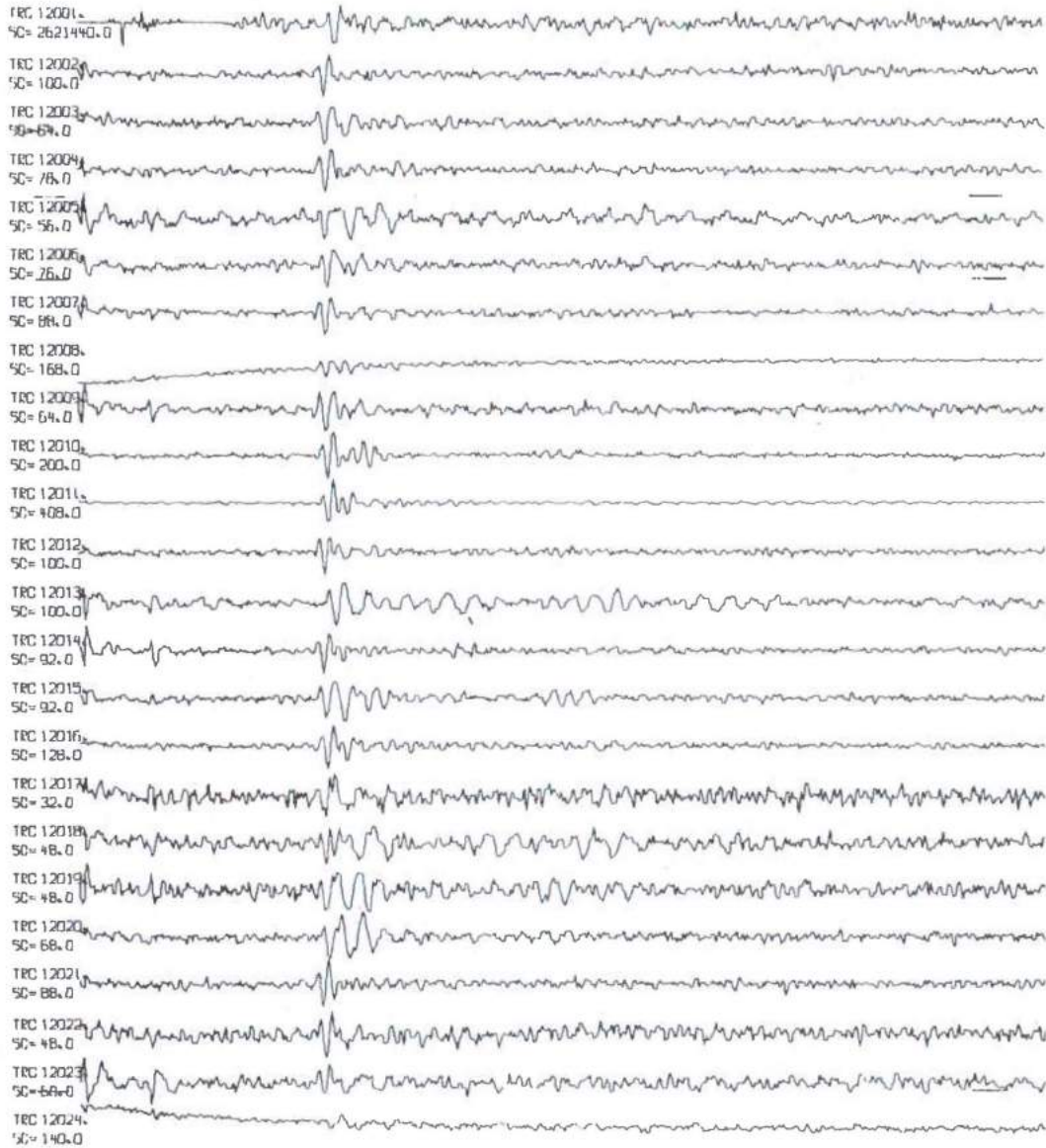


Fig. 3.8 Field records from the Løkken-78 experiment. (50 grams of C4 explosives fired at depth level 720 m). Total trace length is 500 ms.

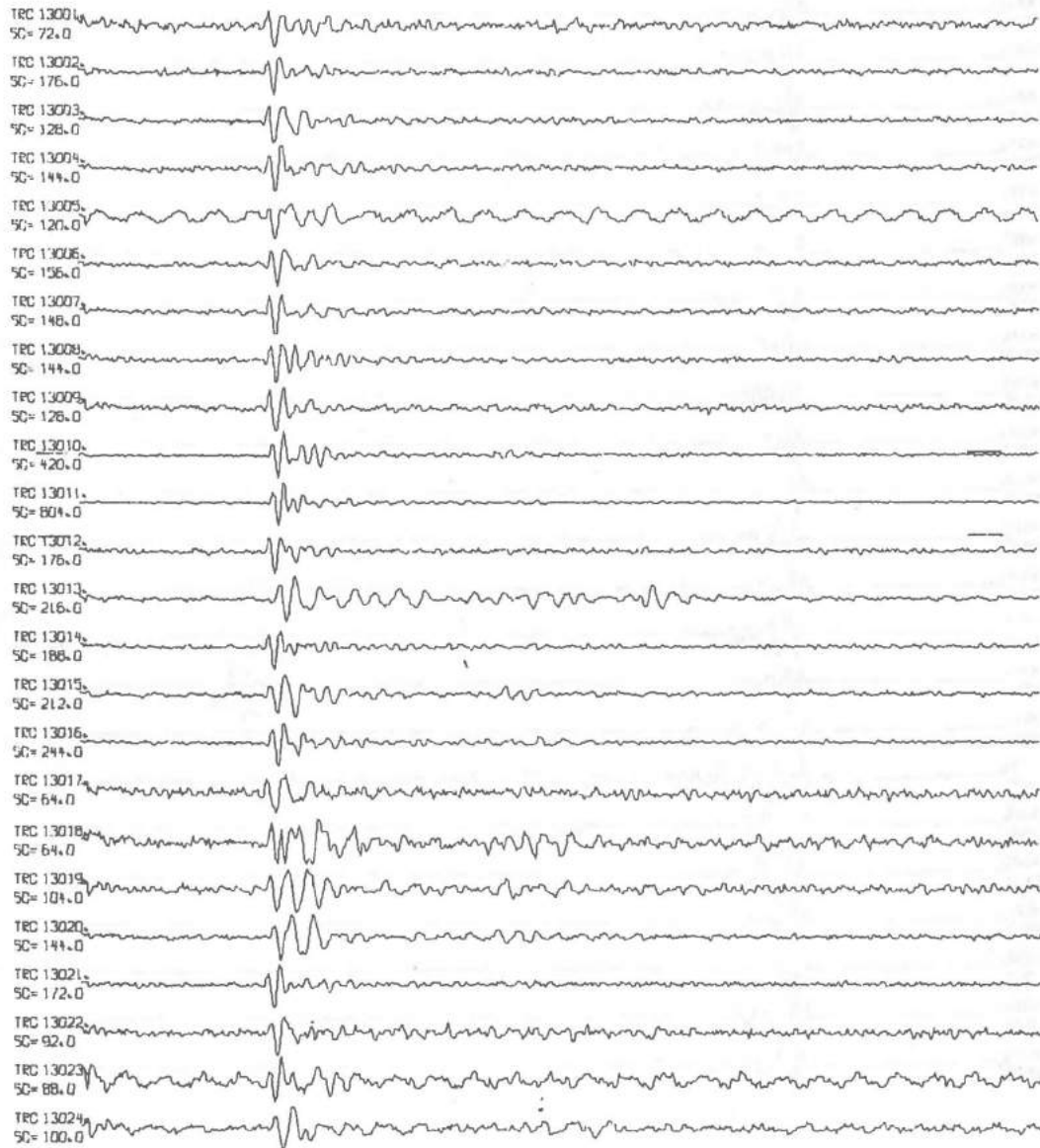


Fig. 3.9 Field records from the Løkken-78 experiment. (100 grams of C4 explosives fired at depth level 720 m). Total trace length is 500 ms.

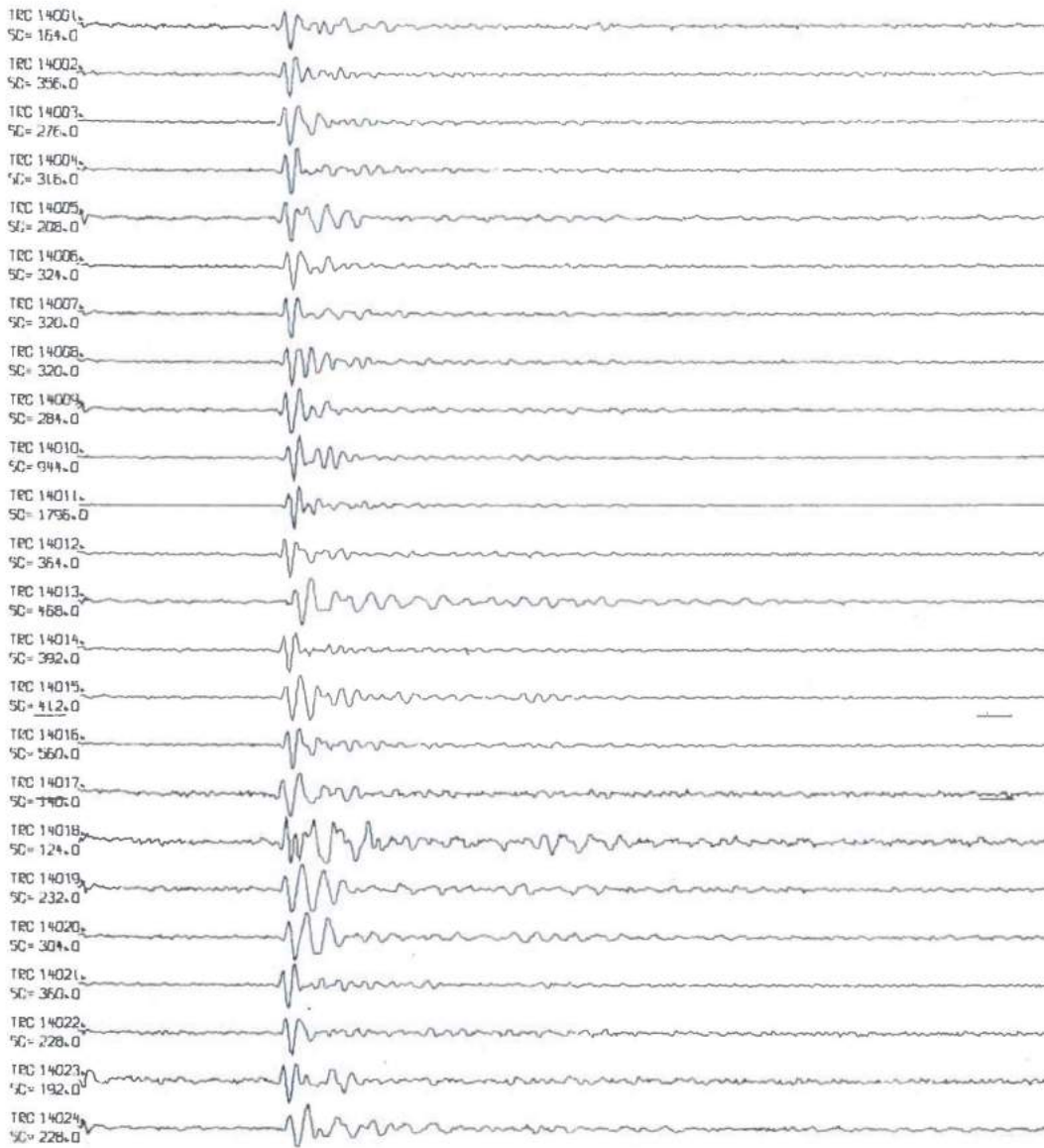


Fig. 3.10 Field records from the Løkken-78 experiment. (200 grams of C4 explosives fired at depth level 720 m). Total trace length is 500 ms.

These values have been obtained by reducing the SNR directly observed for the effects of geometrical spreading and frequency attenuation in accordance with eq. (3.13). It should be noted that these values refer to single geophone records and should be taken as a basis when deciding what stacking fold will at least be necessary in order to increase the SNR above the detection level. It should also be remembered that these values represent 'best cases', since source-generated noise is not present. For these ideal SNR values to be observed in a practical situation, the reflections must arrive in time windows where the source-generated noise does not dominate over the background noise, i.e.,  $n_s < n_b + n_i$ . We shall return to this point later.

From the above results, we may conclude that comprehensive stacking procedures will have to play an ultimate role in the processing of the data, in order to obtain detectable reflections. Even in the ideal case, that is, with no significant source-generated noise in the actual time window, the expected SNR turns out to be so small that a considerable effort should be made just in investigating optimal ways of stacking the data. Moreover, an equally important problem to be solved is what kind of corrections should be performed on the data before stacking in order to get real improvements. For example, a single trace SNR of 0.5 would ideally increase to 2.0 if 16 channels are stacked together. This will require identical signals and completely uncorrelated noise on all channels, in addition to ideal line-up of the signals in time (no uncontrollable phase shift). Especially, the high frequency band we are working with (100-200 Hz), will be extremely sensitive to small phase errors which can very easily be introduced, f.ex., by slightly different rock/ soil conditions close to the receiver sites. Without a relatively good control of this type of errors, one might happen to observe no SNR enhancement at all, even after a considerable stacking effort.

In conclusion we will have to admit the following: The expected signal to-noise ratio given in Table 3.3 shows remarkably small values, in fact, so small that one can hardly expect that stacking/processing will enable a detection of reflected signals from 7-800 m depth.

At this point, remembering that the above values of SNR represent 'best case' (that is, source-generated noise is absent), we had to admit that the prospects for the future were not good. In fact, we were somewhat surprised at the low values, especially because of two factors (for reference, see Ziolkowski and Lerwill, 1979):

- We have seen examples on reflection records from coal prospecting surveys, having a remarkably good SNR on single sensors. The charge size and frequency content of the signals are completely comparable to our case.
- The attenuation constant appearing in these surveys is reported to be considerably greater than our value of  $\alpha=0.0019$ .

The common argument we are faced with when referring to seismic coal prospecting techniques is that coal has a very large reflection coefficient ( $\sim 0.5$ ) and that source-generated noise does not represent a great problem, since one usually has a soft soil layer on top of the sediments. Here we would like to reply that a reflection coefficient of 0.5 will only double the values of Table 3.3, and moreover, the coal prospecting records show good reflections also for deeper layers ( $T\sim 500$  ms), where the energy has propagated through a number of coal layers before returning to the surface. As to the argument about the source-generated noise, it should (once again) be repeated that our values have been obtained in absence of this kind of noise field.

Having the above stated facts in mind, we started to wonder why our noise level should be significantly higher than that obtained by similar comparable observations. Since most of our experiments had been performed under remarkably good weather conditions, we started to be suspicious about the instrument noise. Would it be possible to increase SNR considerably by using another type of instrumentation? Incidentally, it turned out that the deep mine experiments of 1977 had been performed with two different instrumentations (see Geoteam, 1978): 1) Input/output DHR 1632, and 2) A Texas Instruments DFS V.

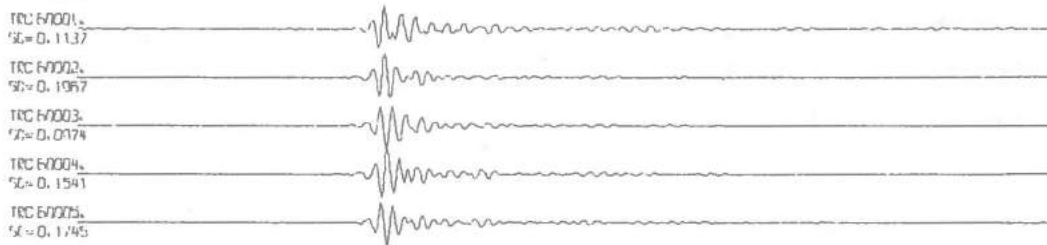
As both instrumentations had been used for recording seismic pulses from the same charges at the same level of the mine, it should be possible to compare the noise level at the two instruments, using the pulse amplitude

as a reference. The results of this comparison were rather dramatic. Fig. 3.11 shows two records of a shot at level 720 in the mine, recorded at the surface. The pulses have been scaled to the same amplitude, emphasizing the enormous difference in noise level. In fact, the noise levels differ by a factor of 20-30 dB, which means that the DHR 1632 equipment has an instrument noise level of at least the same value. This, of course, is quite unsatisfactory, in fact, one would never have a chance to detect reflections from an ore body with this kind of instrument noise level. Furthermore, this is a rather dramatic conclusion, since the DHR equipment has been used in nearly all seismic profiling work in the period 1976-78. At first sight, this must be characterized as a rather negative conclusion, since it shows that very much of the data recorded until now has very little value; but on the other hand, a discovery like this also allows us to be more optimistic as to the future, as it no doubt reveals a hidden potential of increase in SNR.

The observant reader may come up with the question of why the DHR 1632 was used during the 1978 experiments, as long as data from 1977 were able to show so clearly the superior performance of the DFS V. The answer is regrettable, though very simple: The DFS V instrumentation had been applied only in a limited number of experiments due to an accidental malfunctioning of the DHR 1632. It is generally occupied in marine seismic surveys and is consequently very seldom available for ore prospecting purposes. All the 1977 data had been analyzed prior to NORSAR's engagement (June 1978), however, no statement or comment was made in earlier reports which could point towards the above conclusion. Consequently, this very important discovery was not made until the DFS V data were analyzed at a later stage - that is, not until we started to be suspicious about the DHR noise level. Needless to say, an earlier discovery of this fact could have saved a large amount of money and effort. However, we would like to add that the analysis programs used by the processing company - specially designed for oil prospecting purposes - were not too well suited for investigations of the above kind.

In the next sections we shall look more closely at the signal and noise characteristics, as these are the most important factors to be considered when designing optimal shot/receiver configurations and corresponding stacking procedures.

### DFS V



### DHR 1632

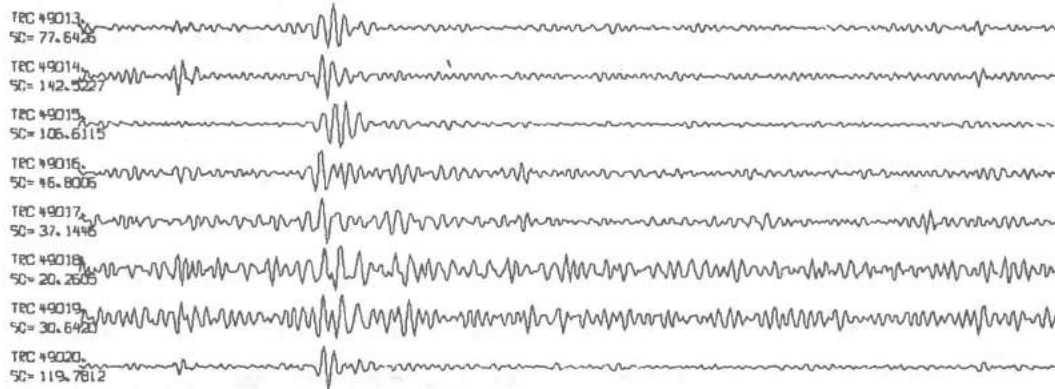


Fig. 3.11 Comparison between traces recorded with DFS V and DHR 1632 (100 gram explosives at 720 m depth).

#### 4. THE EFFECT OF SHOT DEPTH ON SOURCE-GENERATED NOISE - THE HADELAND 78 EXPERIMENT

##### 4.1 The Hadeland 78 Experiment

As a part of the general attempt to find methods for suppressing source-generated noise, it was decided to carry out supplementary experiments late in 1978. These experiments were especially aimed at studying the dependence of shot-generated noise on the depth of the surface shot.

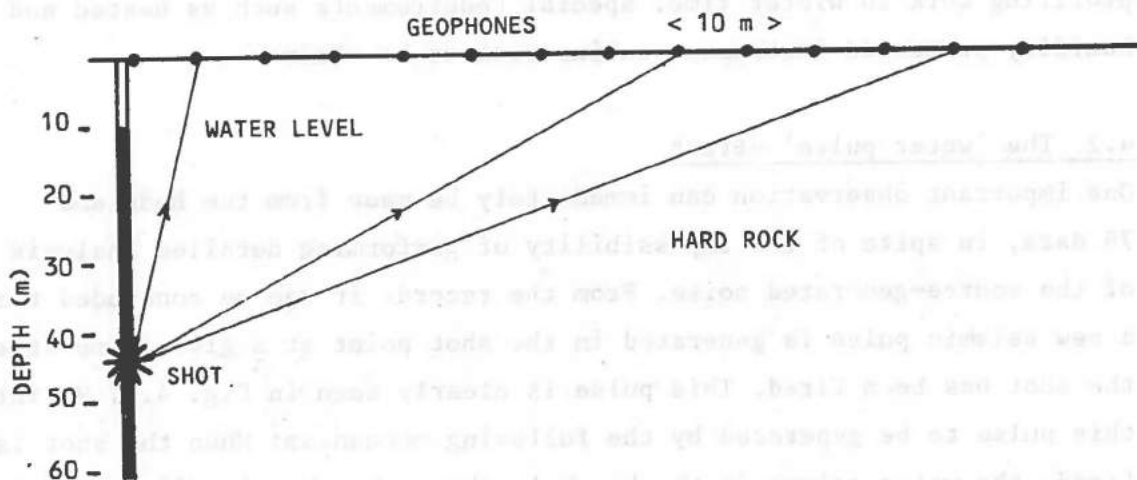


Fig. 4.1 Schematic lay-out of the Hadeland 78 borehole experiment.

Fig. 4.1 shows the simple lay-out of the experiment. A 60 m deep water-filled borehole located at Hov, Hadeland, (actually one of the old NORSAR instrument sites which is no longer in operation) was used for the shots, and a simple 24 channel geophone line was laid out from the hole. Shots (50 g of C4 explosive) were fired at different levels in the hole, starting at 60 m and going up to 10 m at 5 m intervals. Recording equipment used was a T.I. DFS V, operated by A/S Geoteam. Unfortunately, the field display equipment (field plotter) broke down already at the start



of the data recording, so that data control in the field became impossible. However, relying on the automatic gain control of the DFS V, we decided to complete the experiment without possibilities of field display.

Some typical recordings from this experiment are shown in Fig. 4.2. Regrettably, most of the traces are severely contaminated by a set of strong non-seismic waveforms which were, by the operator, explained by crossfeed in the instrumentation due to an open channel which was not in use. Because of the very bad quality of these data, we found it useless to carry out the planned analysis. It was, however, decided to repeat the experiment at a later time - this would only include one day's work, since the profile is completely prepared with geophone bolts, etc. One important conclusion which could be immediately drawn from this experiment was that there are considerable problems tied to carrying out seismic profiling work in winter time. Special requirements such as heated and humidity protected instrument cabins seem to be ultimate.

#### 4.2 The 'water pulse' effect

One important observation can immediately be made from the Hadeland 78 data, in spite of the impossibility of performing detailed analysis of the source-generated noise. From the records it can be concluded that a new seismic pulse is generated in the shot point at a given time after the shot has been fired. This pulse is clearly seen in Fig. 4.3. We interpret this pulse to be generated by the following mechanism: When the shot is fired, the water column in the borehole above the shot is lifted a certain distance, which obviously depends on factors such as charge size and weight of the water column. After a certain time, the generated 'hole' collapses and a new seismic pulse is generated. This effect is quite similar to the well-known 'bubble-pulse effect' observed in marine seismic recordings, where air-guns are fired, generating 'air bubbles' giving rise to new pulses when collapsing.

We have named this effect the 'water pulse' effect, and we can, at this stage, at least state the following conclusion: If we are going to use shot holes that are too deep for the charge to blow all the water out of the hole immediately after the detonation, some parameters must be carefully selected in order to prevent 'water pulses' arriving in interesting time intervals. Such effects may place considerable restrictions on our possibility to choose freely important field parameters (such as charge size) in a practical situation.

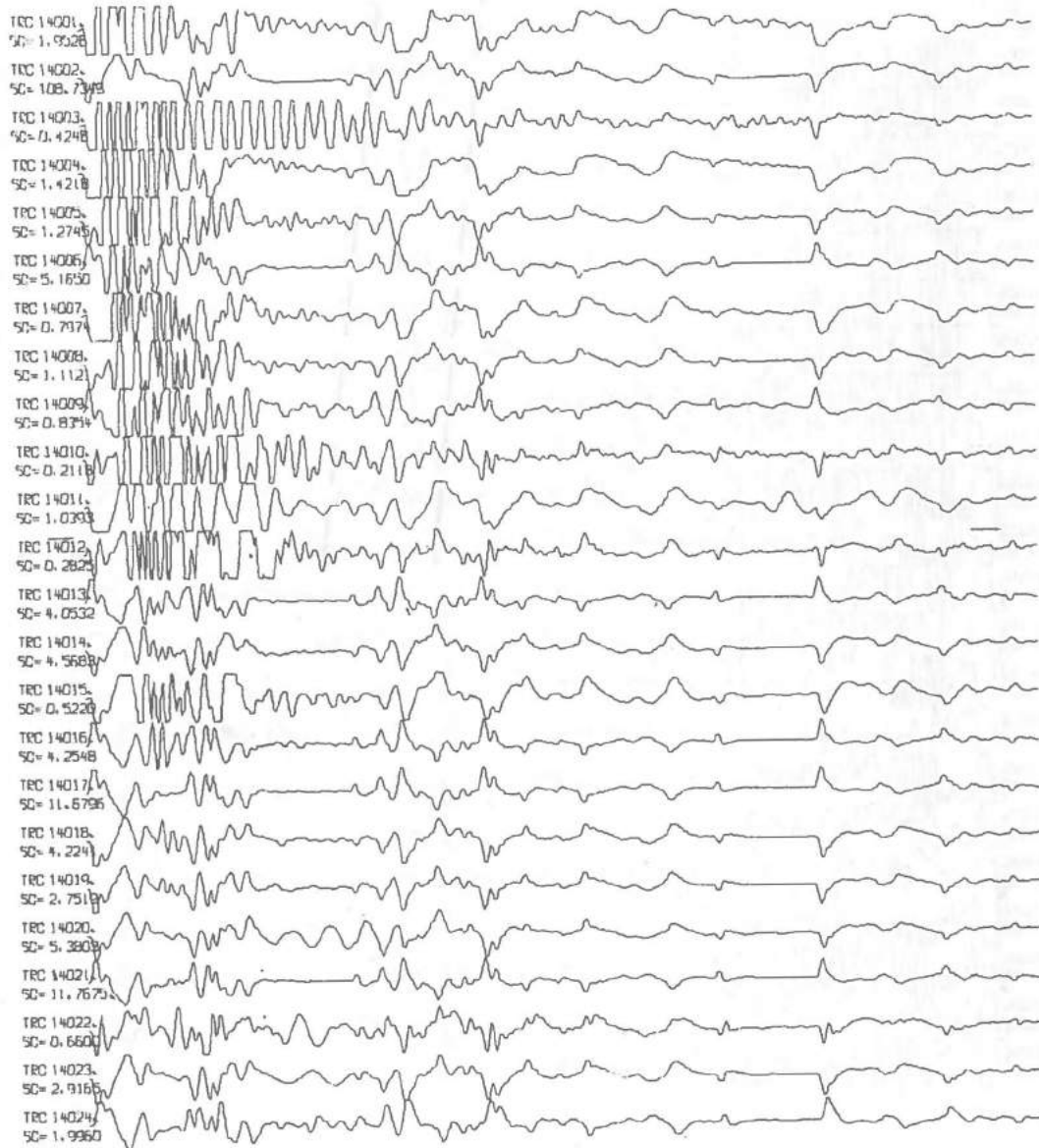


Fig. 4.2 Typical recording from the Hadeland-78 experiment. Note the strong non-seismic waveforms that are superimposed on the traces. 50 g of explosives are fired at 10 m depth. Total trace length is 500 ms.

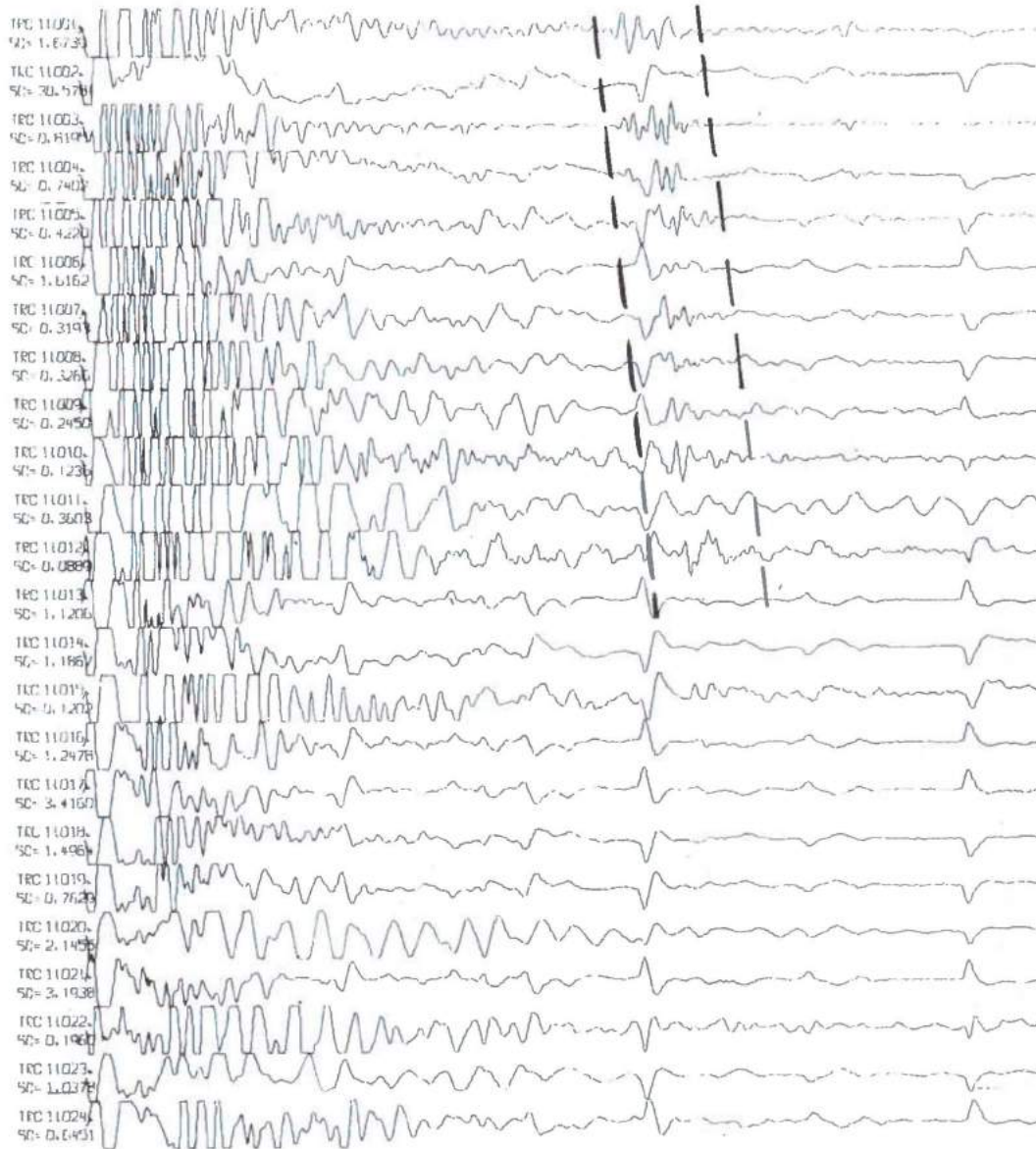


Fig. 4.3 Recording from the Hadeland-78 experiment, showing the 'water pulse' effect within the dotted lines. 50 g of explosives are fired at 23 m depth. Total trace length is 500 ms.

5. SIGNAL/NOISE CHARACTERISTICS AND CORRESPONDING CRITERIA FOR OPTIMUM DESIGN OF SHOT/RECEIVER GEOMETRY

5.1 Source generated noise - Løkken 1978

One of the main objectives of the Løkken-78 experiments was to study the source generated noise (direct P, S and surface waves) and design shot/receiver arrays that were able to cancel this kind of noise in an effective way. Since very little had been done in this field earlier, we decided to perform the experiments with a number of shot/receiver geometries in order to compare a relatively wide range of possible shot/receiver combinations during the following data analysis. Fig. 5.1 shows the various configurations used during the experiment. For each configuration, shooting was performed both in the mine (depth = 720 m) and at the surface.

CASE NO.	CONFIGURATION NO.	SURFACE SHOT	MINE SHOT	FIG. NO.
1	I	50	50	5.2
2	I	50	100	5.3
3	I	25	25	5.4
4	I	25	50	5.5
5	I	25	100	5.6
6	I	50		5.7
7	I	25		5.8
8	I		12.5	5.9
9	I		25	5.10
10	I		50	5.11
11	I		100	5.12
12	I		200	5.13
13	II	50		5.14
14	II		100	5.15
15	III	50		5.16
16	III		100	5.17
17	IV	50		5.18
18	IV		100	5.19

Table 5.1

Table showing various combinations of charge sizes (in grams of explosives) fired at the surface and in mine (depth =720 m). The table also shows the configuration used in each case (see Fig. 5.1) and a reference to the figures displaying the corresponding records.

The actual experiments are summarized in Table 5.1, showing the size and location of the charge in each case. Figs. 5.2-5.19 show a selection of shot files from the experiment. A preliminary analysis of the data unfortunately showed that most records, including surface shots, had a quite

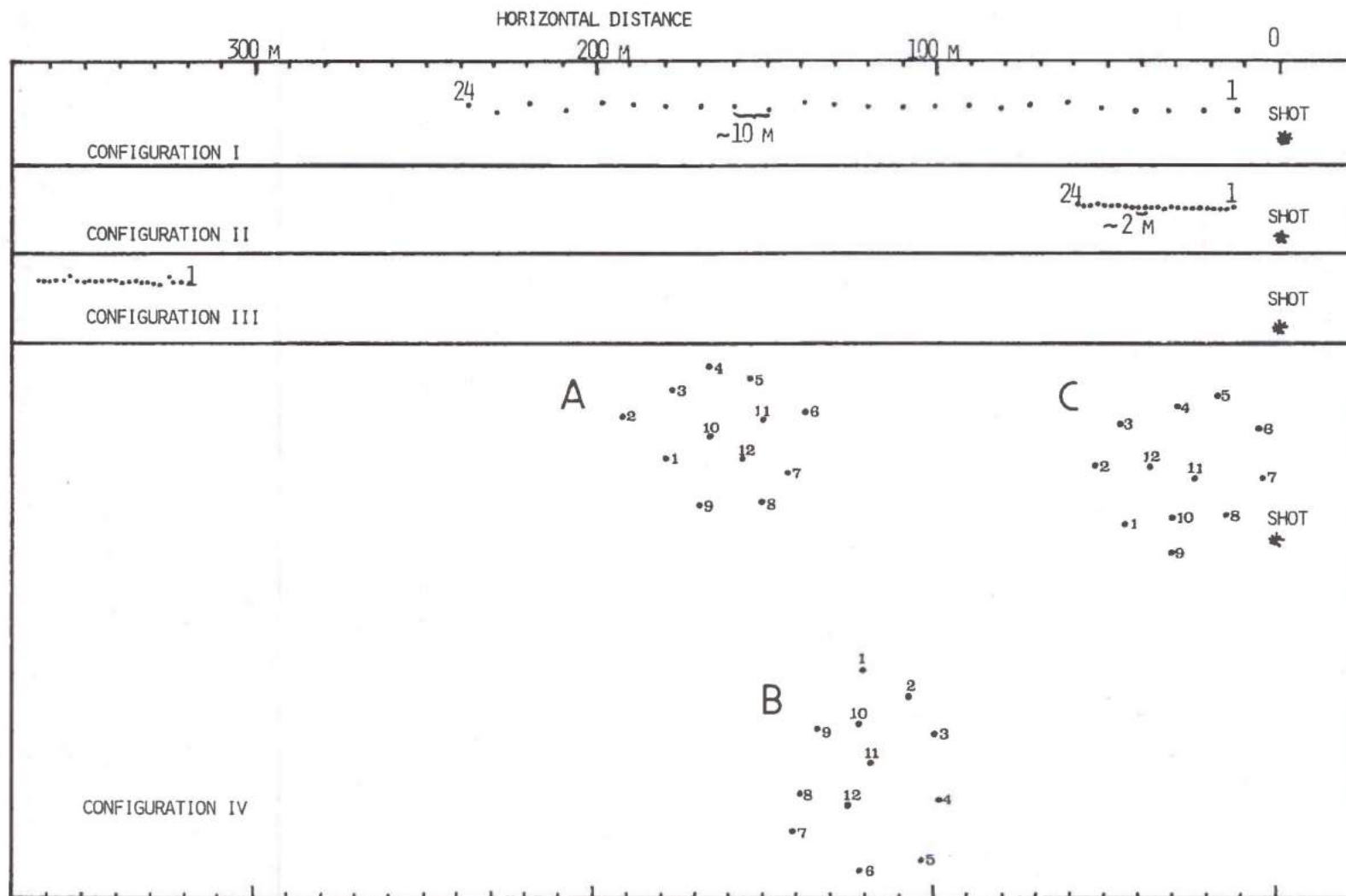


Fig. 5.1 Horizontal map of the four different shot/receiver configurations used during the Løkken-78 seismic experiment. The shot is indicated by a star, the geophones by a dot.

unsatisfactory noise level. The main reason for this was that the constant instrument gain of the DHR 1632 was selected in such a way that the very strong early surface waves (0-100 ms) passed unclipped through the recorder thereby 'consuming' the entire dynamic range of the system. This is illustrated in Fig. 5.20, showing a seismic trace recorded 10 m from the shot point. When using the whole dynamic range of the system for recording the strong surface wave, there will be nothing left for the later low level part of the trace, where deep reflections are expected to arrive. The result is that the electronic noise of the recording system is dominating after approximately 100 ms on the channels located closest to the shot, that is, the channels having the lowest preset gain.

In short, this had the fatal consequence that most of the data were useless with respect to the study of the source generated noise conditions in the interesting time interval 200-400 ms (i.e., reflector depth 600-1200 m). On the basis of this discovery, we became suspicious as to earlier data recorded with the DHR 1632, especially the profiling data recorded over the known Løkken ore body in 1976 (see page 5). An analysis of these data showed exactly the same effect - at least 70-80% of the data in the actual reflection time window were completely dominated by instrument noise. The very 'good' reflections from the ore body that could be seen on the corresponding stacked sections were now, in fact, placed in a somewhat strange light. Although we did not undertake a very comprehensive study of these data, it was concluded that the 'reflections' could possibly be coherent instrument noise that was stacked in phase. In fact, it had earlier been commented upon that the major 'reflections' seemed to be somewhat later than should be expected from the known depth of the ore body. As we did not want to put too much money and effort into a more thorough analysis of these data, we just concluded that a completely new data base would be necessary in order to perform a reasonable study of the source generated noise characteristics.

At this stage, it was also remarked that if the 'reflections' appearing on the 1976 sections should happen to be real - in spite of the fact that 70-80% of the traces contained pure instrument noise - we should be in a rather happy situation!

Figs. 5.2-5.19. Displays of records from the Løkken-78 seismic experiment. The shot/receiver configurations and charge sizes used in each case are given in Fig. 5.1 and Table 5.1, where reference is given to the various figures. The two trace panels displayed in each figure are the same data plotted with different scale factors. In the first case (a) the data have been scaled relative to the maximum value in the time window 20-500 ms; in the second case (b) the corresponding time window has been 200-500 ms. Total trace length is 500 ms.

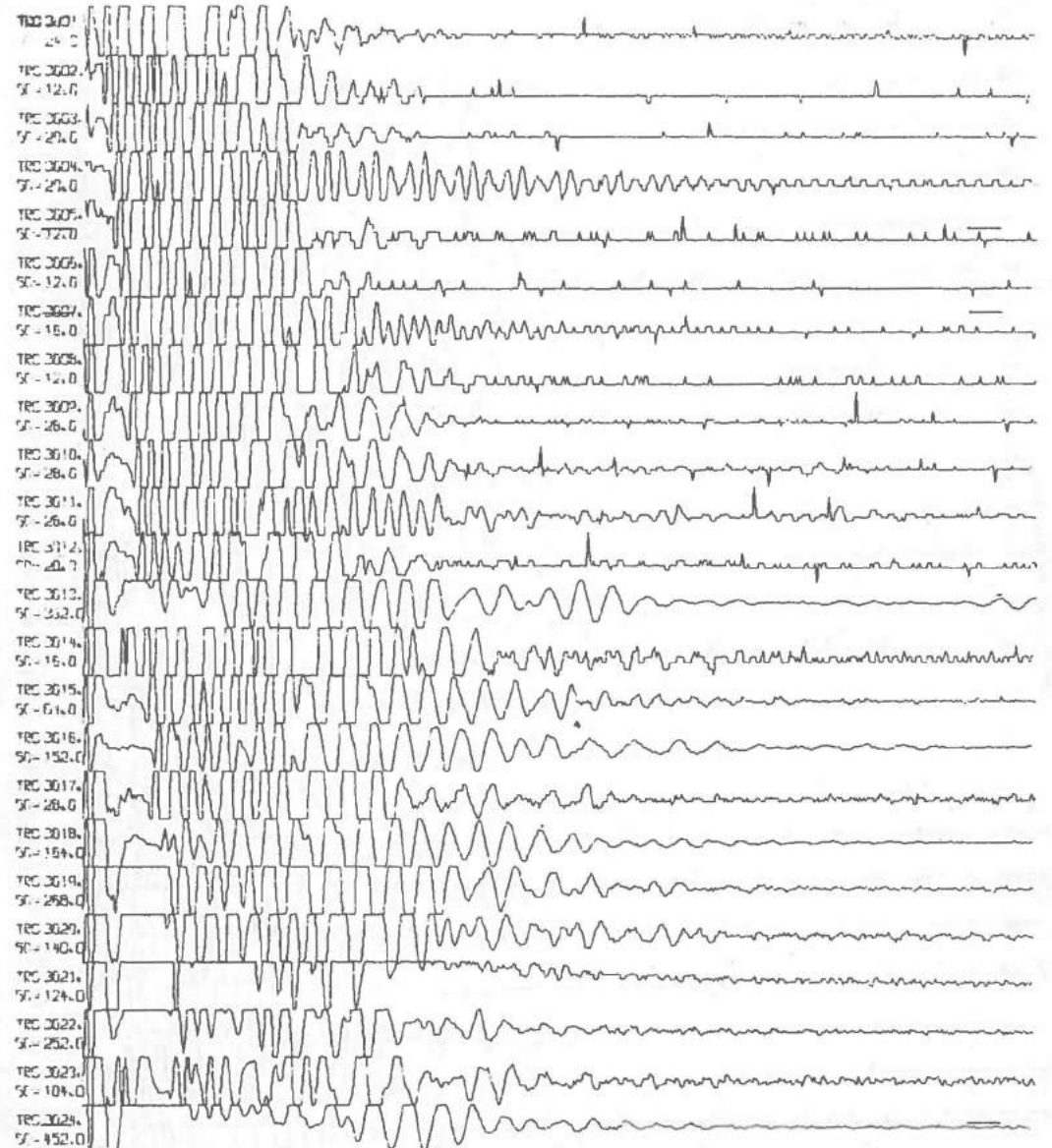
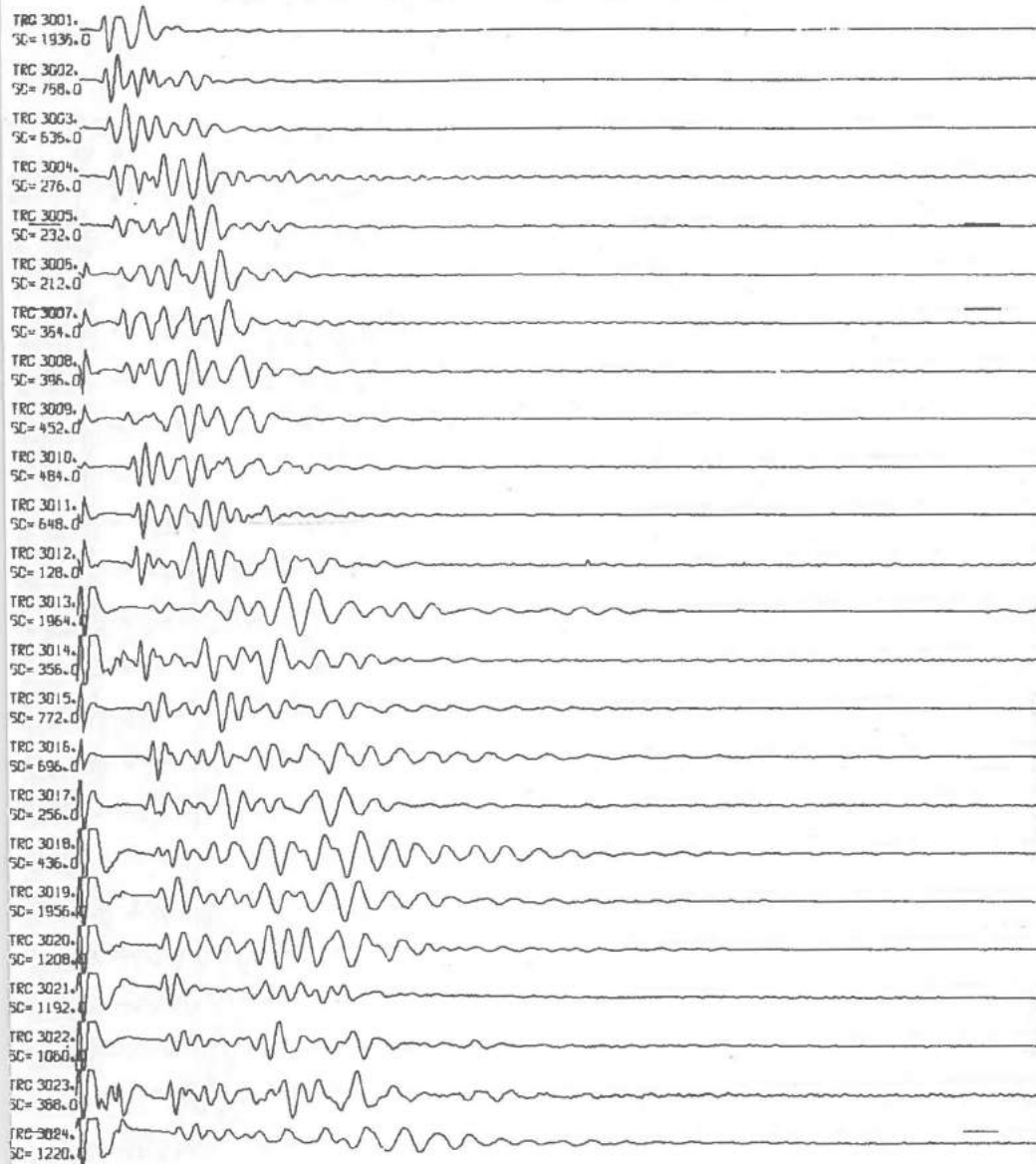


Fig. 5.2 Configuration No. I. Surface shot = 50 g, mine shot = 50 g.



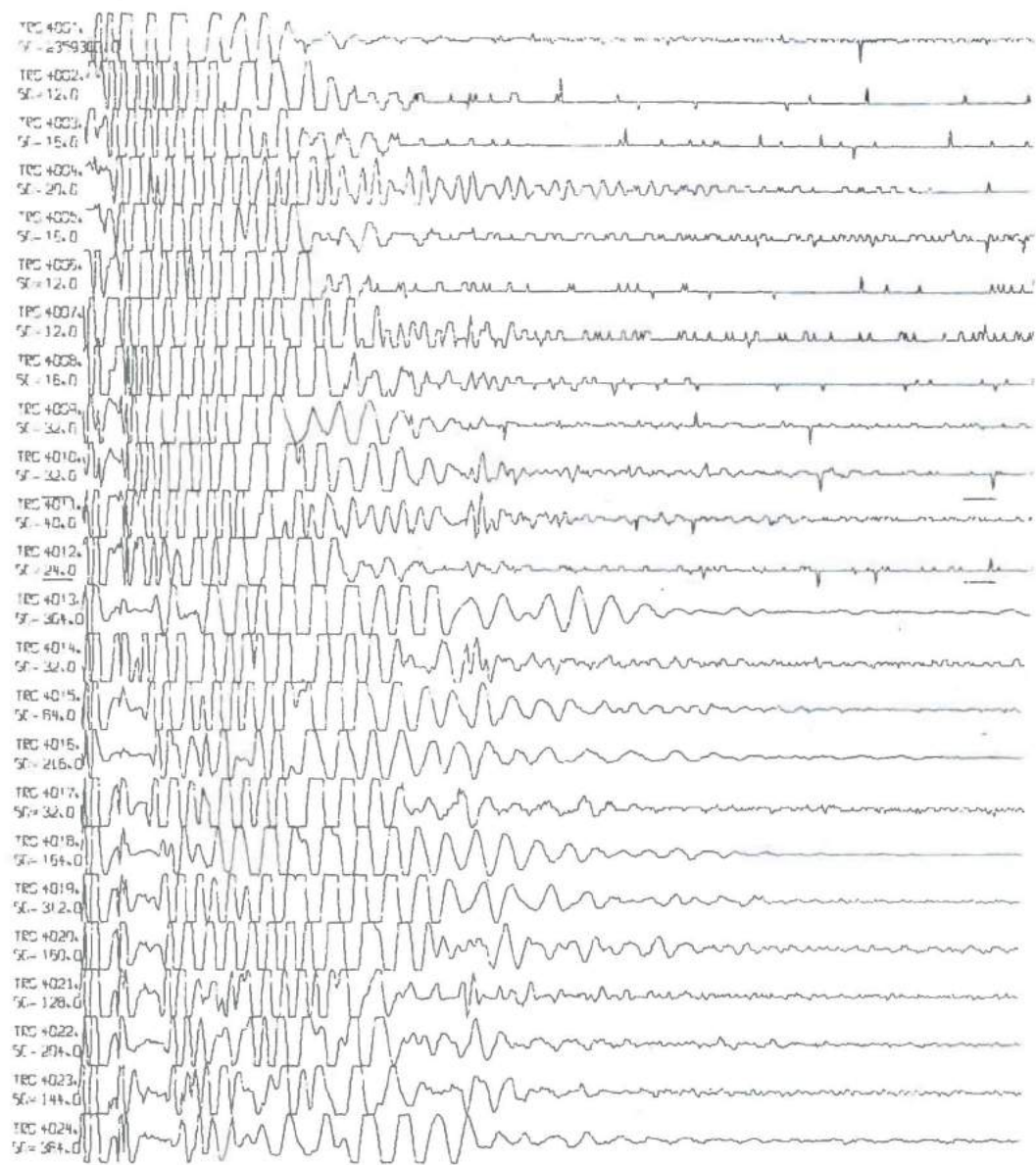
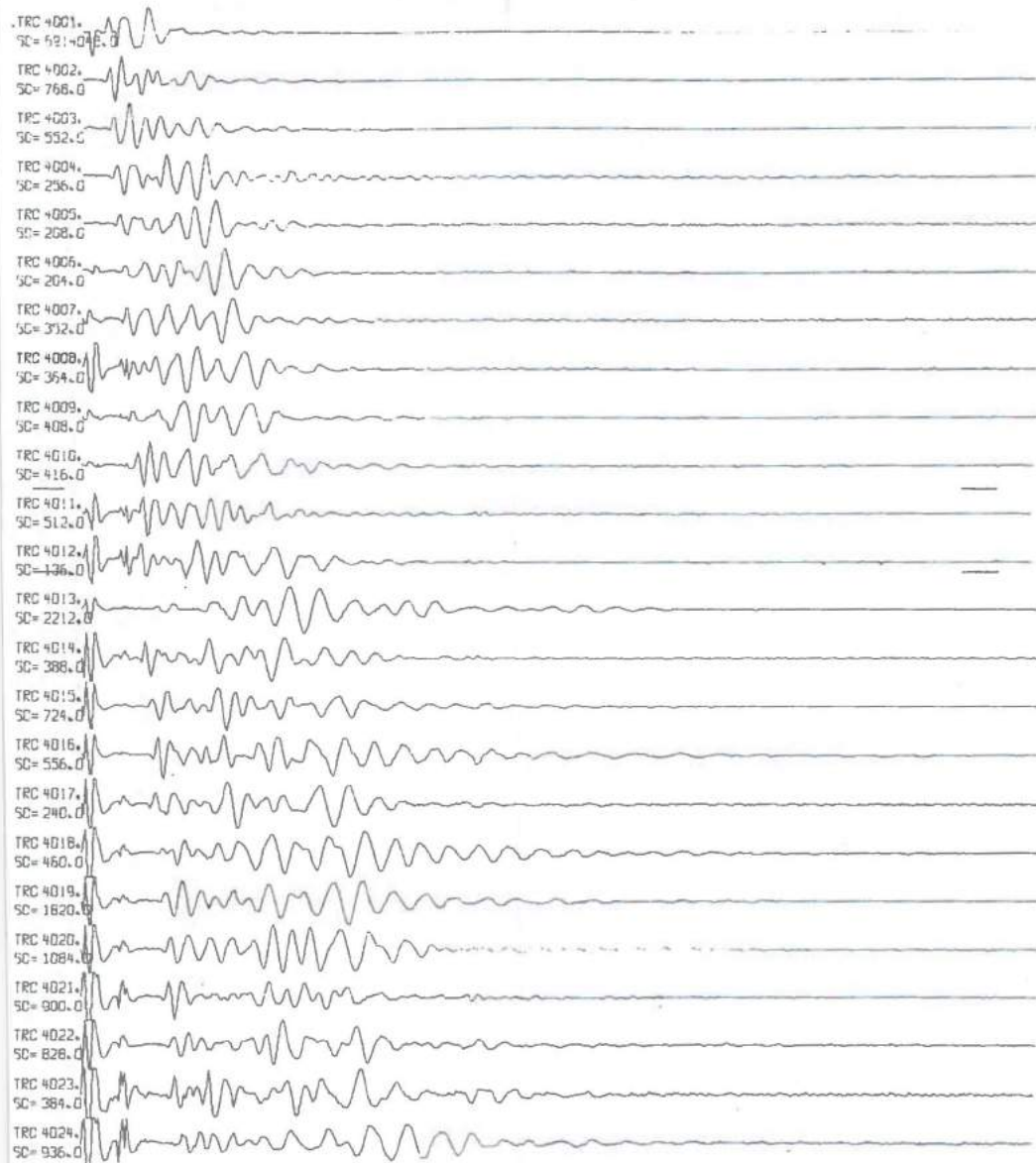


Fig. 5.3 Configuration No. I. Surface shot = 50 g, mine shot = 100 g.

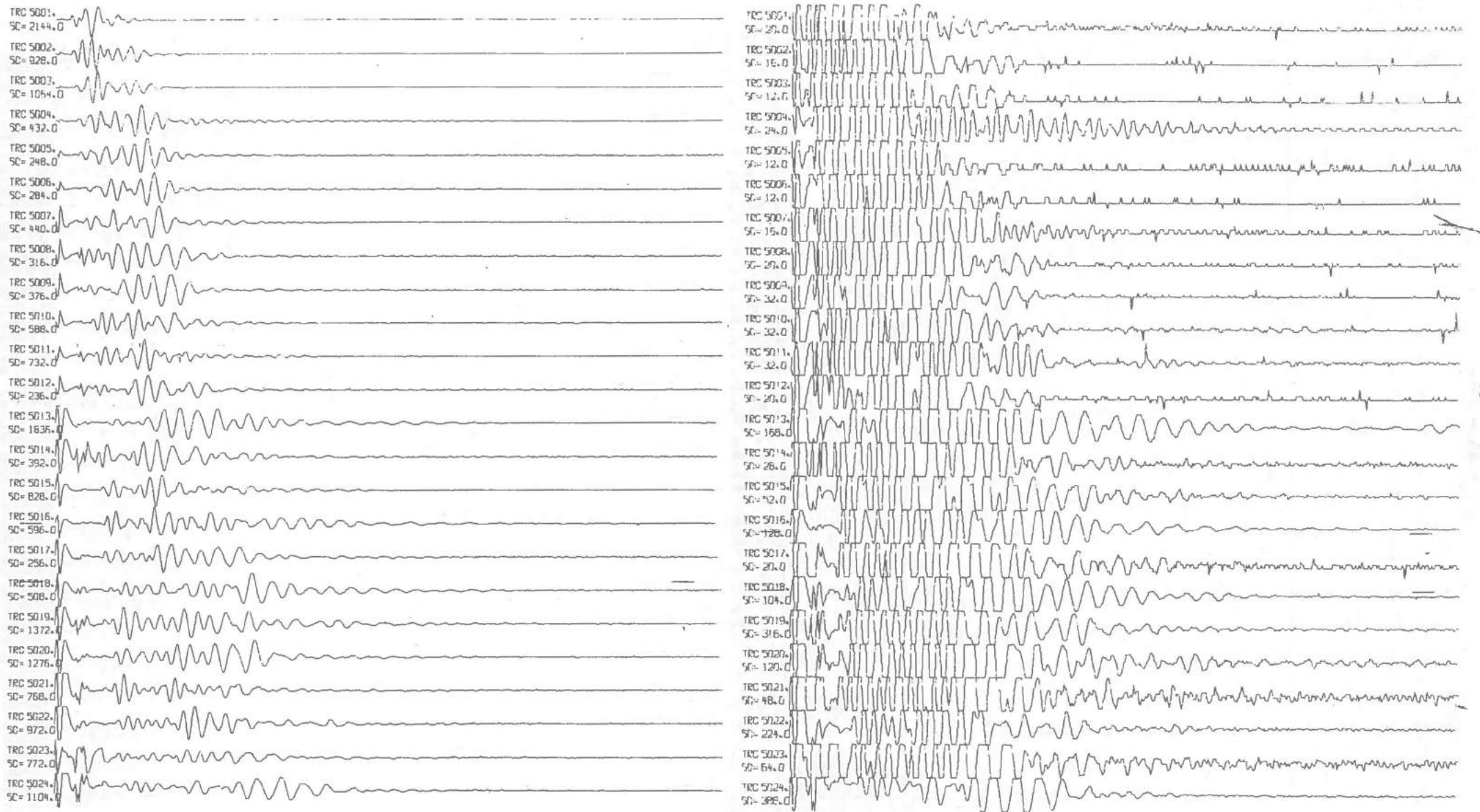


Fig. 5.4 Configuration No. I. Surface shot = 25 g, mine shot = 25 g.

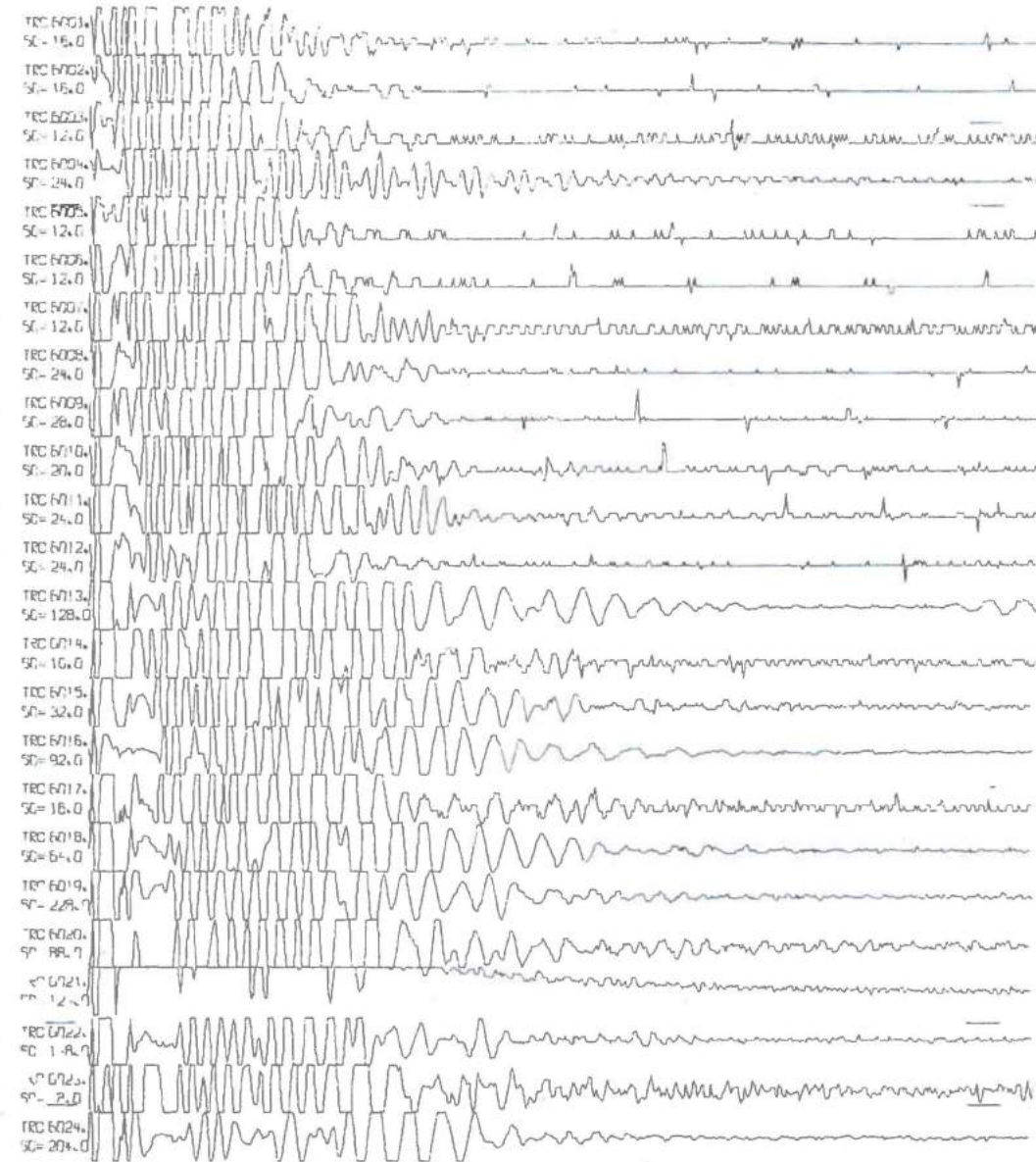
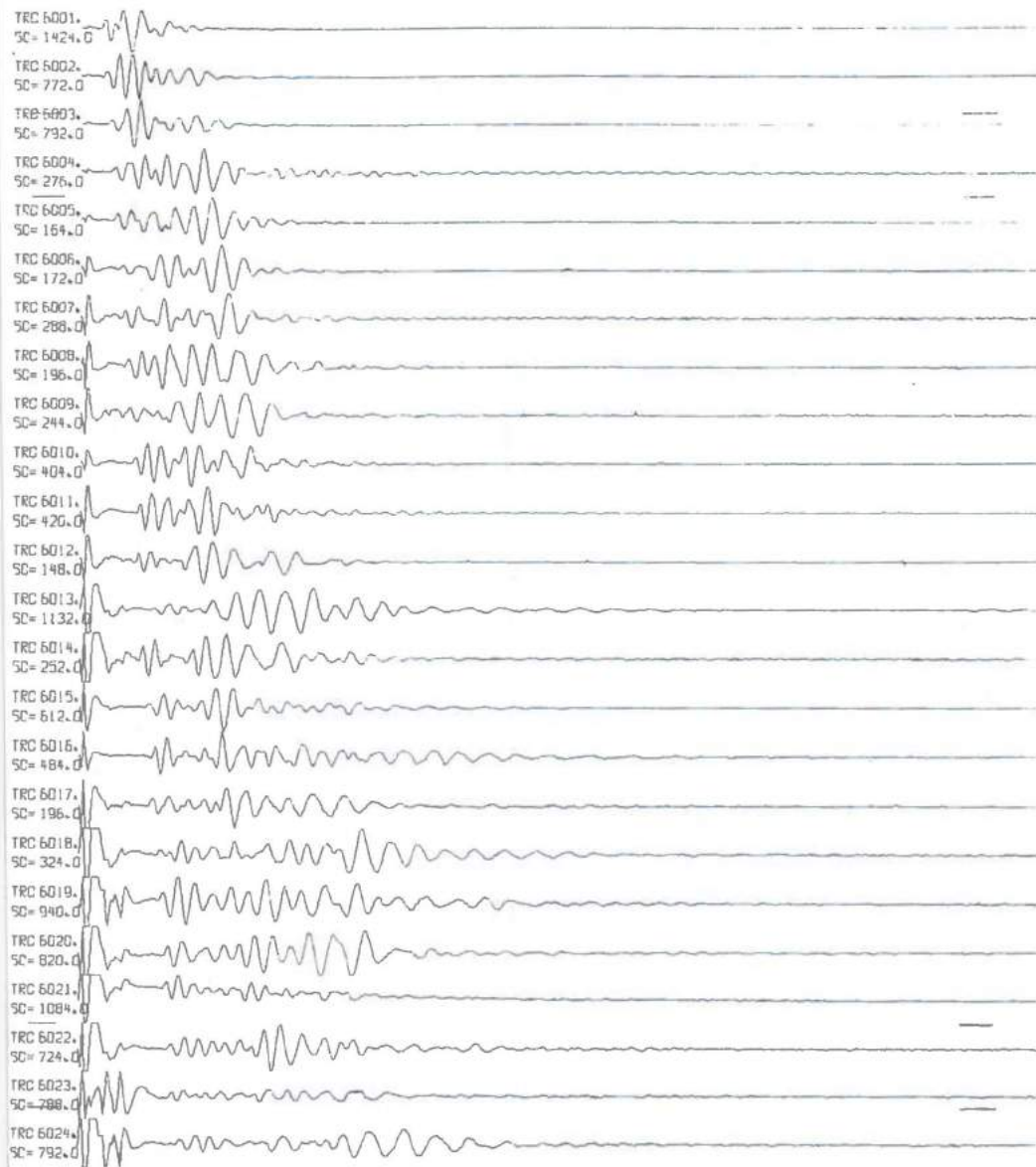


Fig. 5.5 Configuration No. I. Surface shot = 25 g, mine shot = 50 g.

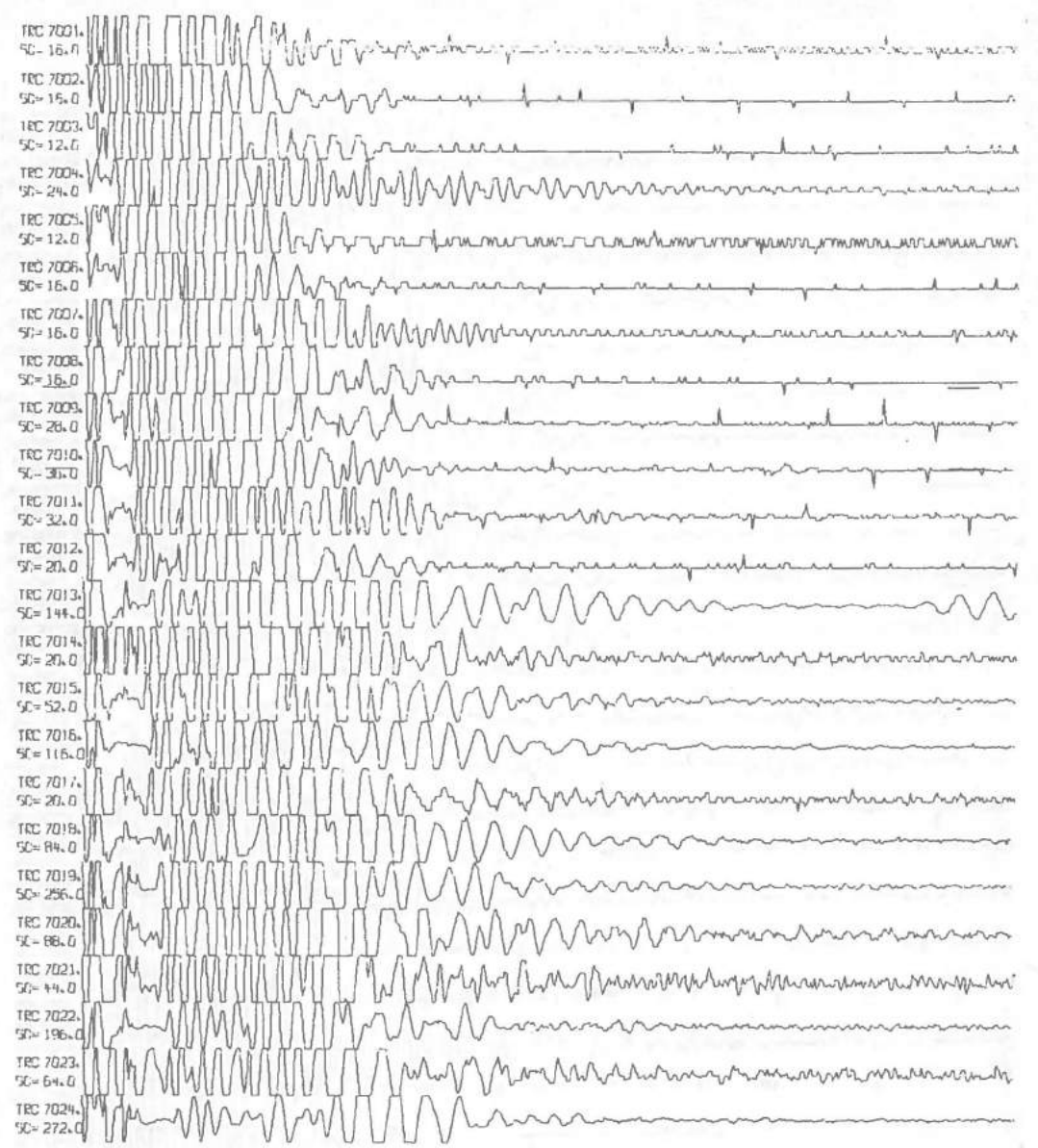
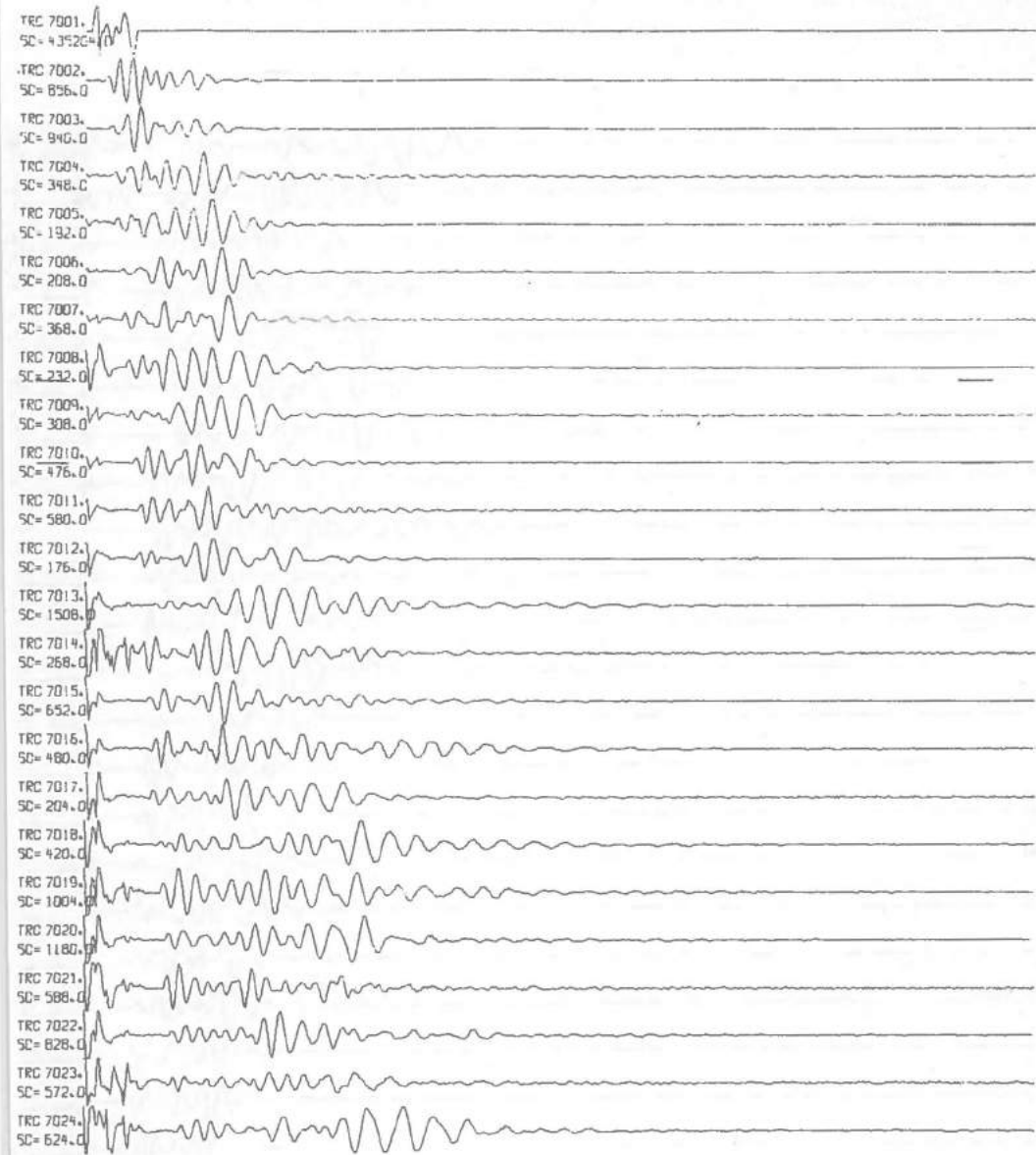


Fig. 5.6 Configuration No. I. Surface shot = 25 g, mine shot = 100 g.

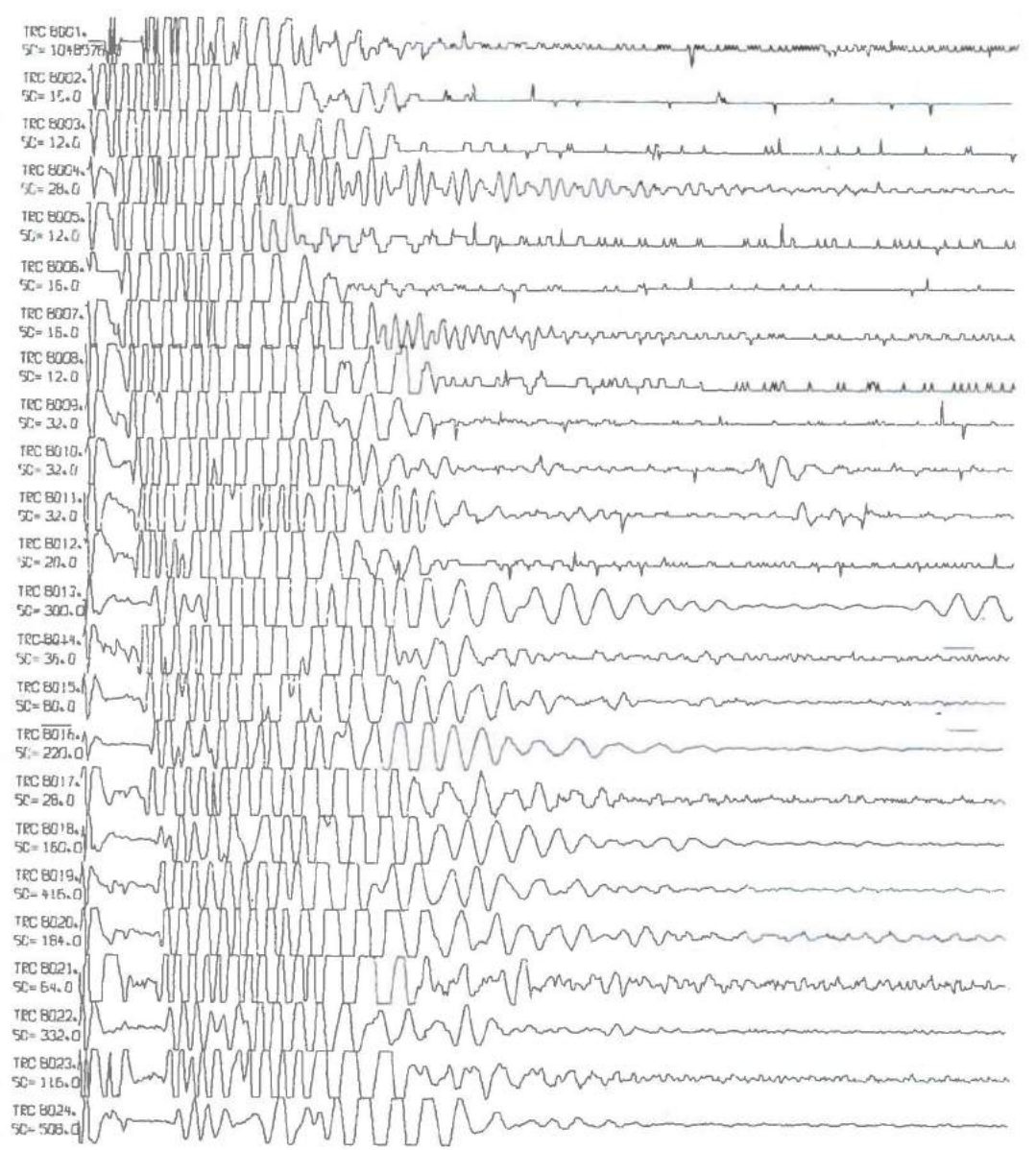
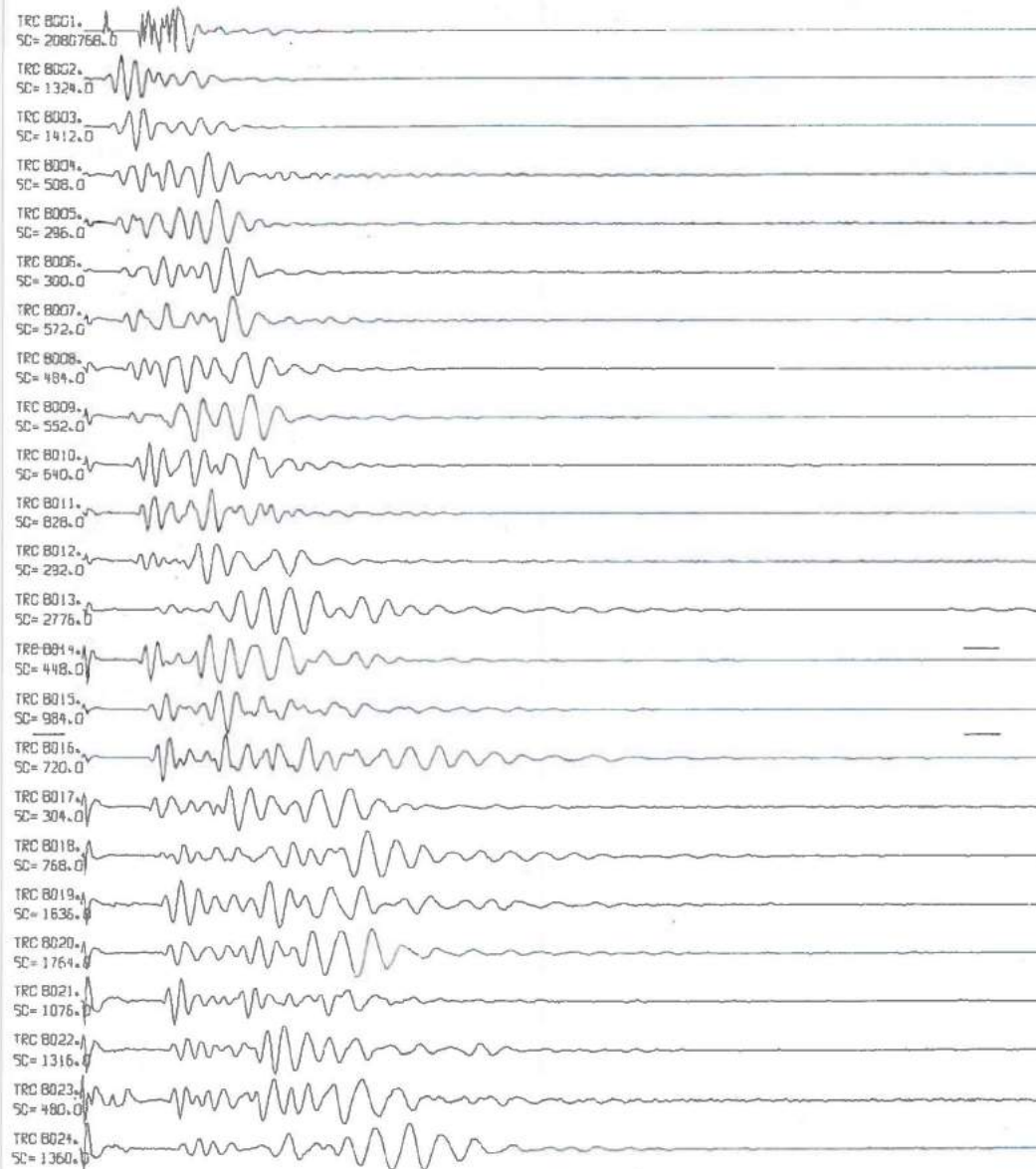


Fig. 5.7 Configuration No. I. Surface shot = 50 g, mine shot = 0.

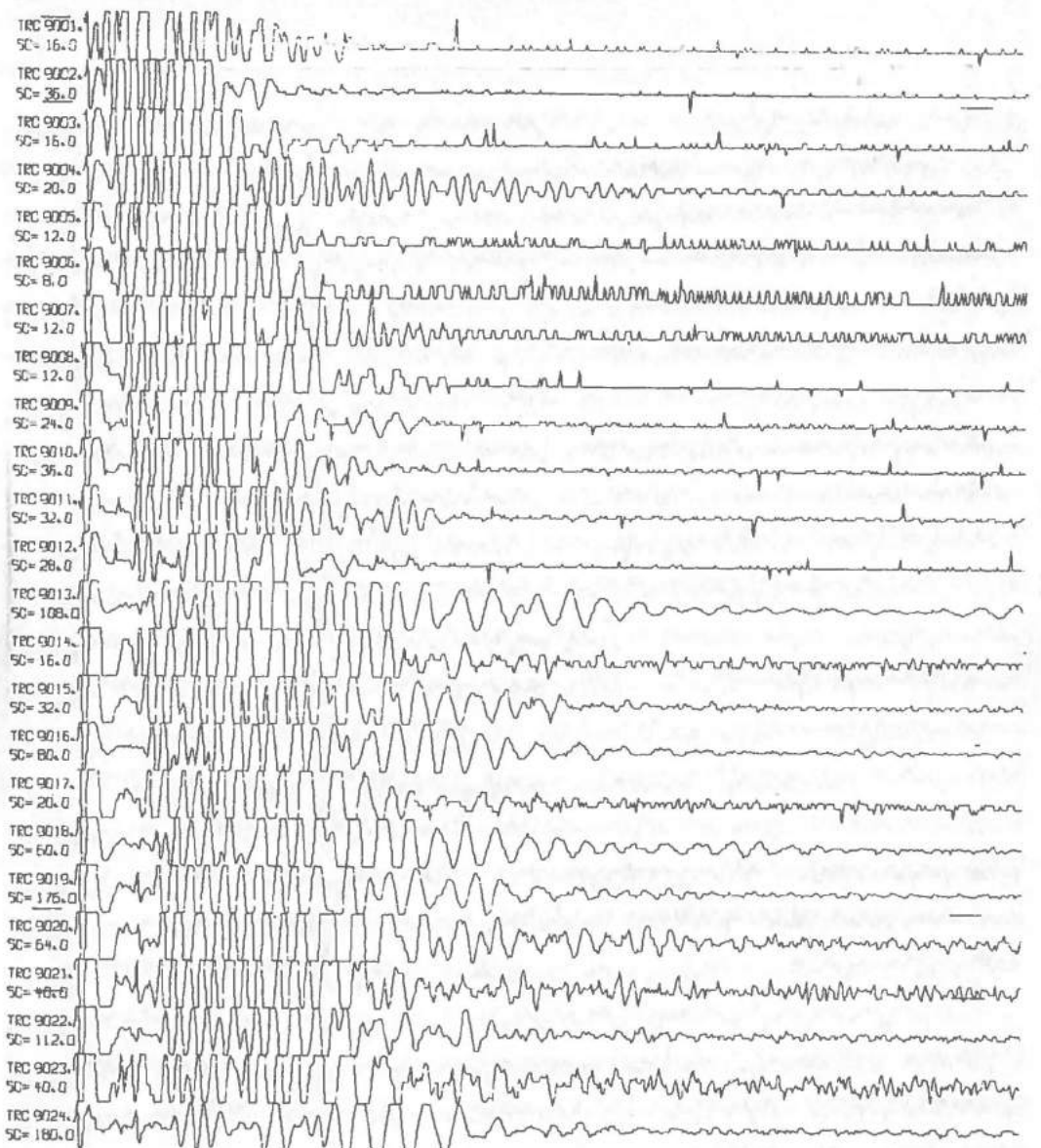
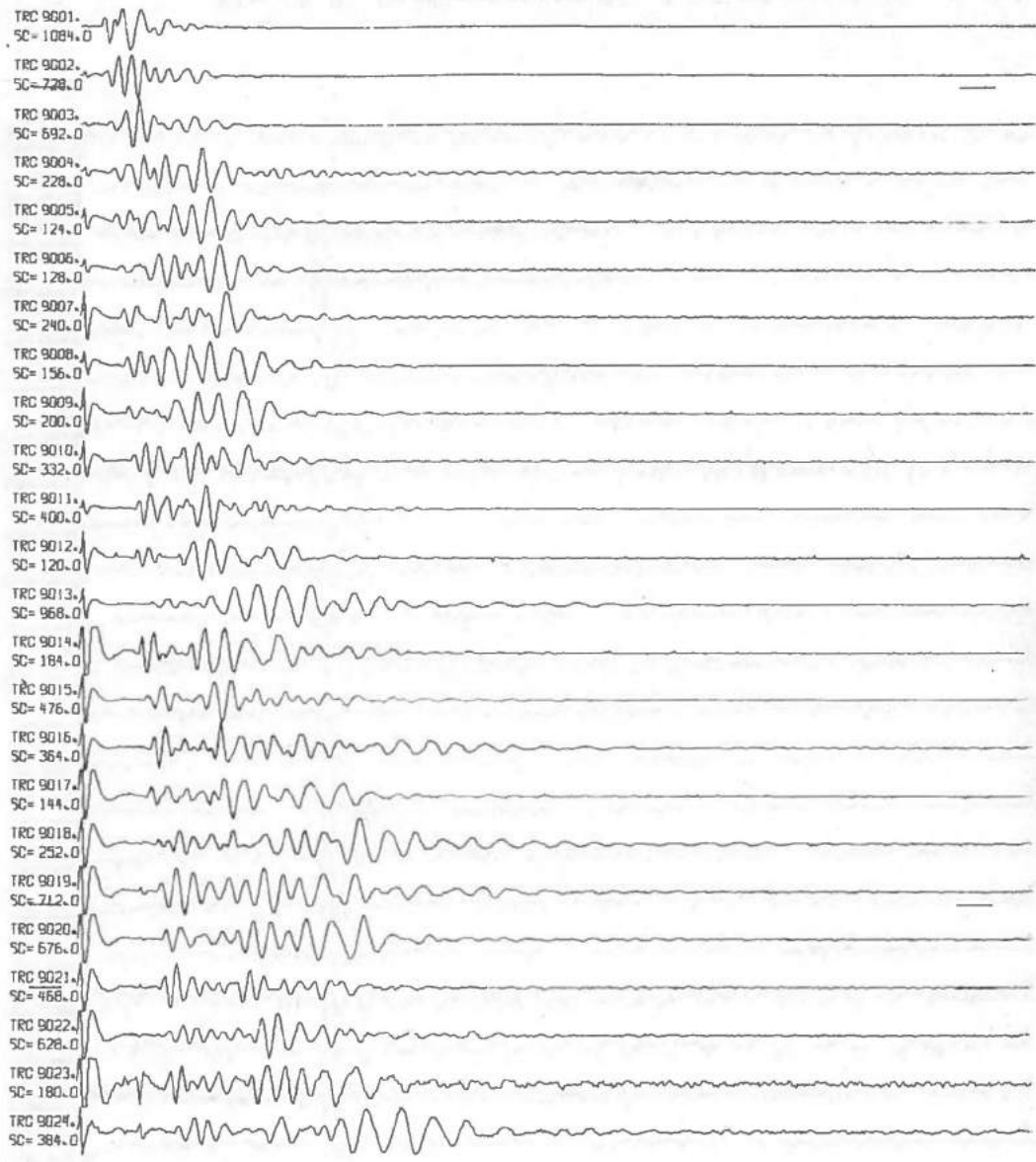


Fig. 5.8 Configuration No. I. Surface shot = 25 g, mine shot = 0.

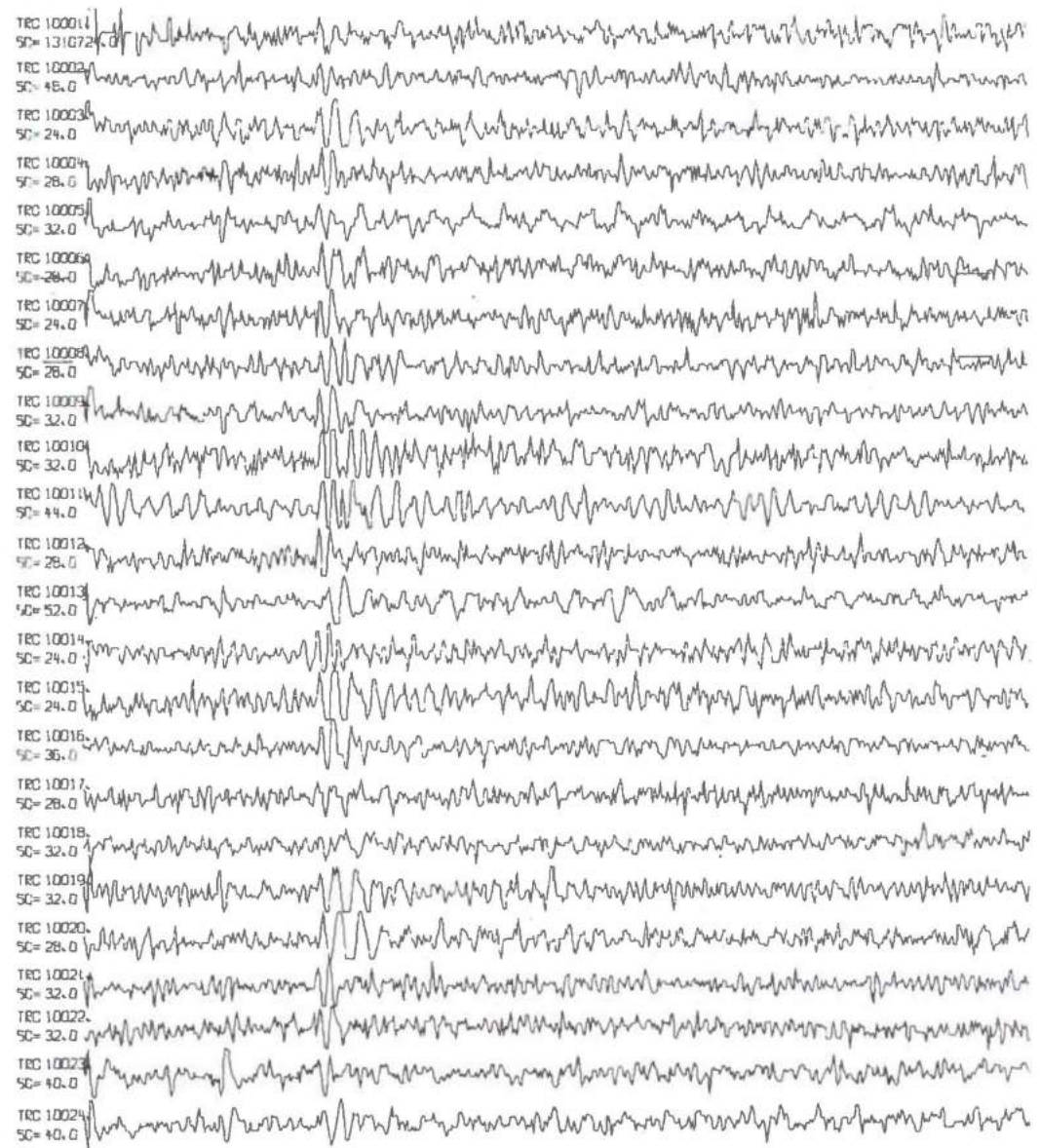
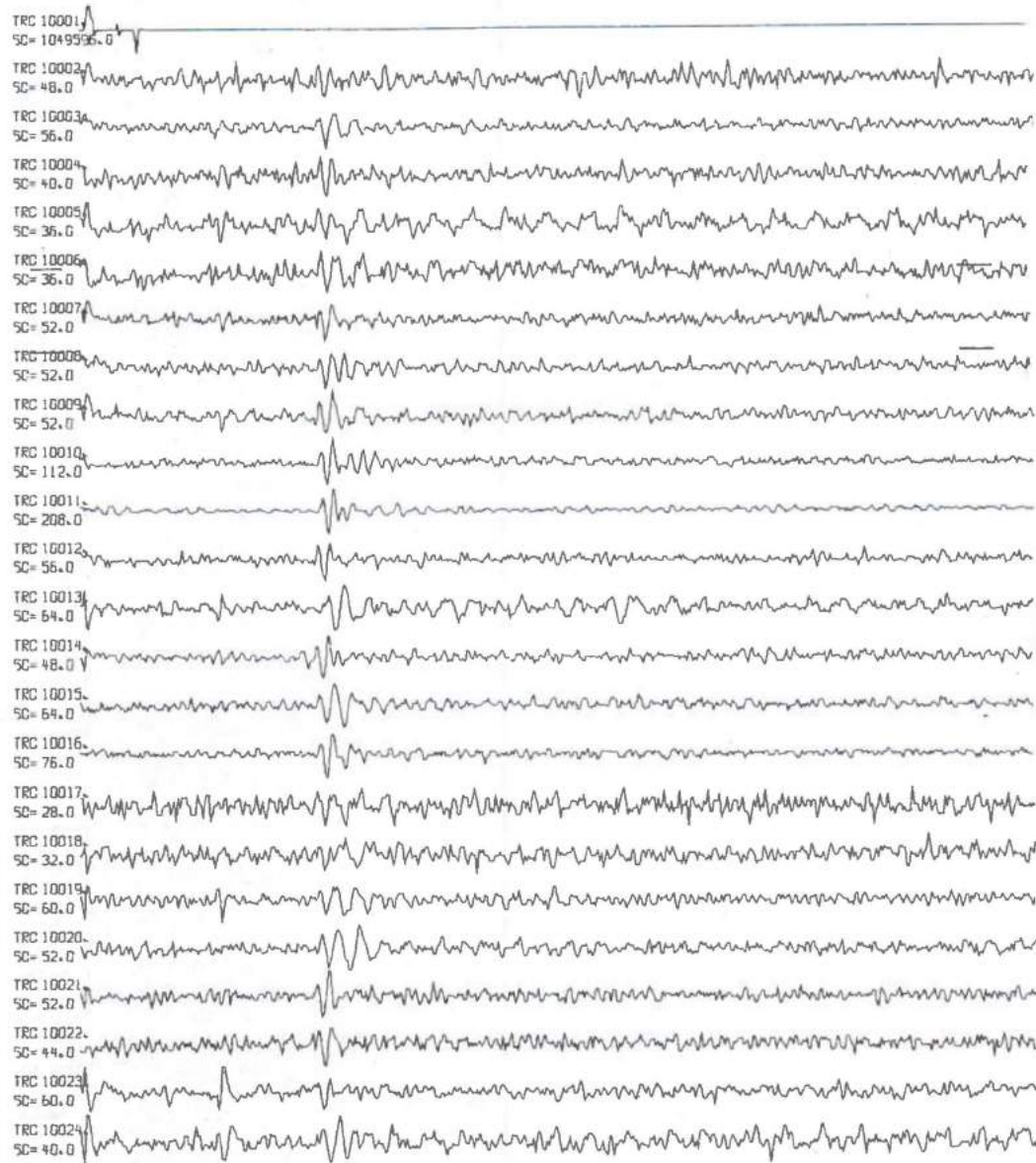


Fig. 5.9 Configuration No. I. Surface shot = 0, mine shot = 12.5.

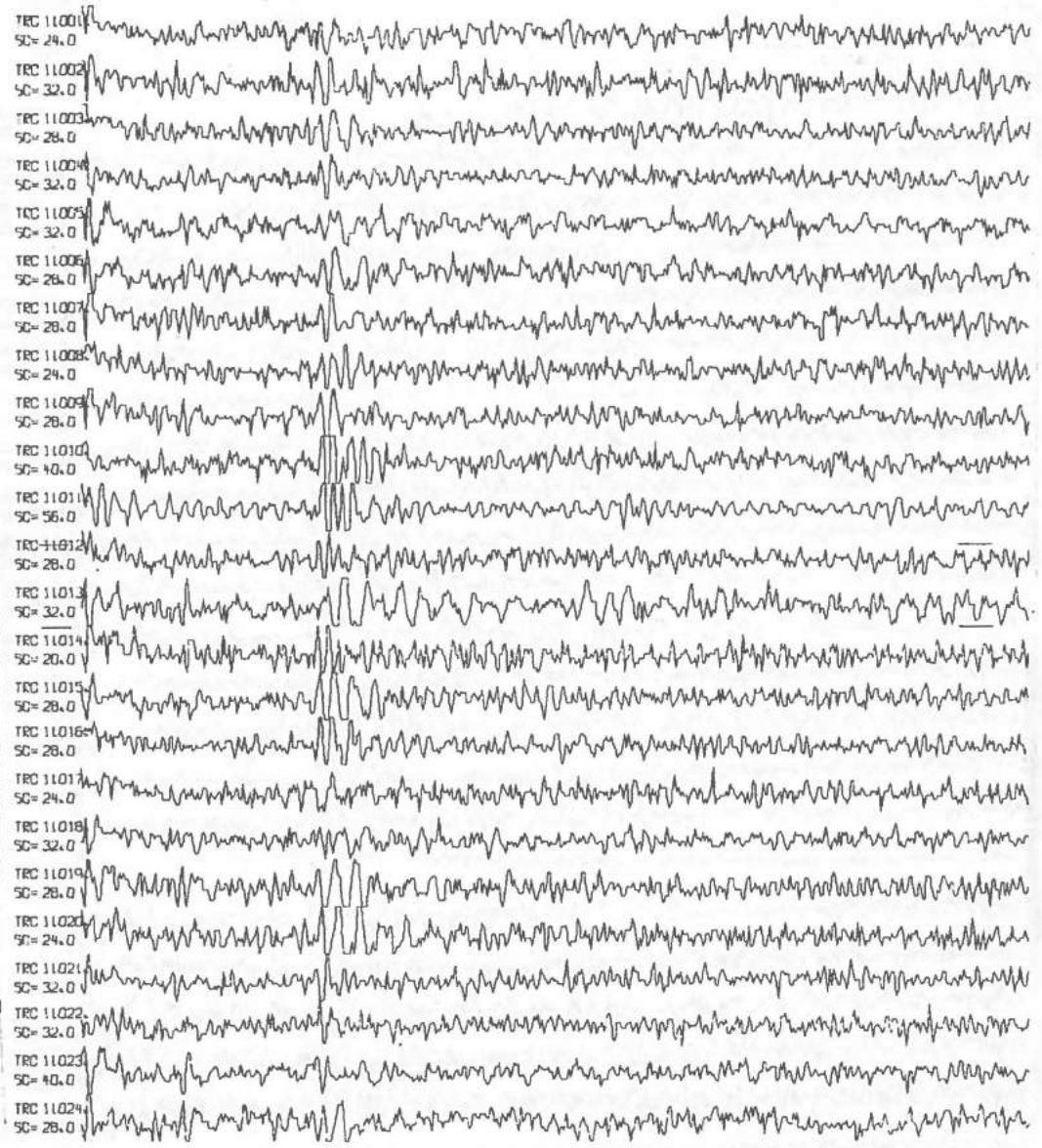
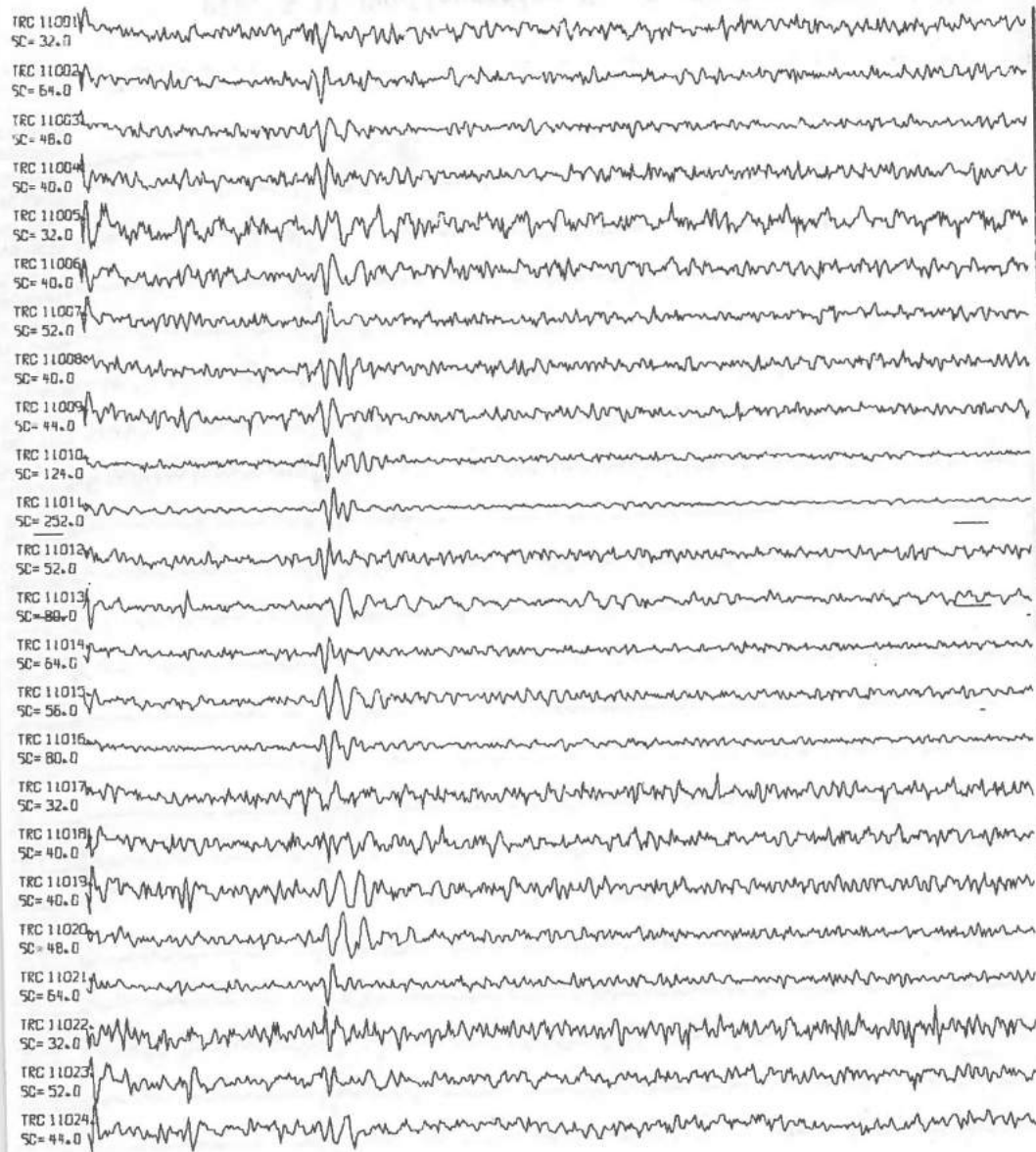


Fig. 5.10 Configuration No. I. Surface shot = 0, mine shot = 25 g.



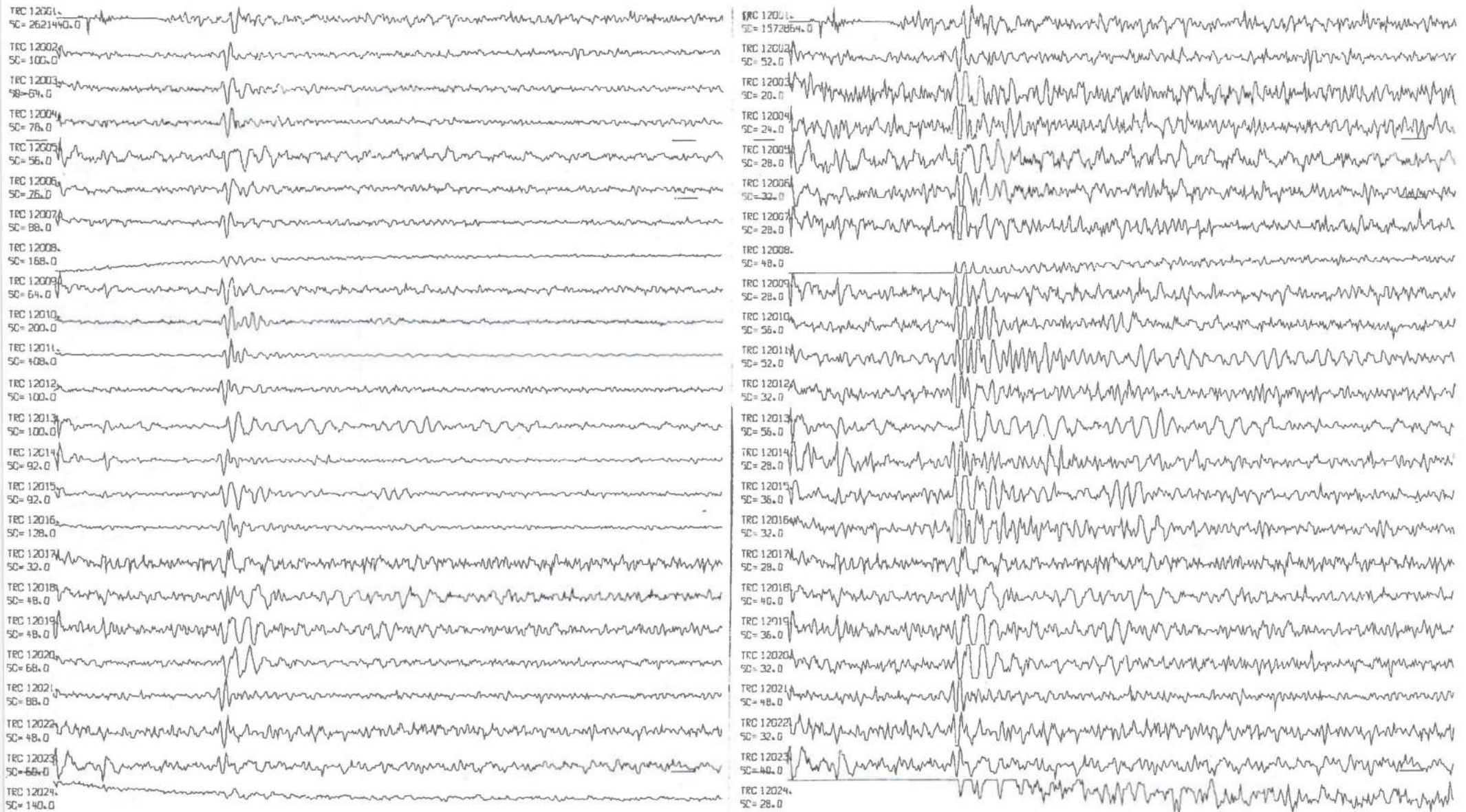


Fig. 5.11 Configuration No. I. Surface shot = 0, mine shot = 50 g.

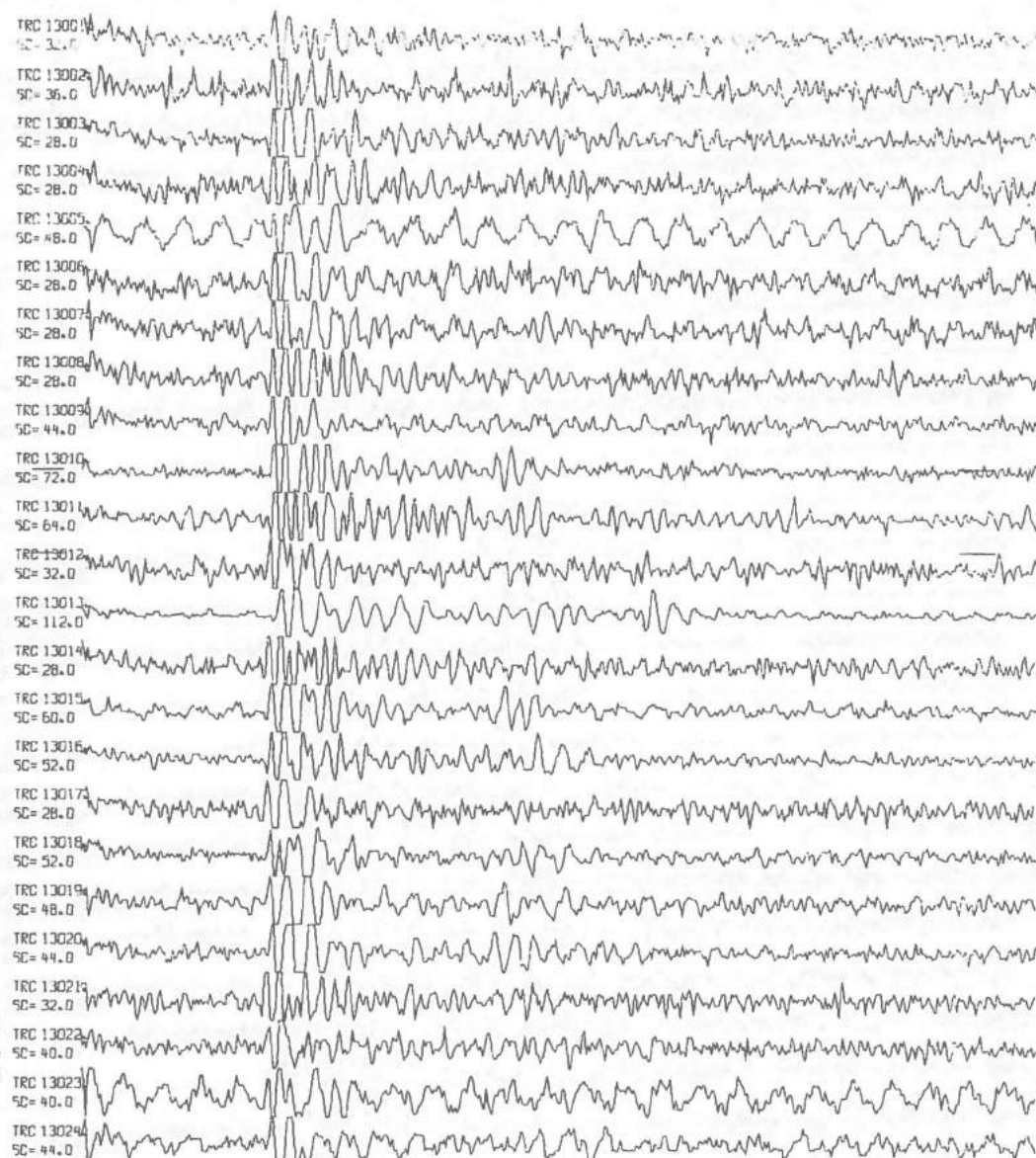
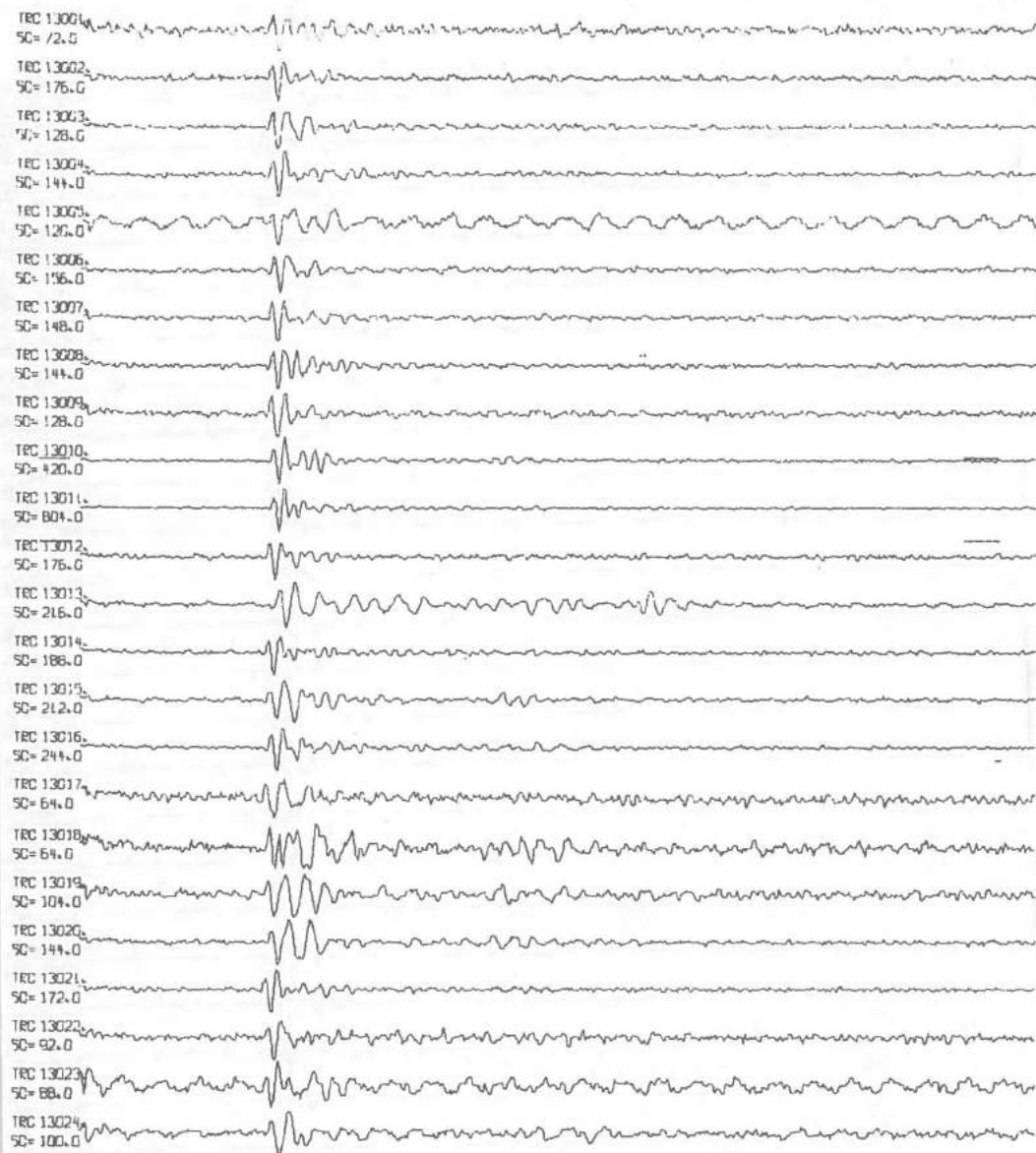


Fig. 5.12 Configuration No. I. Surface shot = 0, mine shot = 100 g.

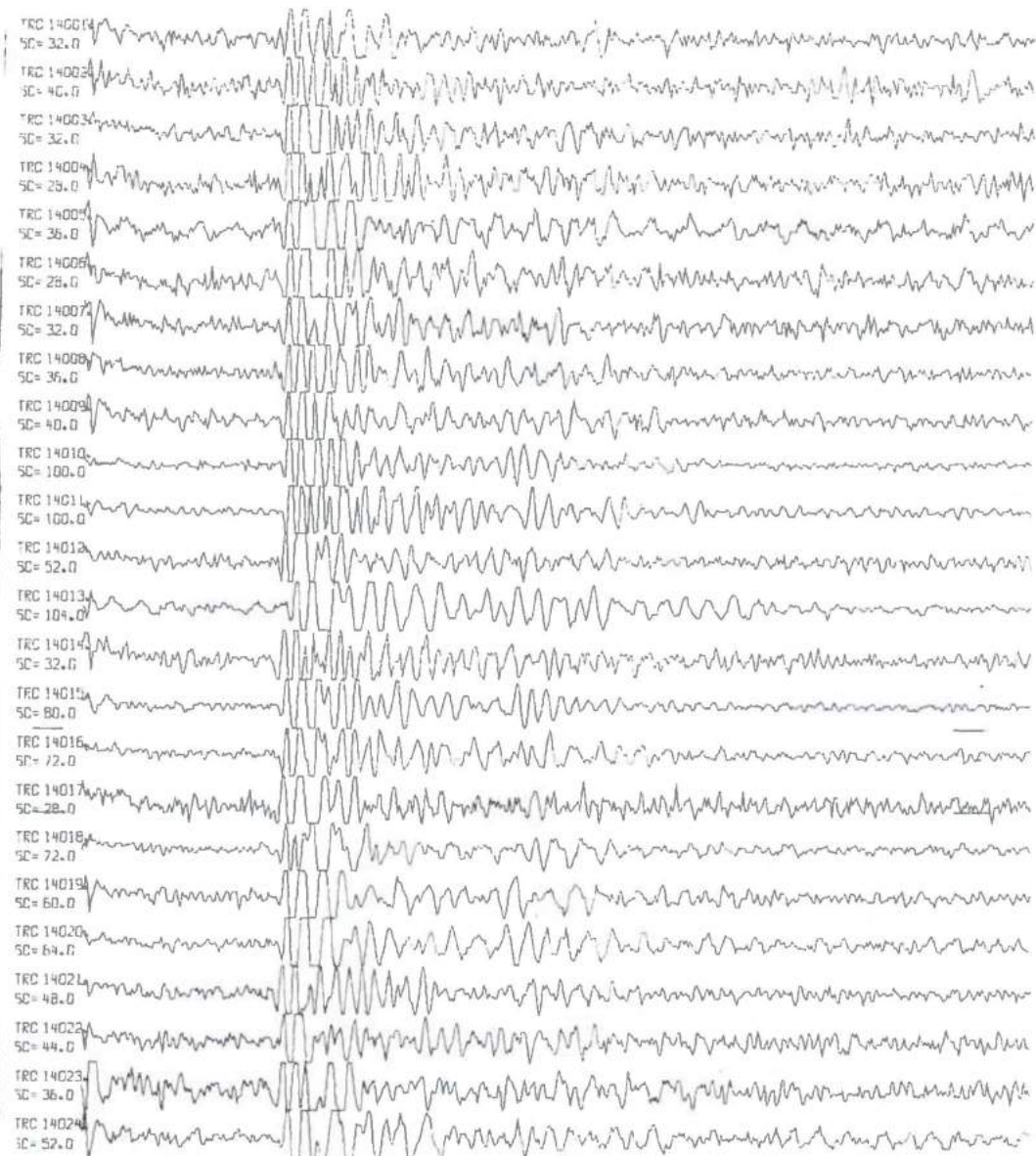
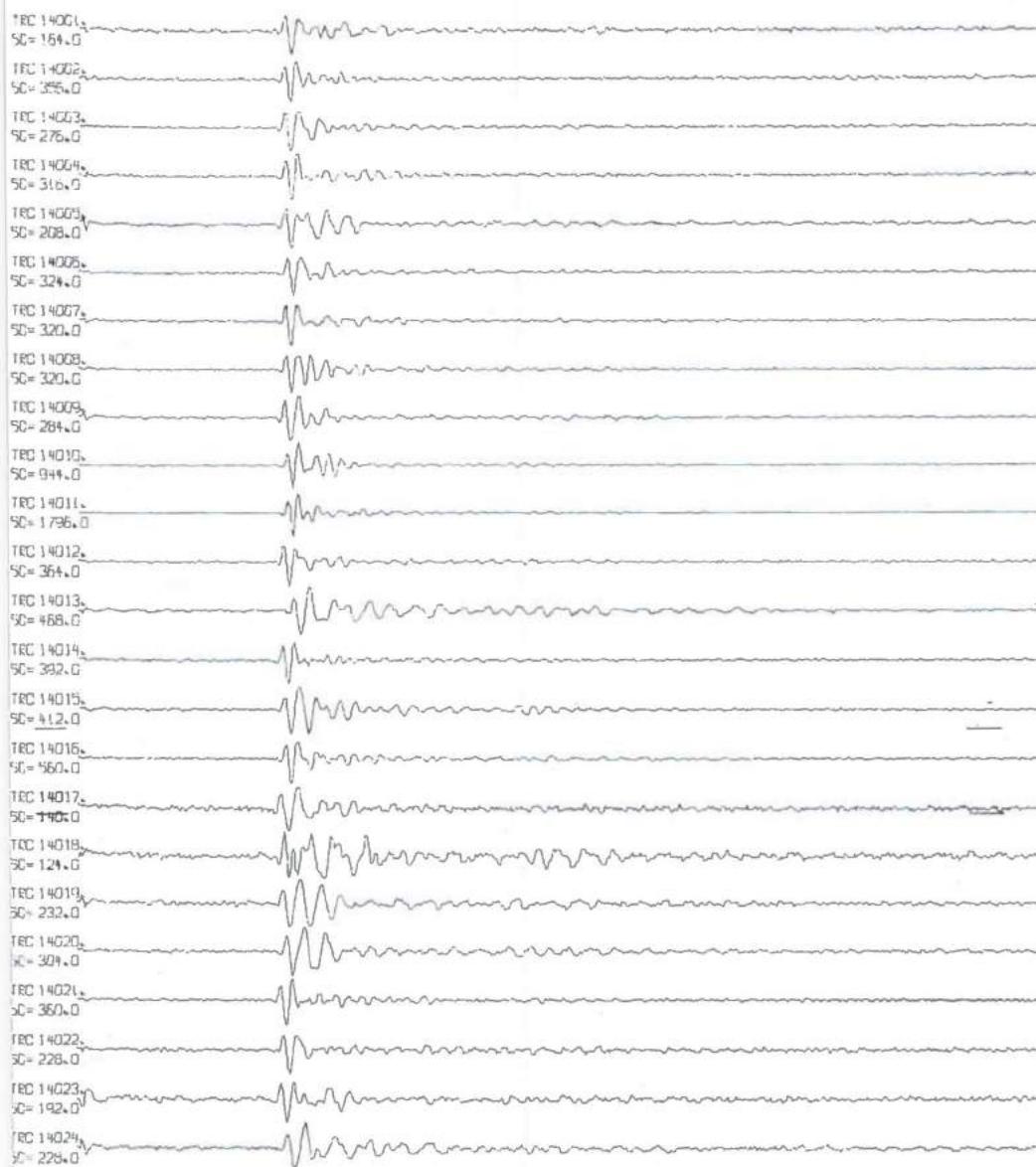


Fig. 5.13 Configuration No. I. Surface shot = 0, mine shot = 200 g.

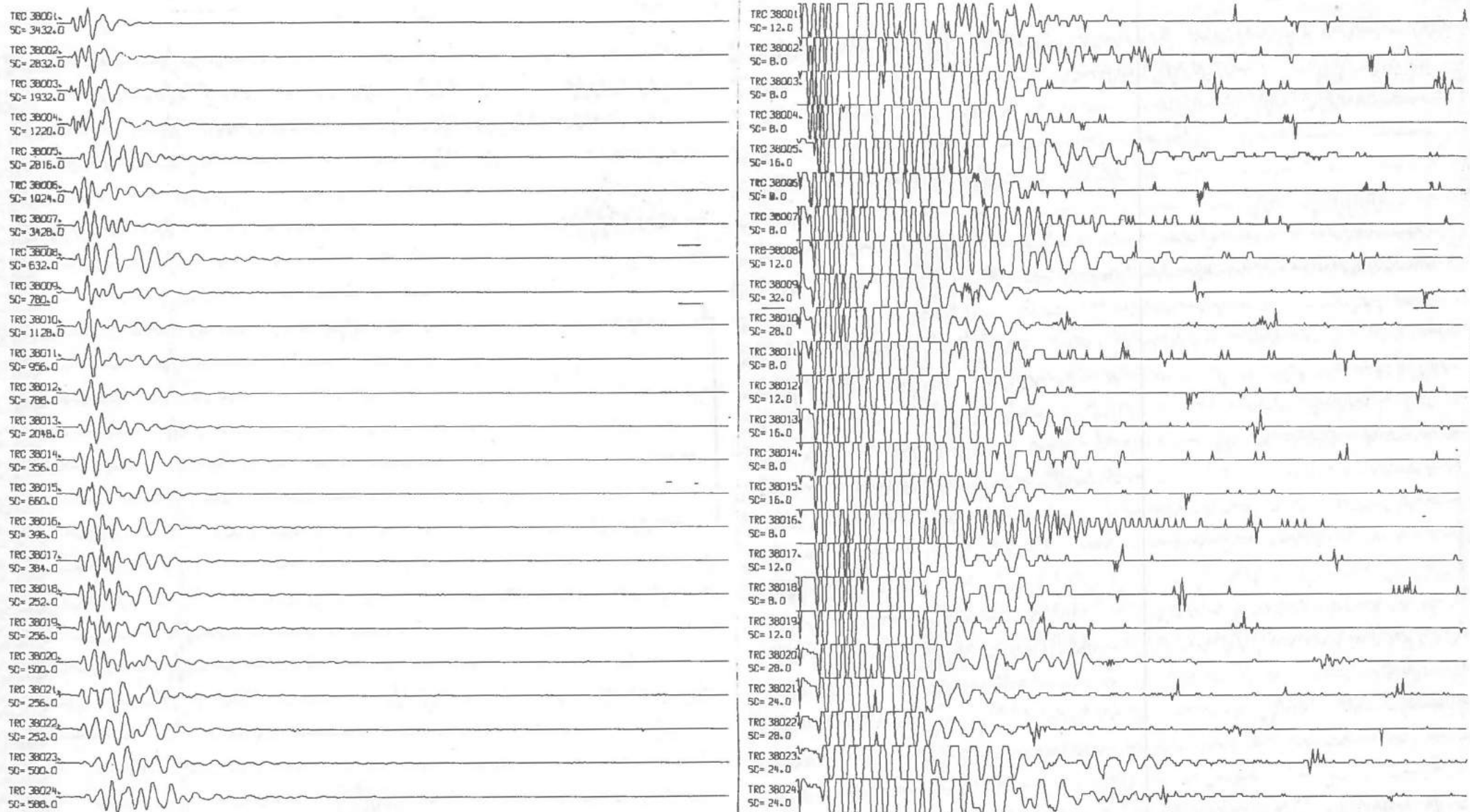


Fig. 5.14 Configuration No. II. Surface shot = 50 g, mine shot = 0.

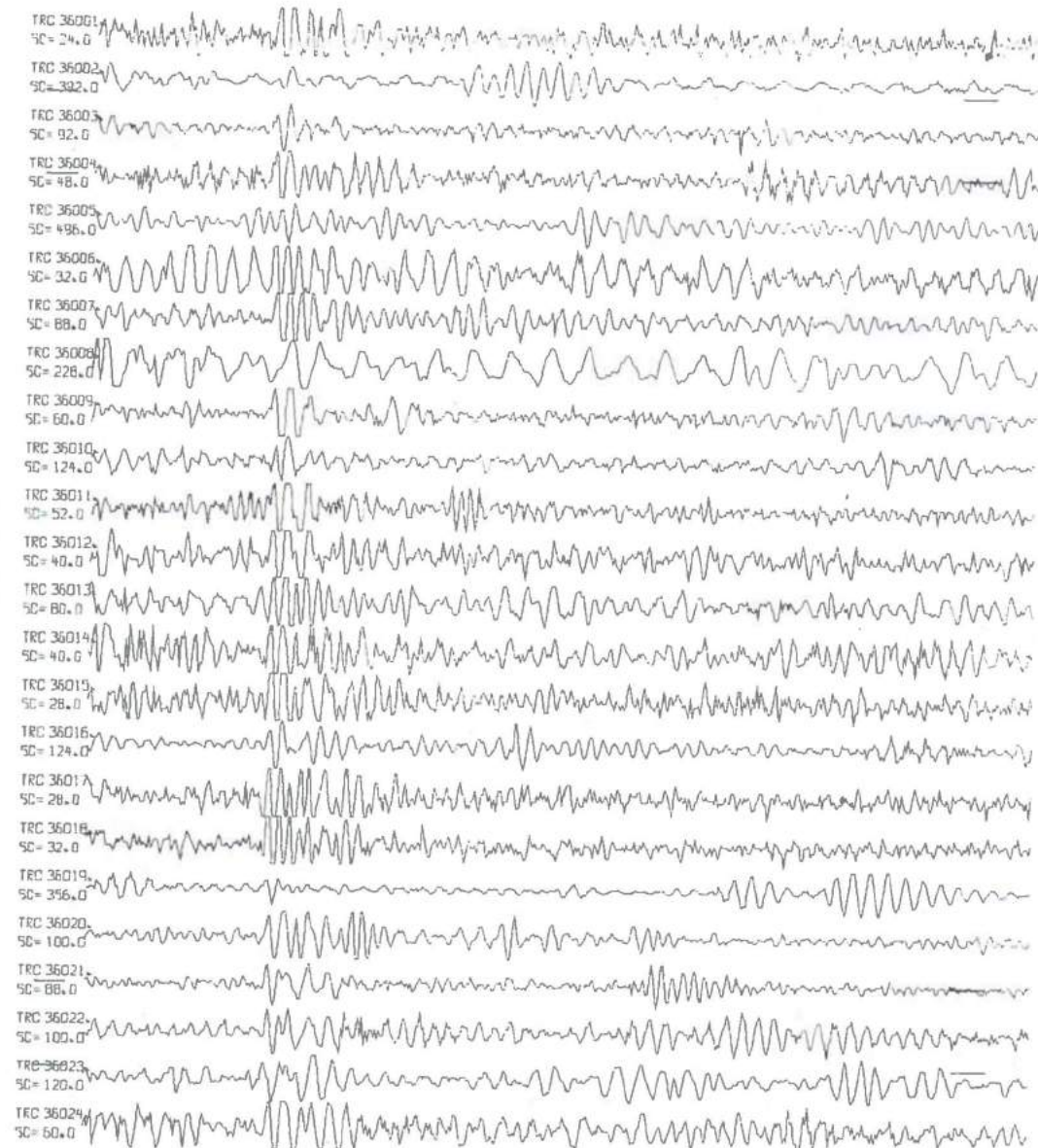
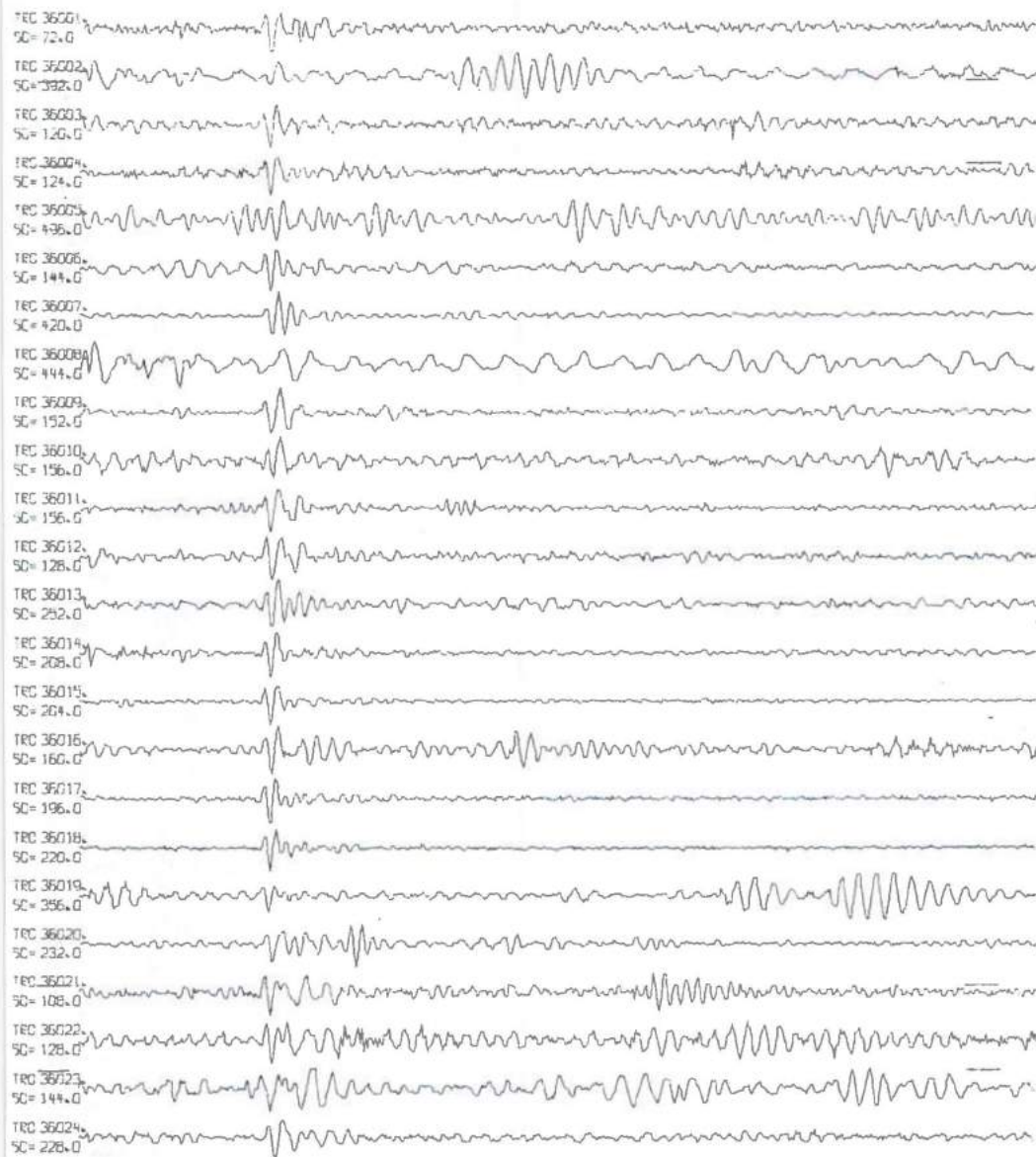


Fig. 5.15 Configuration No. II. Surface shot = 0, mine shot = 100 g.

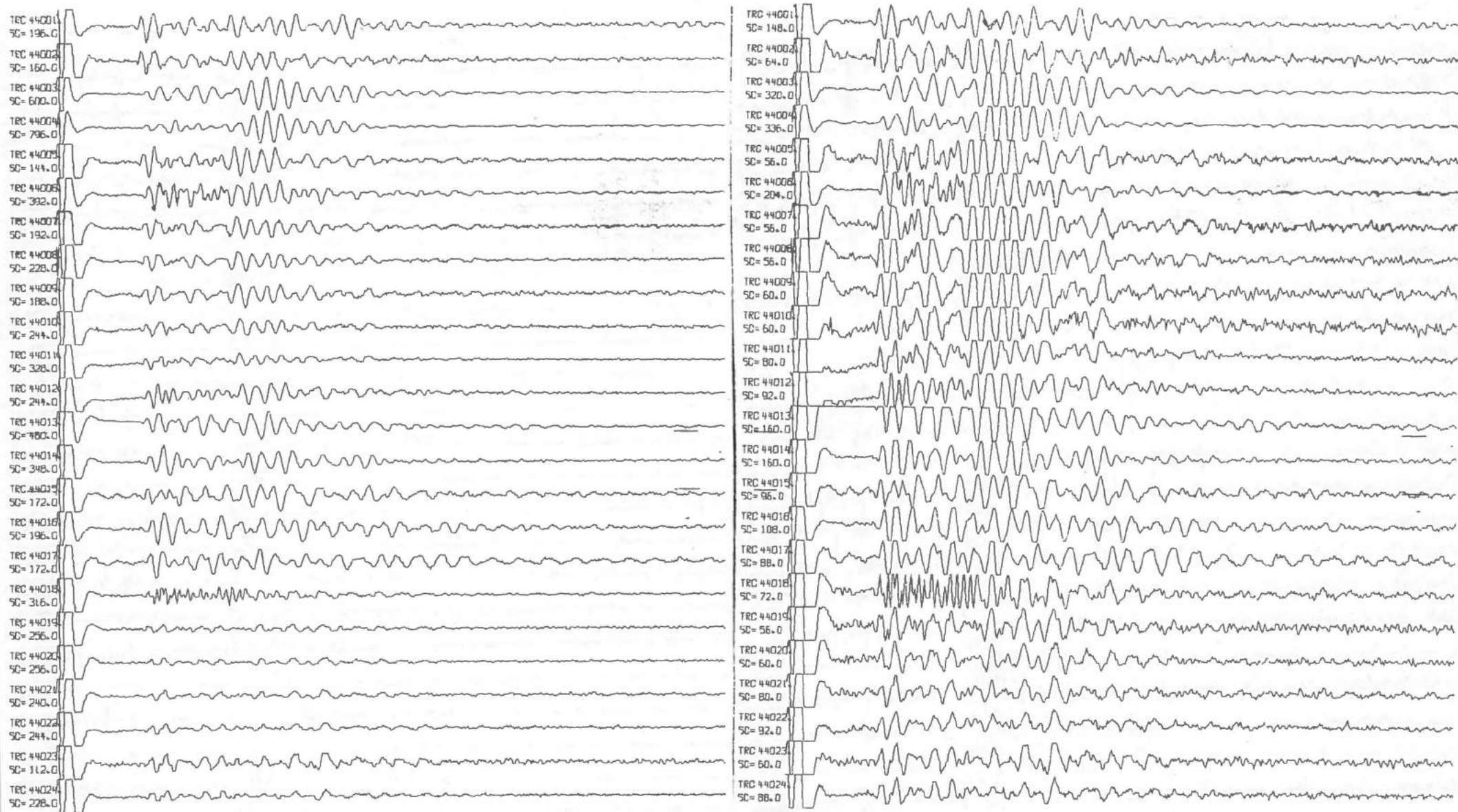


Fig. 5.16 Configuration No. III. Surface shot = 50 g, mine shot = 0.

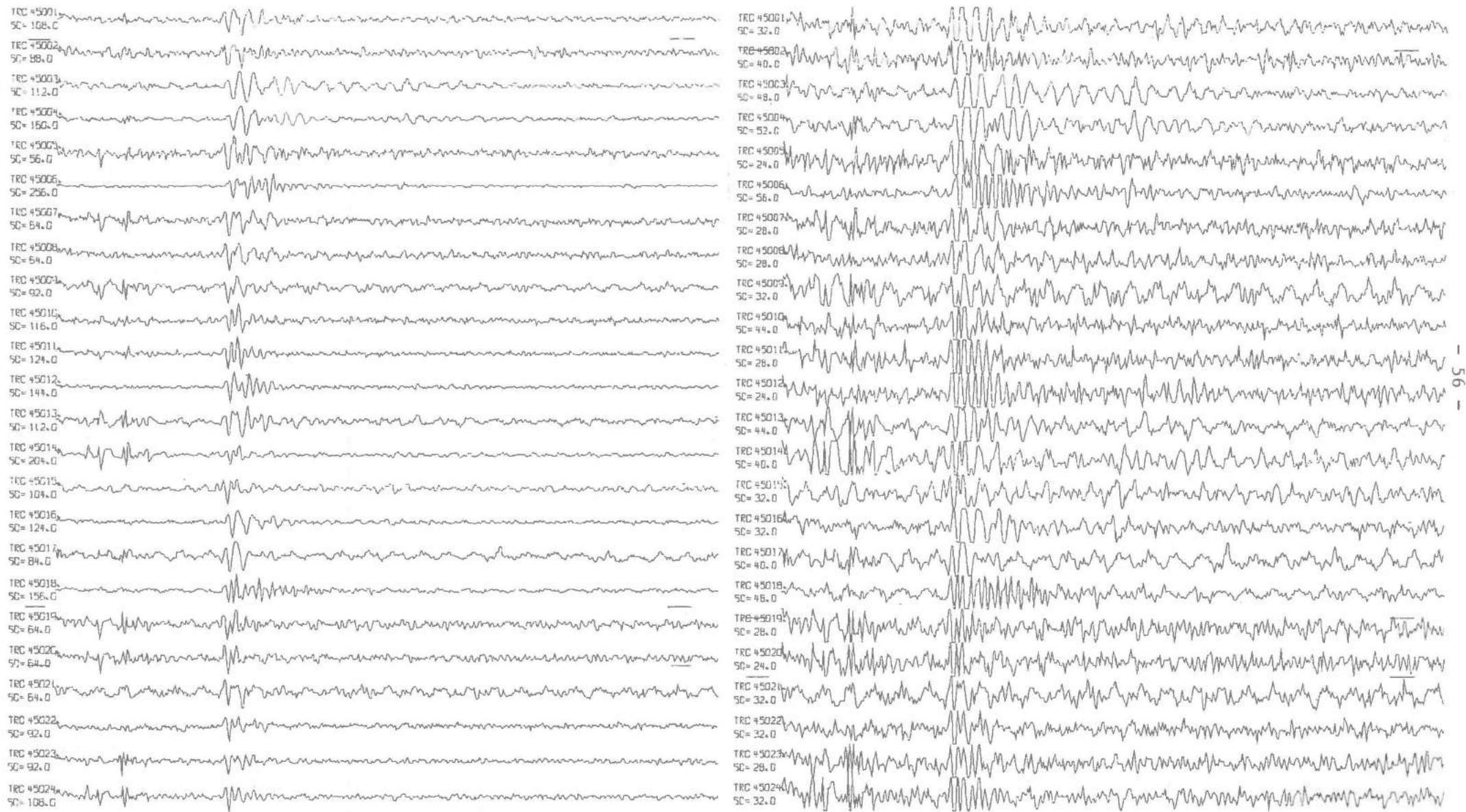


Fig. 5.17 Configuration No. III. Surface shot = 0, mine shot = 100 g.

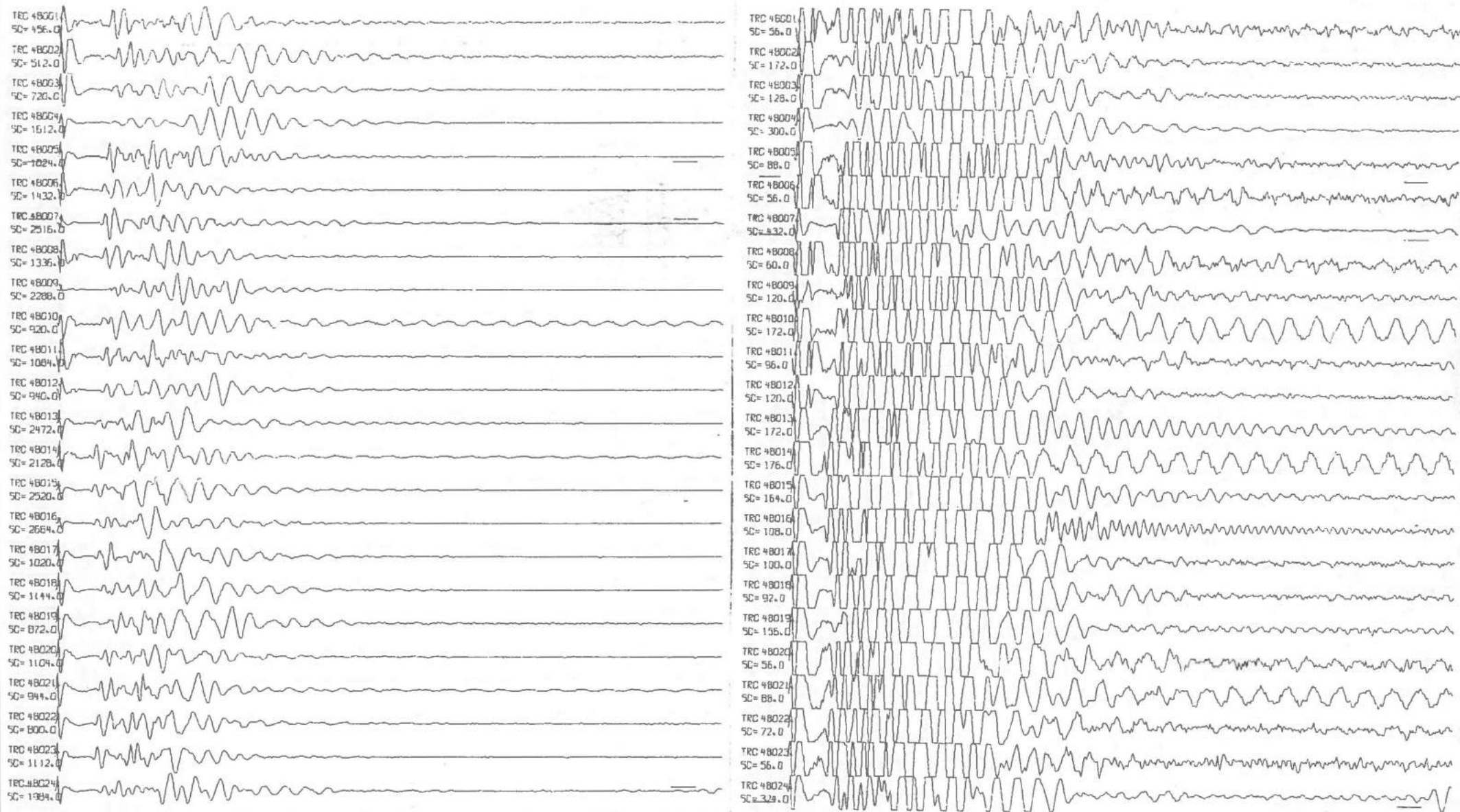


Fig. 5.18 Configuration No. IV. Surface shot = 50 g, mine shot = 0. Array A = trace 1-12, array B = trace 13-24.



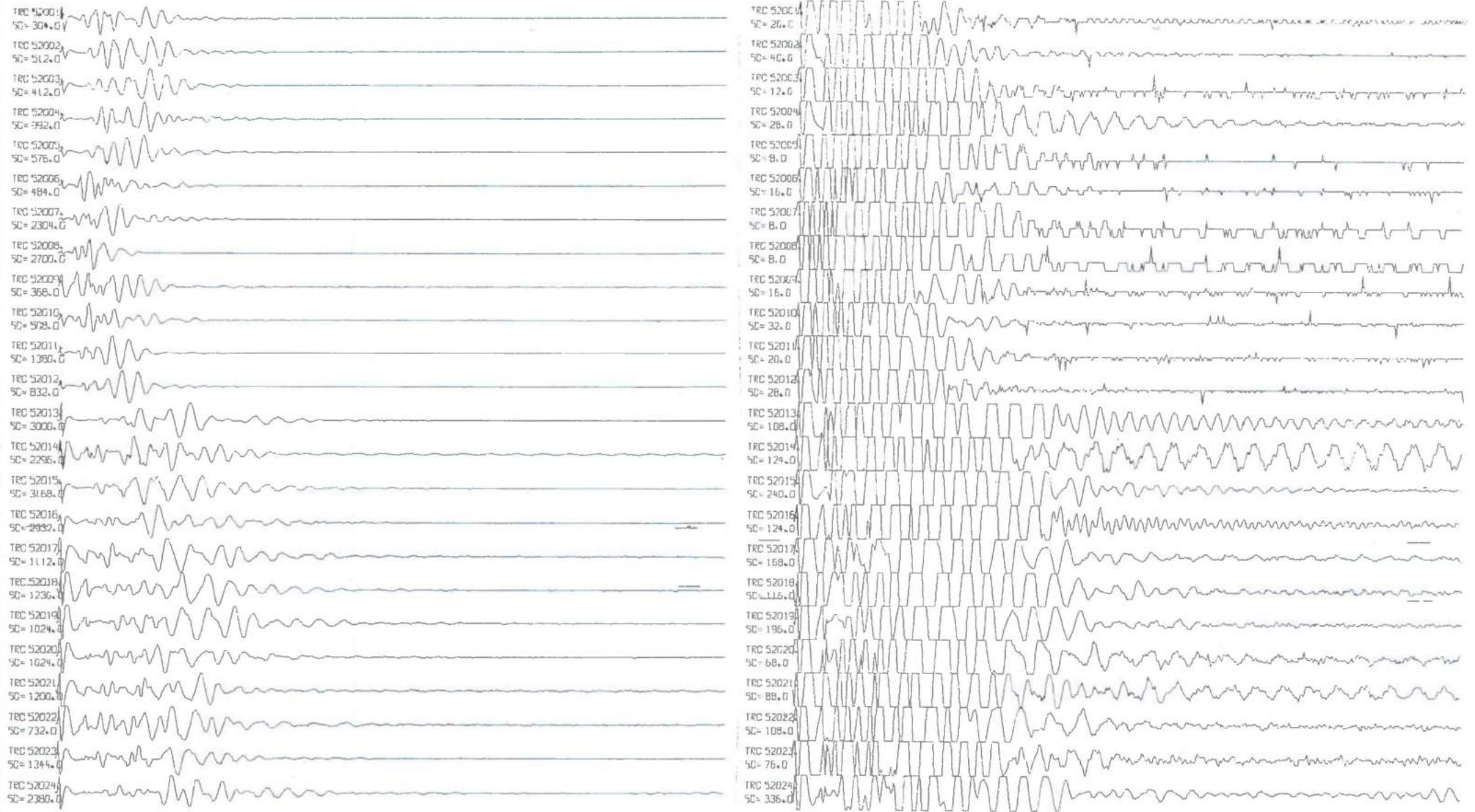


Fig. 5.18 (cont.) Array C = trace 1-12, array B = trace 13-24.

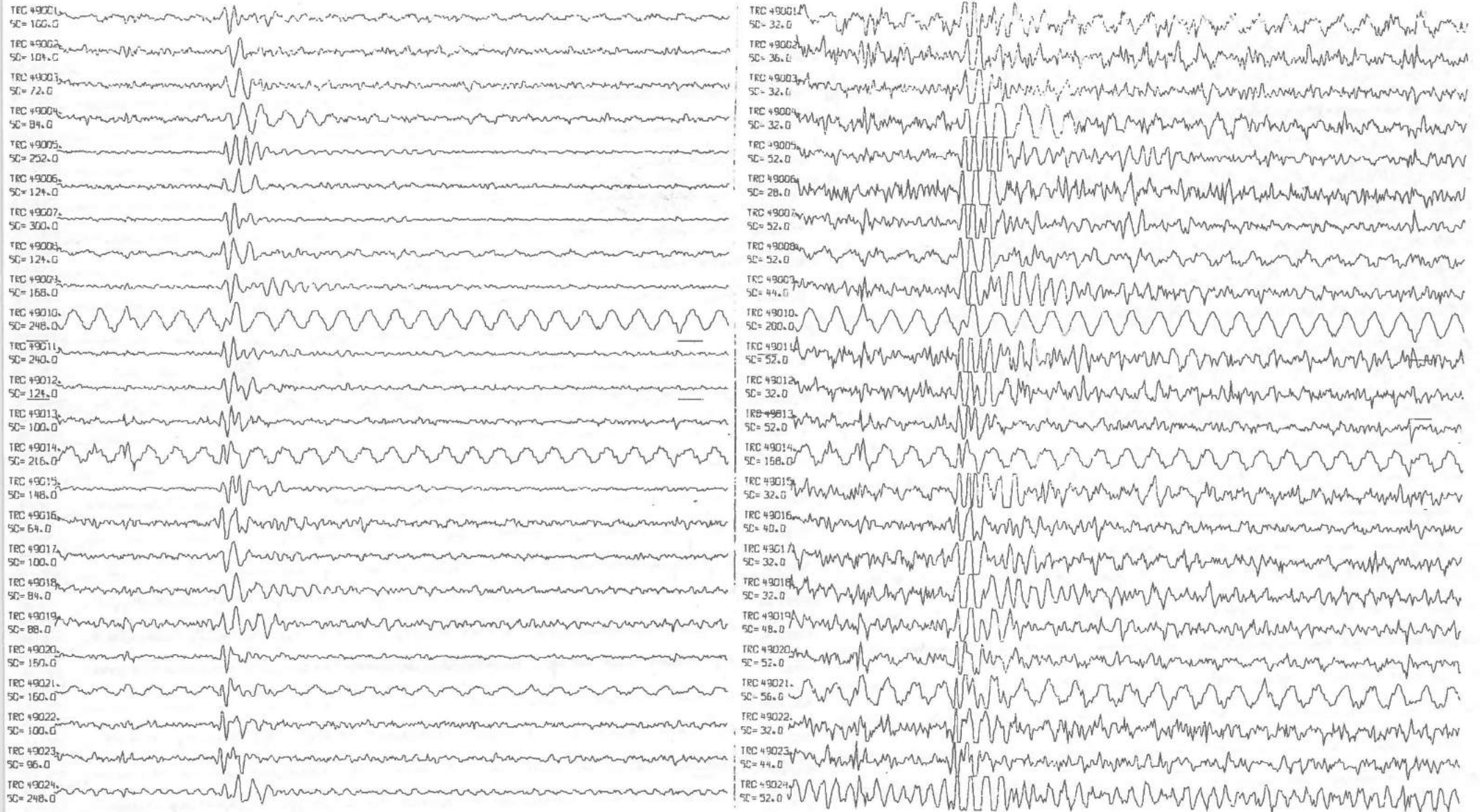


Fig. 5.19 Configuration No. IV. Surface shot = 0, mine shot = 100 g. Array A = trace 1-12, array B = trace 13-24.

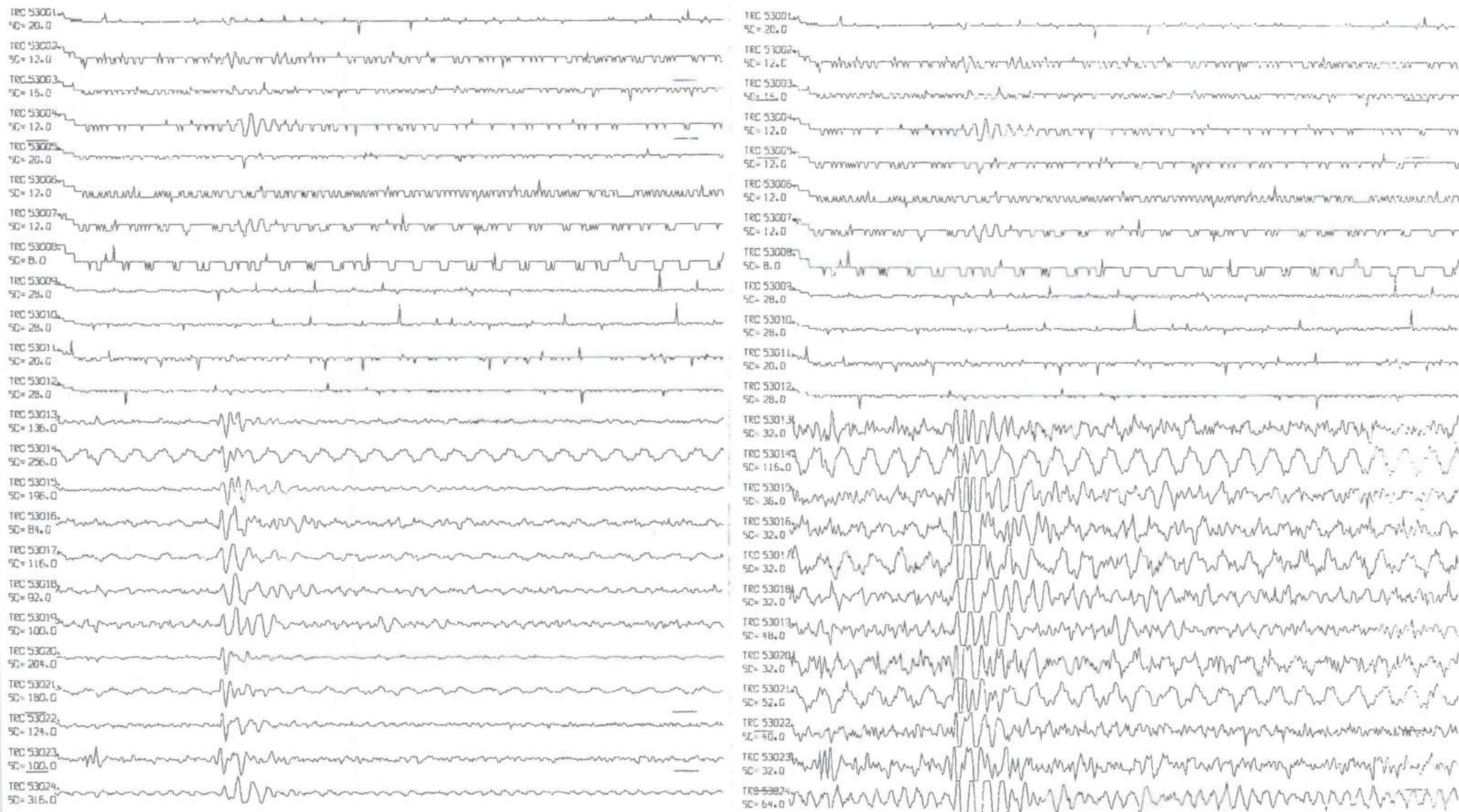


Fig. 5.19 (cont.) Array C = trace 1-12, array B = trace 13-24.

5.2 Analysis of static corrections

As mentioned, the 1978 station data had very little variation with respect to noise statistics, and thereby with respect to the choice of noise configurations, since one of the major objectives of the noise configurations is just the ability of noise suppression. However, the data could still be used for other purposes, and one very important effect to be studied was the so-called 'static', which is the time-varying being introduced due to the very inhomogeneous conditions due to the surface.

Fig. 5.21 shows a recording of a shot that shows a frequency spectrum. We observe that the pulses are most or less uniform in amplitude to each other; more, i.e., the very great shift between stations 11 and 12. Obviously, this effect was not corrected for in the data. He stretched (stretched) together the processing of the data.

The question is now how to perform this correction. When the noise ratio is good for this station, the noise ratio is good for the other stations. However, if SNR is rather poor, as should be expected for the other stations, a correlation procedure will hardly give the proper correction.

The noise reduction which has been performed in this recording is a unique possibility to check the performance of station and to identify need for finding the 'static correction'.

Fig. 5.22 shows a rather large variation from station to station, especially the amount of noise around the very large stations. This is due to the very low station-to-station ratio in the receiver. The corresponding 'static' for the different stations are shown, compared relative to a linear arrival time function shown in Fig. 5.23. It turns out that the low ratio of static correction shows a very good correlation, which means that static corrections of different stations using the surface can be used for finding an effective time correction.

**Fig. 5.20 Seismic trace recorded at 10 m distance from the shot (50 g charge), illustrating the dynamic range of the recordings. The right trace is simply a blow-up of the later part of the left trace. Total trace length (left) = 500 ms.**

## 5.2 Analysis of 'static corrections'

As mentioned, the 1978 Løkken data had very little value with respect to noise studies, and thereby with respect to the choice of shot/receiver configurations, since one of the major optimizing criteria for these configurations is just the ability of noise suppression. However, the data could well be used for other purposes, and one very important effect to be studied was the so-called 'statics', which is the phase shifts being introduced due to the very inhomogeneous conditions close to the surface.

Fig. 5.21 shows a recording of a mine shot along a geophone line at the surface. We observe that the pulses are more or less shifted relative to each other; note, f.ex., the very great time shift between channels 12 and 13. Obviously, this effect must be corrected for if traces are to be stacked (summed) together during the processing of the data.

The question is now how to perform this correction. When the signal-to-noise ratio is good (as for this strong pulse from the mine shot), the time correction may obviously be found by a simple correlation procedure. However, if SNR is rather poor, as should be expected for real reflections, a correlation procedure will hardly give the proper corrections.

The mine shooting which has been performed in this experiment gives us a unique possibility to check the performance of another method frequently used for finding the 'static correction'.

Fig. 5.22 shows static time corrections measured from the records in Fig. 5.21. We observe a rather large variation from sensor to sensor. Especially the sensors mounted on loose ground show very large statics, which is due to the very low wave velocity close to the receiver site. Fig. 5.23 shows corresponding 'statics' for the 'direct' P arrival from a surface shot, computed relative to a linear arrival time function shown in Fig. 5.24. It turns out that the two sets of static corrections show a very good correlation, which means that static time measurements of direct P-waves from the surface shot can be used for lining up reflections from below.

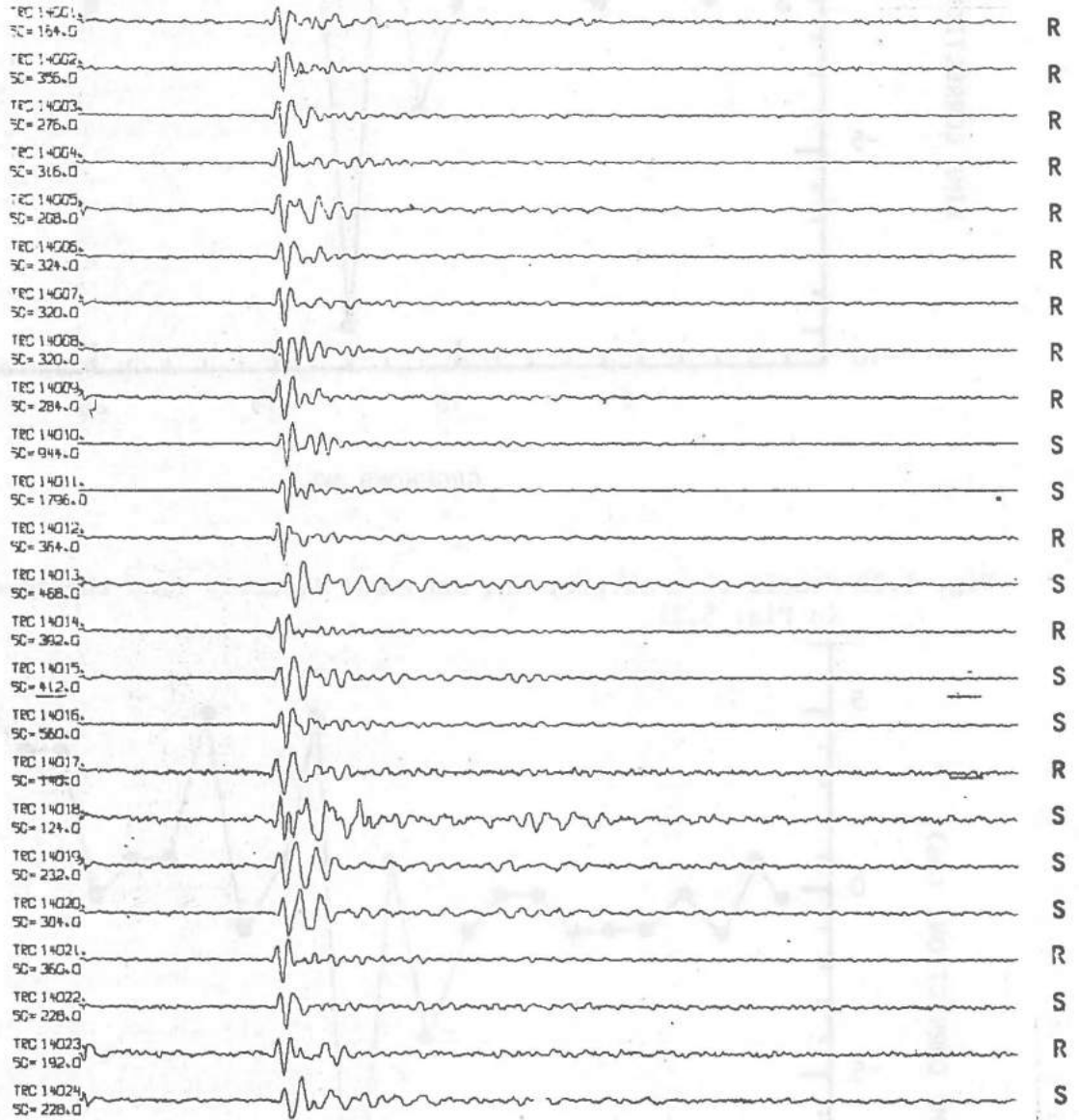


Fig. 5.21 Recordings of a mine shot (200 g charge at 720 m depth) along a geophone line at the surface. (Configuration No. I, Fig. 5.1). R = rock mounted geophone, S = soil mounted geophone. Total trace length is 500 ms.

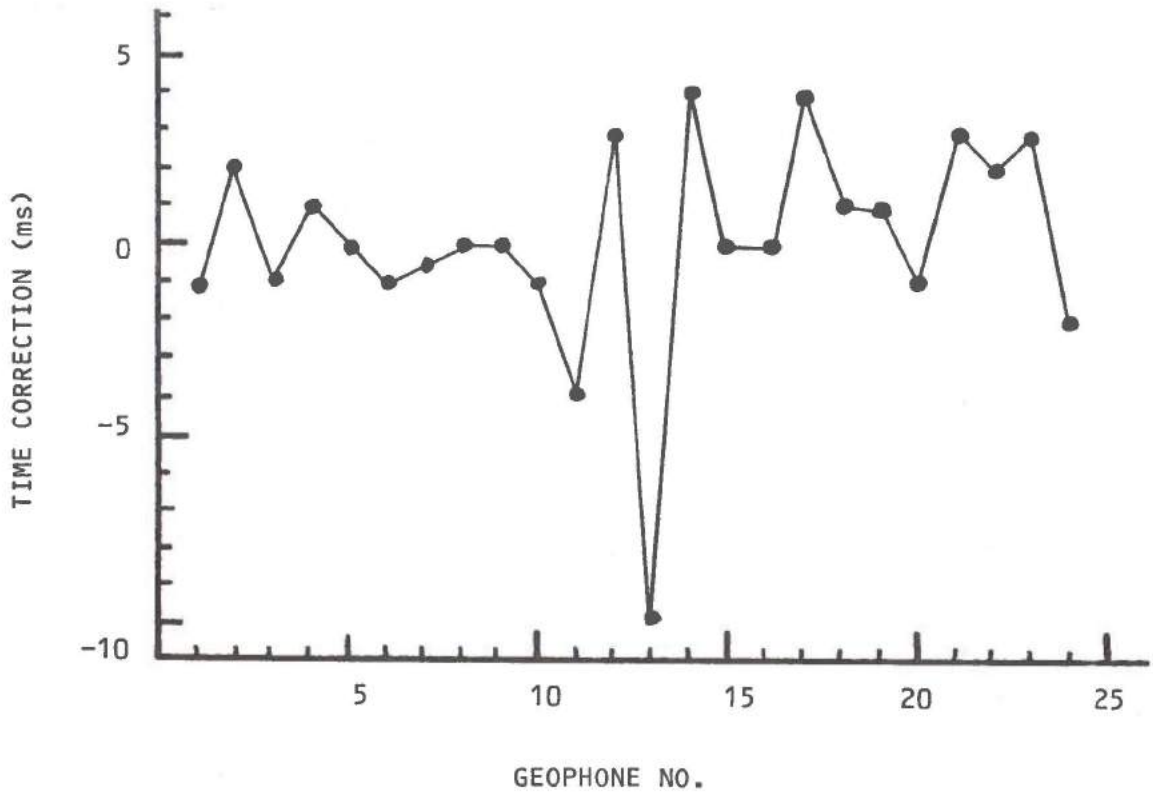


Fig. 5.22 Static time corrections measured directly from the records in Fig. 5.21.

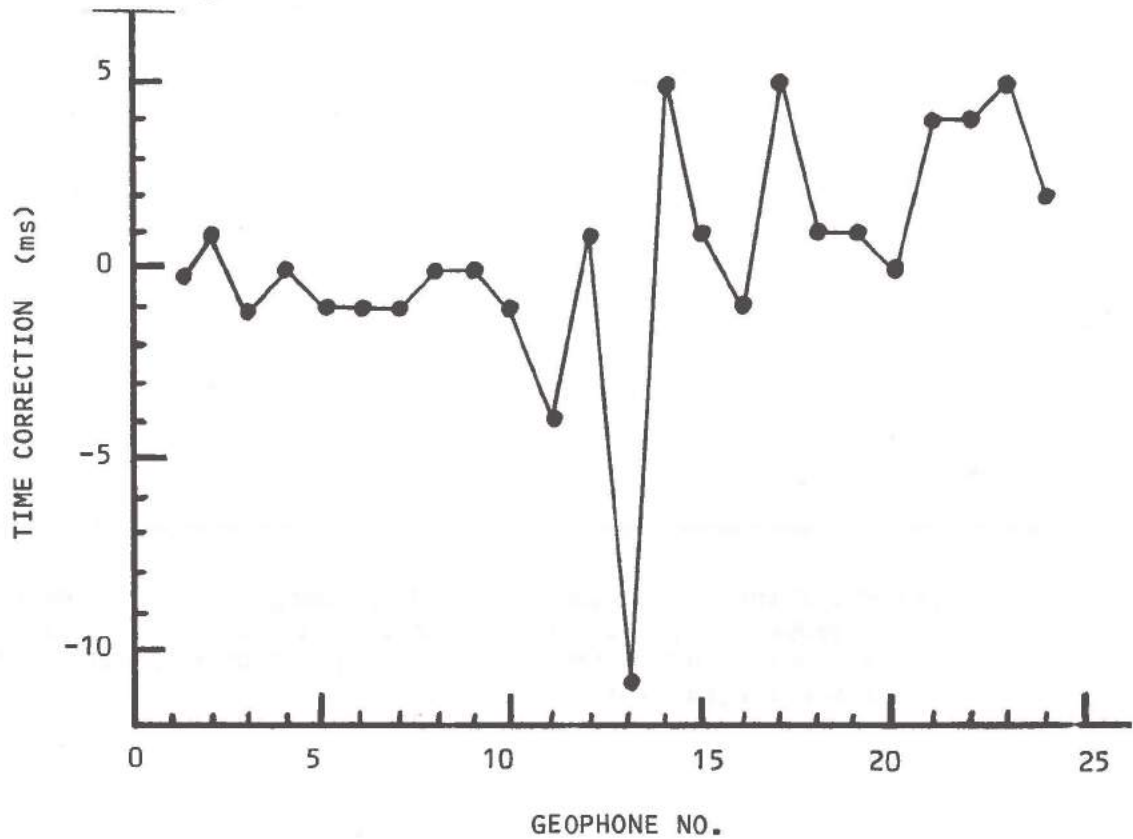


Fig. 5.23 Static time corrections for the direct P arrival along the surface, computed relative to the linear arrival time function shown in Fig. 5.24.

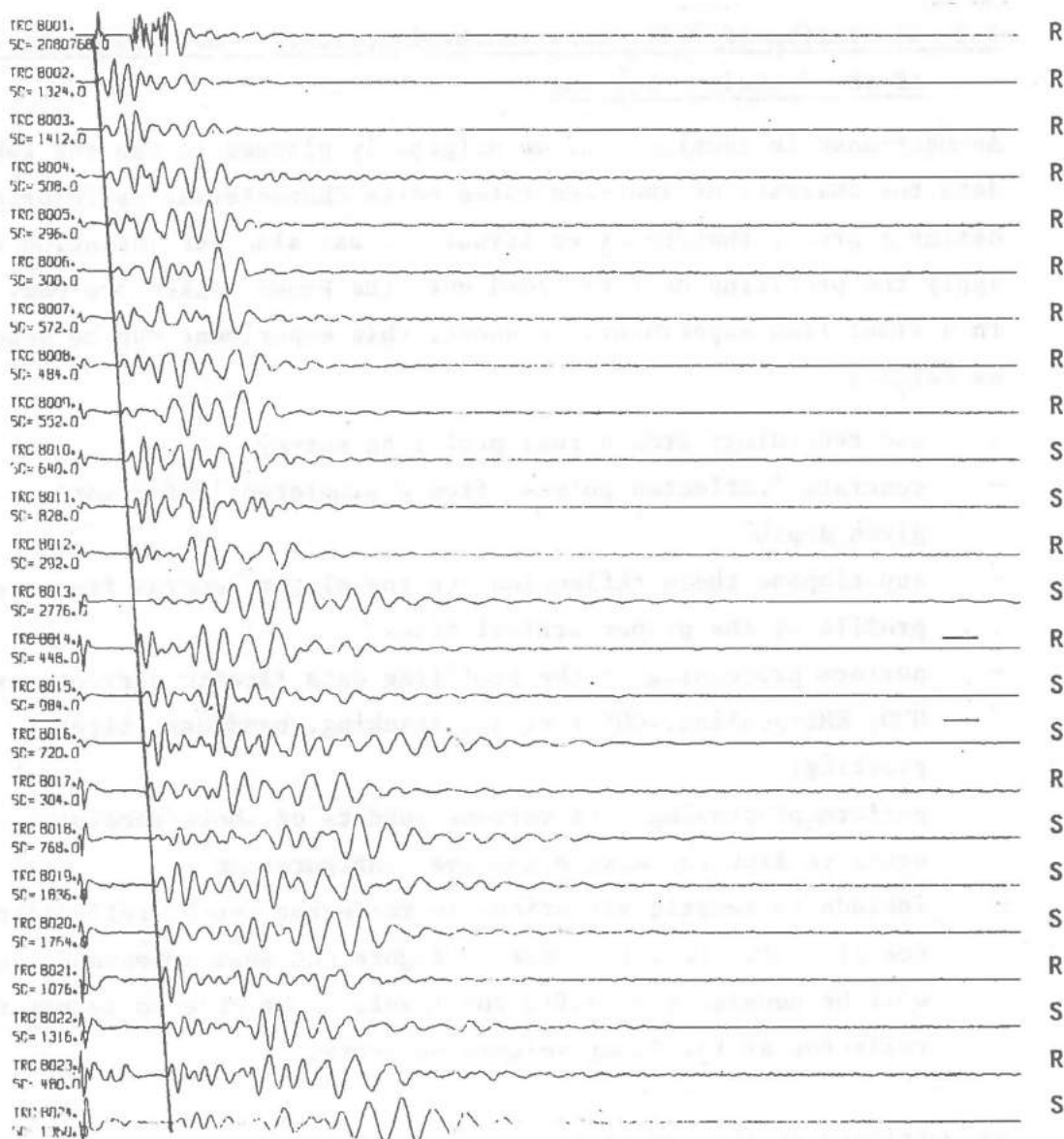


Fig. 5.24 Recordings of a surface shot (50 g charge) along a geophone line at the surface (Configuration No. I, Fig. 5.1). R = rock mounted geophone, S = soil mounted geophone. Total trace length is 500 ms. A linear arrival time function is indicated, corresponding to a velocity of 5300 m/s.



An example of applying this principle in practice is reproduced in Fig. 5.25. The first trace is a sum ('stack') of traces from a simultaneous shooting experiment (shooting simultaneously in the mine and at the surface), without having performed any static corrections to the records. The second trace is a corresponding 'stack' after static corrections based on first P arrivals. The example proves a considerable improvement of the SNR of the stacked trace.

### 5:3 Simulation of reflectors to obtain criteria for optimum design of shot/receiver lay-out

As mentioned in section 5.1, we originally planned to use the Løkken-78 data for analysis of shot-generated noise characteristics in order to design a proper shot/receiver layout. It was also our intention to apply the profiling data recorded over the known Løkken ore body in 1976 in a simulation experiment. In short, this experiment can be described as follows:

- use recordings from a real profiling survey
- generate 'reflected pulses' from a simulated 'reflector' at a given depth
- superimpose these reflections on the single records from the profile at the proper arrival times
- perform processing of the profiling data (static corrections, NMO, RMS-scaling, CDP sorting, stacking, bandpass filtering plotting)
- perform processing with various subsets of shots/receivers in order to find the most effective configuration
- include systematic variations in reflector depth, reflection coefficient, etc., in order to figure out what impedance contrasts will be necessary at different levels to be able to detect the reflector at the final seismic sections.

As mentioned at the end of section 5.1, it later turned out that the Løkken-1976 data - due to the very unfavorable gain setting - were strongly contaminated by instrument noise in the time windows of interest. We therefore could not see much value in applying the above simulation experiment to these data, as these data had not been subject to a real geophysical noise situation. Fortunately, it turned out that a seismic profile had been shot in Sulitjelma late in 1978 with the DFSV instrument (due to a break-down of the DHR 1632), and it was decided to perform the planned simulation experiment on these data.

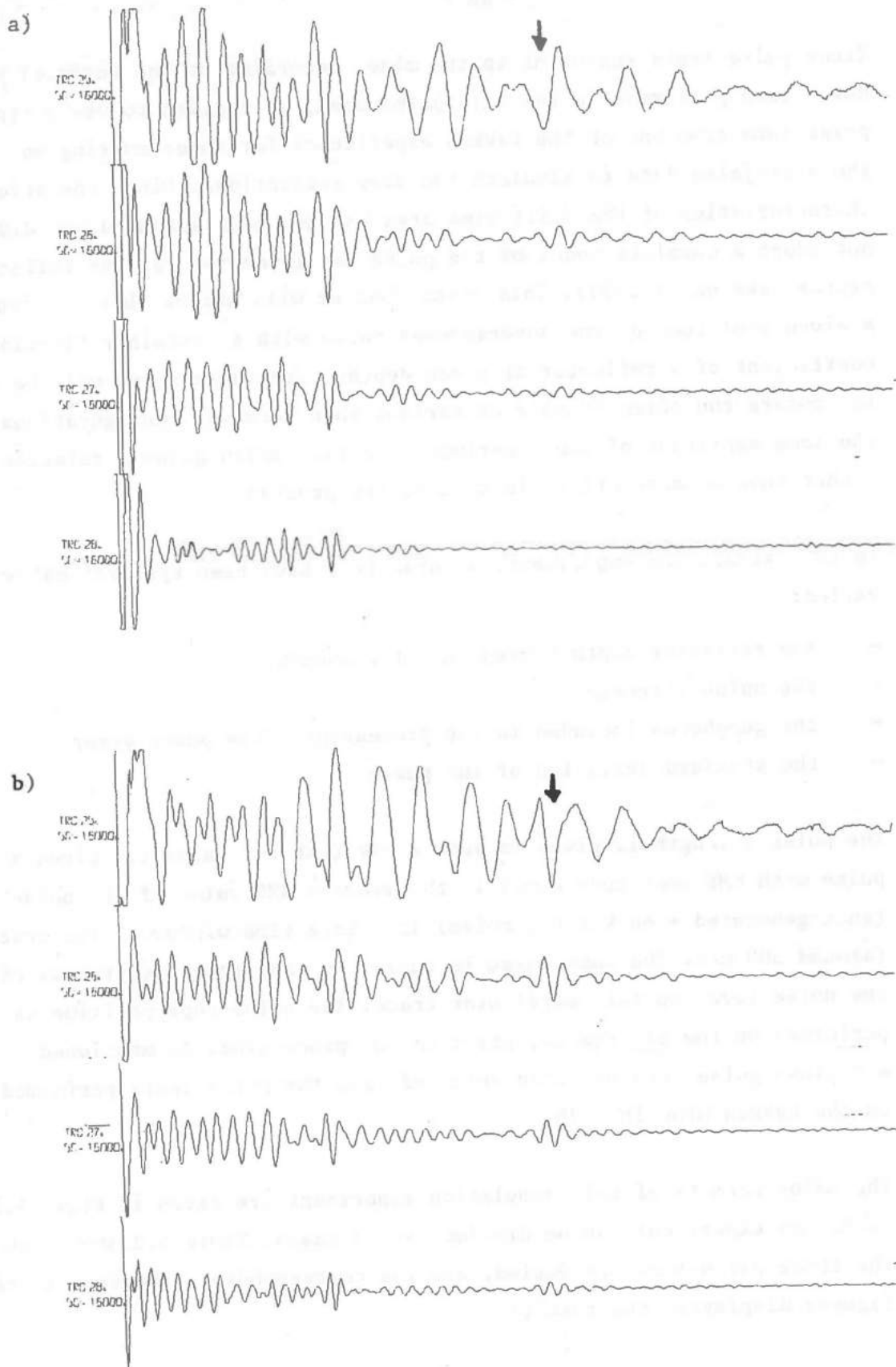


Fig. 5.25 Each trace is a stack of the 24 traces shown in Fig. 5.6, where shots have been fired simultaneously in the mine and at the surface. The pulse from the mine shot is indicated by an arrow. Total trace length is 250 ms. Different bandpass filters are used.  
a) No static corrections applied to the data before stack  
b) Static corrections applied, computed from surface shot direct P arrivals (see Fig. 5.24).

Since pulse tests (shooting in the mine, recording at the surface) had never been performed in the Sulitjelma area, we decided to use a typical pulse form from one of the Løkken experiments for superimposing on the Sulitjelma data to simulate the deep reflections. Since the attenuation characteristics of the Sulitjelma area had not been measured, we did not adopt a complete model of the pulse amplitude for various reflector depths (see eq. (3.12)). This means that we will not be able to associate a given amplitude of the superimposed pulse with a certain reflection coefficient of a reflector at given depth. Nevertheless, we will be able to compare the effectiveness of various shot/receiver configurations for the same amplitude of the superimposed pulse, which gives a relative rather than an absolute evaluation of the problem.

In this simulation experiment, 4 parameters have been systematically varied:

- the reflector depth (given in milliseconds)
- the pulse strength
- the geophones included in the processing pulse phase error
- the standard deviation of the phase.

The pulse strength is given in such a way that the value 1.0 gives a pulse with RMS amplitude equal to the average RMS value of the noise (shot-generated + background noise) in a late time window of the traces (around 300 ms). The same pulse is summed on each trace regardless of the noise level on this particular trace. The pulse superposition is performed on the raw traces, prior to any processing. As mentioned, a typical pulse form has been selected from the pulse tests performed in the Løkken mine in 1978.

The major results of this simulation experiment are given in Figs. 5.26-5.45. The experiment can be divided into 3 cases. Table 5.2 shows how the three parameters are varied, and the corresponding reference to the figures displaying the results.

Case	Reflector Depth (m)	Pulse Amplitude	Geophones Used	Phase Error (ms)	Figure Reference
I	250	0.5	G1-G24	0	5.26
			G1-G12		5.27
			G13-G24		5.28
			G1-G8		5.29
			G9-G16		5.30
			G17-G24		5.31
			G9-G24		5.32
II	300	1.0	G1-G24	0	5.33
	200	1.0			5.34
	175	1.0			5.35
	150	1.0			5.36
	150	2.0			5.37
	150	5.0			5.38
	125	5.0	G1-G24		5.39
III	250	0.5	G1-G24	0	5.40
	250	0.3	G1-G24		5.41
	250	0.2	G1-G24		5.42
IV	250	0.5	G1-G24	1	5.43
	250	0.5	G1-G24	2	5.44
	250	0.5	G1-G24	4	5.45

Table 5.2

Table showing how the parameters have been varied during the simulation experiment. The resulting data sections are displayed in the figures referred to in the rightmost column.

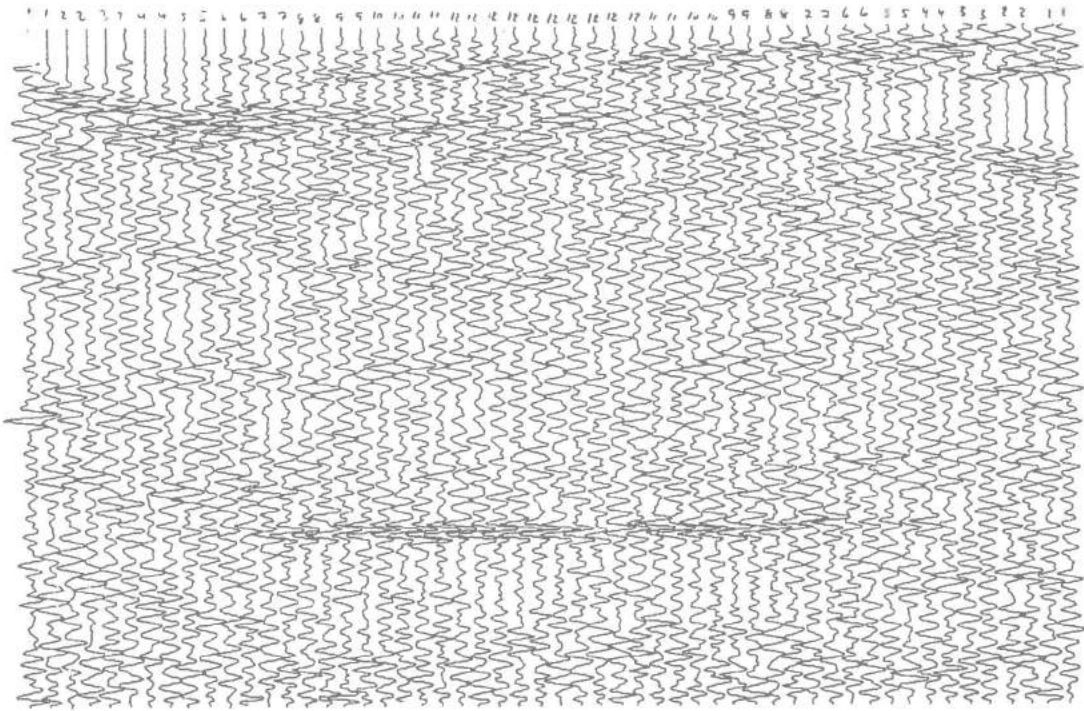


Fig. 5.26 Reflector depth = 250 ms, pulse amp. = 0.5, G1-G24, phase error = 0.

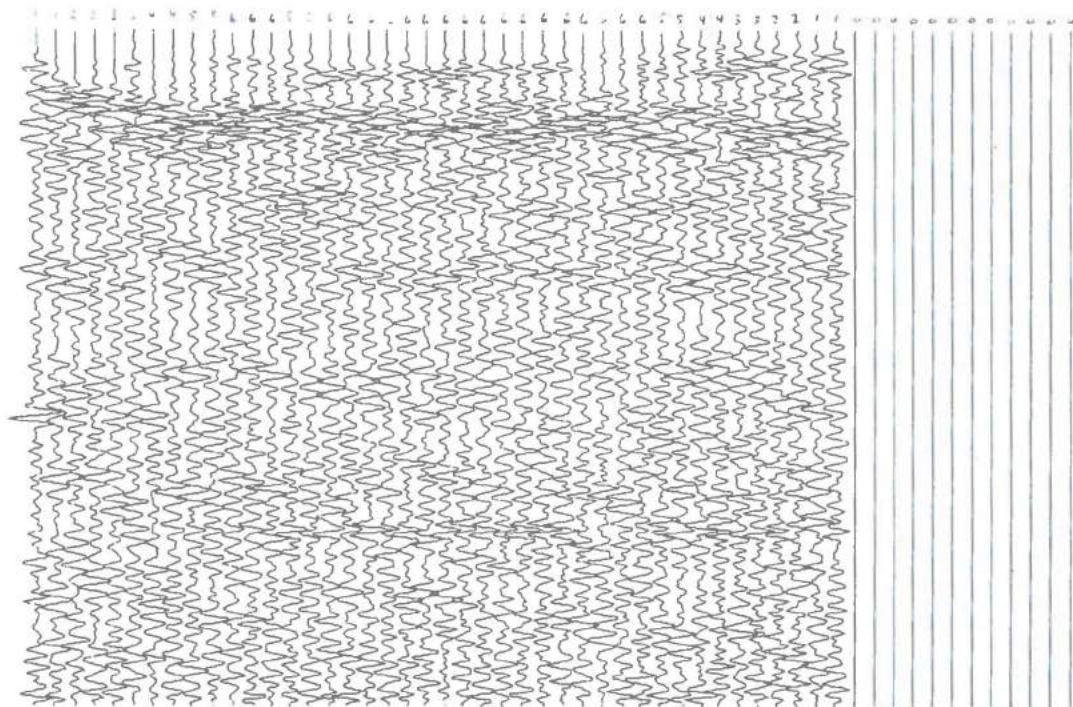


Fig. 5.27 Reflector depth = 250 ms, pulse amp. = 0.5, G1-G12, phase error = 0.

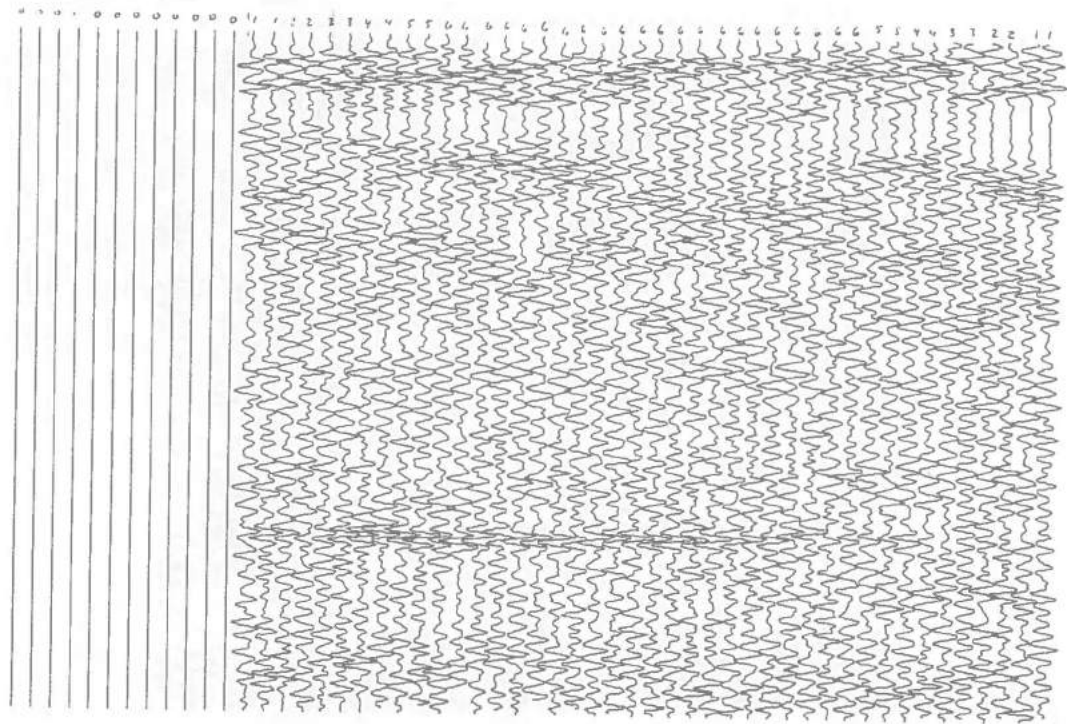


Fig. 5.28 Reflector depth = 250 ms, pulse amp. = 0.5, G13-G24, phase error = 0.

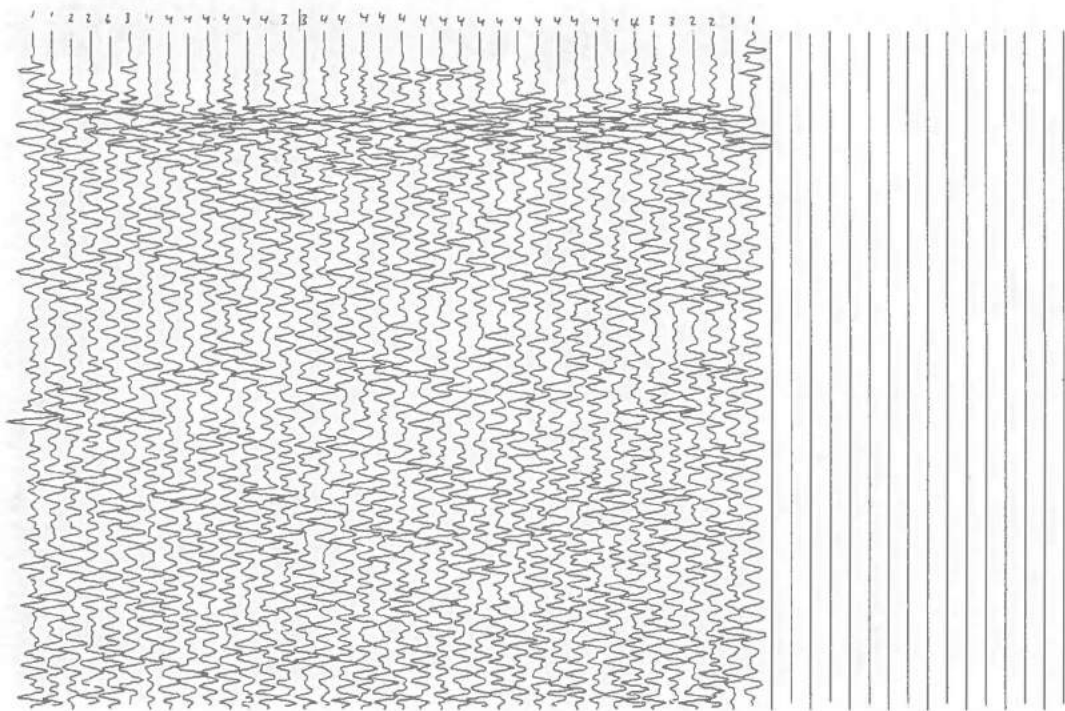


Fig. 5.29 Reflector depth = 250 ms, pulse amp. = 0.5, G1-G8, phase error = 0.

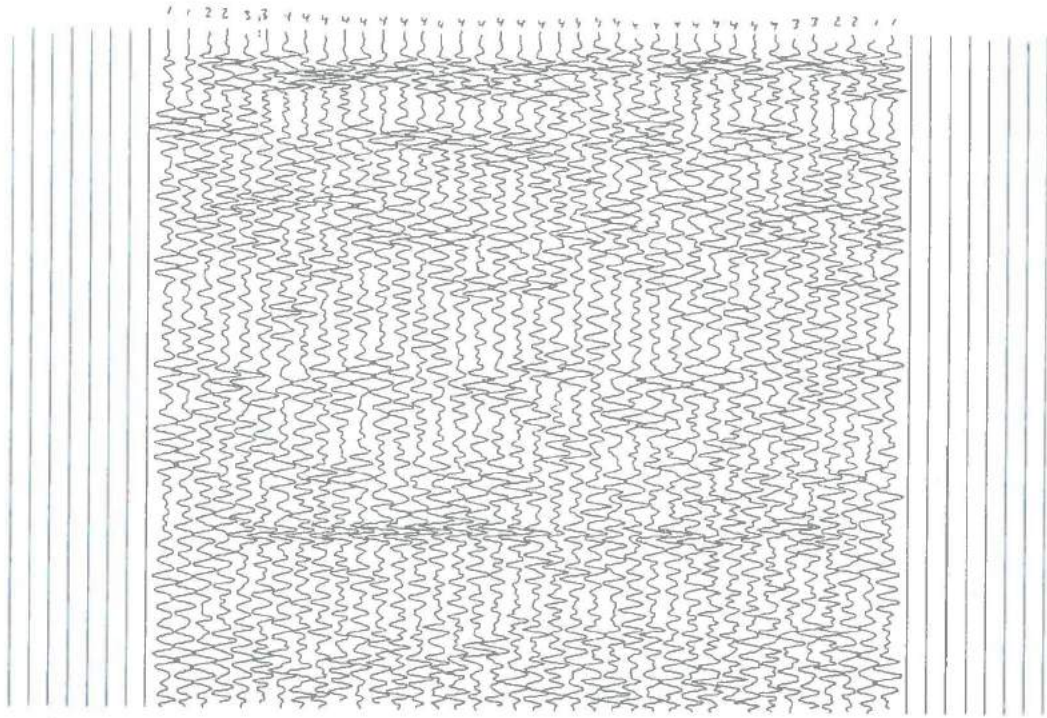


Fig. 5.30 Reflector depth = 250 ms, pulse amp. = 0.5, G9-G16, phase error = 0.

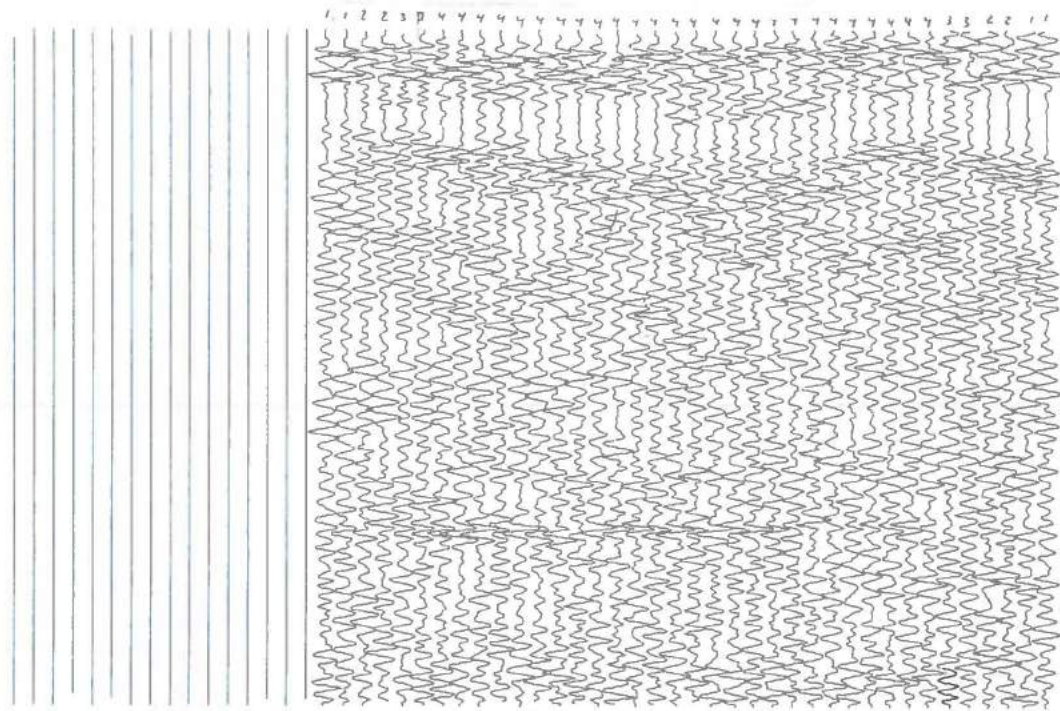


Fig. 5.31 Reflector depth = 250 ms, pulse amp. = 0.5, G17-G24, phase error = 0.

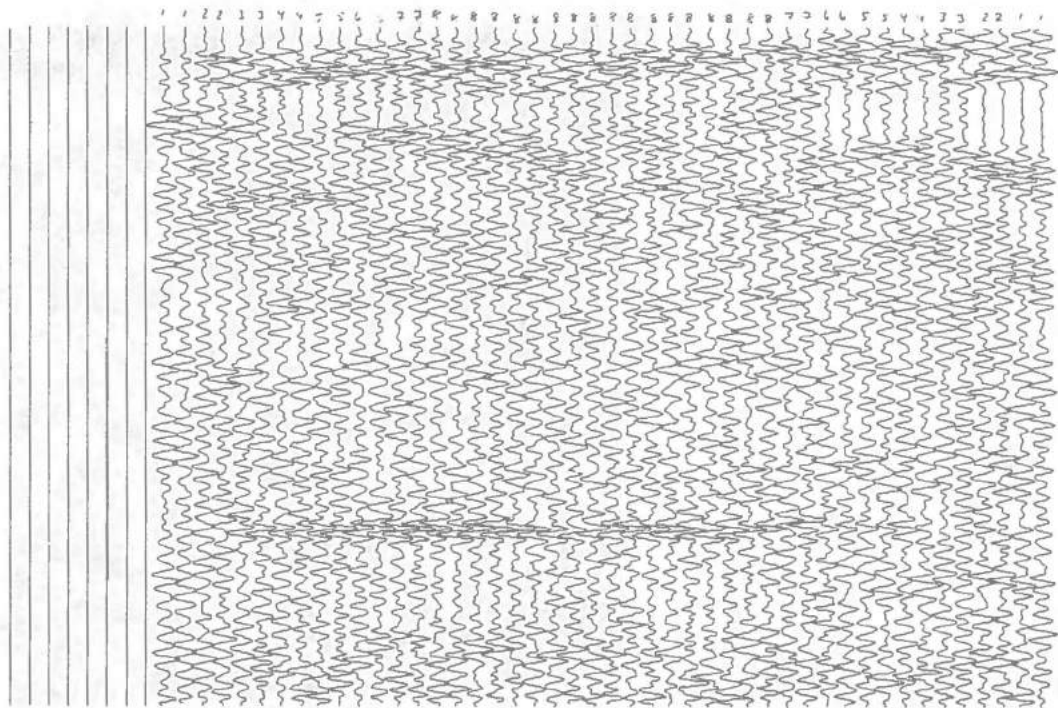


Fig. 5.32 Reflector depth = 250 ms, pulse amp. = 0.5, G9-G24, phase error = 0.

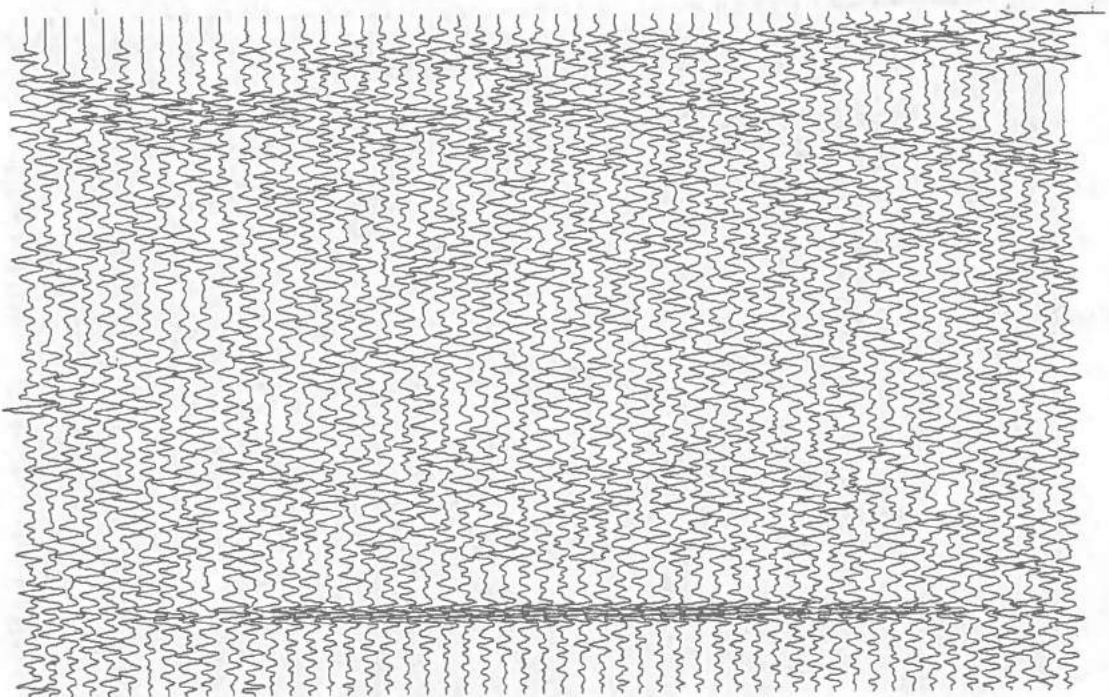


Fig. 5.33 Reflector depth = 300 ms, pulse amp. = 1.0, G1-G24, phase error = 0.



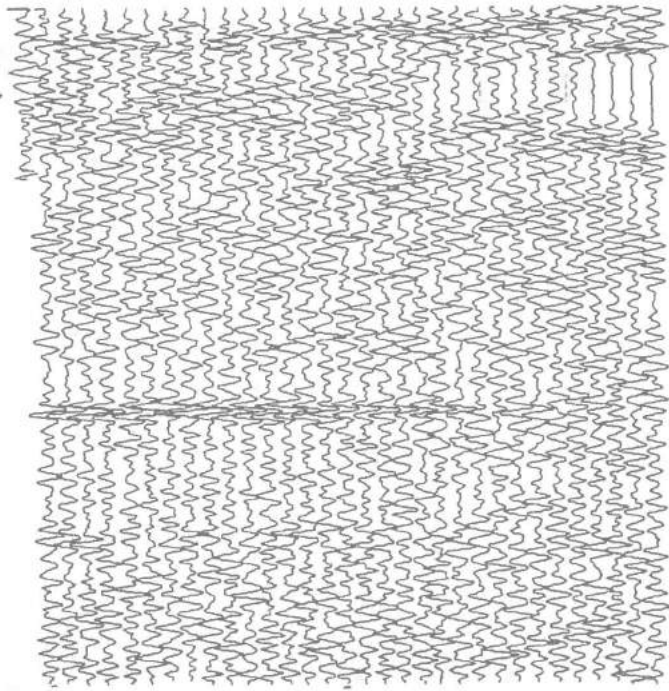


Fig. 5.34 Reflector depth = 200 ms, pulse amp. = 1.0, G1-G24, phase error = 0.

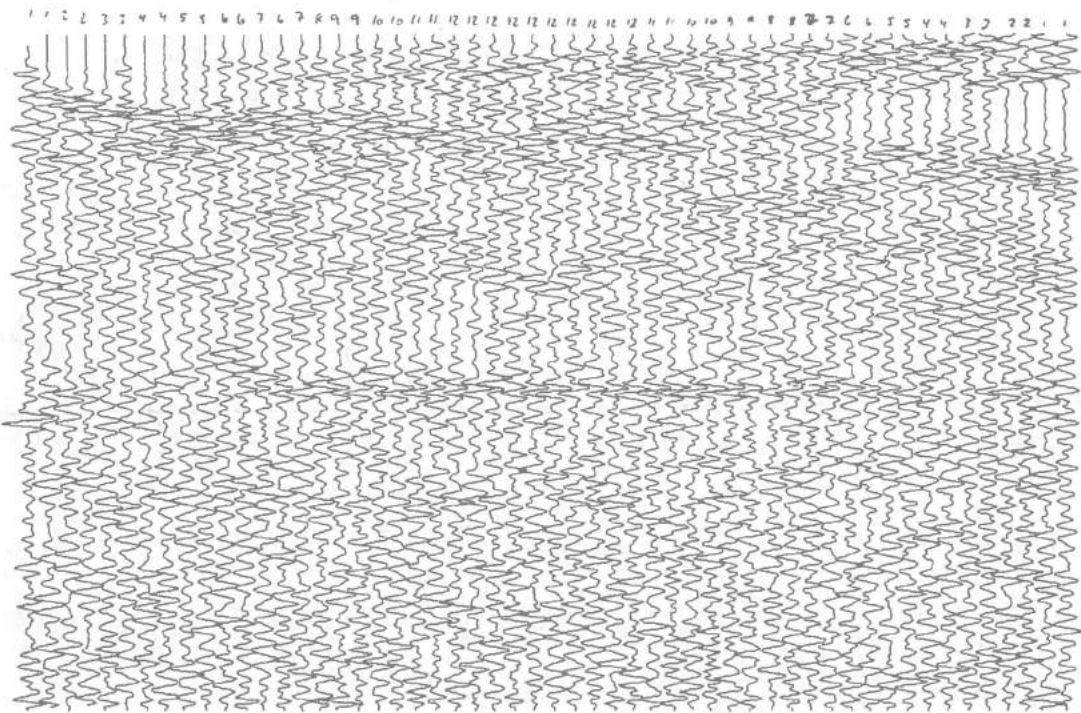


Fig. 5.35 Reflector depth = 175 ms, pulse amp. = 1.0, G1-G24, phase error = 0.

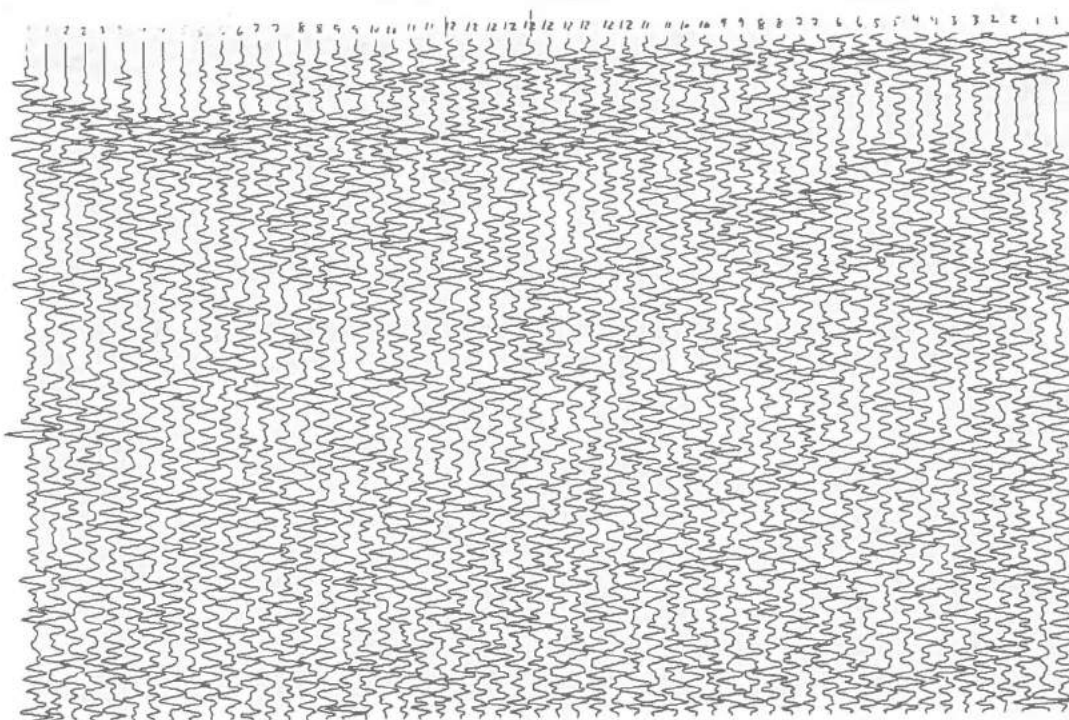


Fig. 5.36 Reflector depth = 150 ms, pulse amp. = 1.0, G1-G24, phase error = 0.

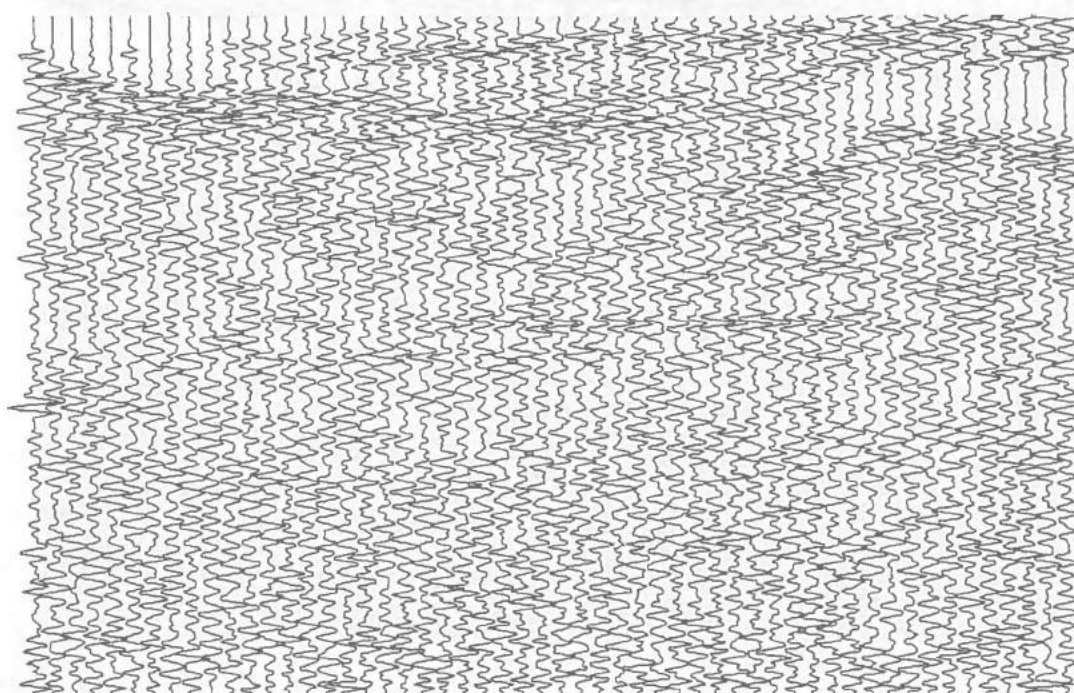


Fig. 5.37 Reflector depth = 150 ms, pulse amp. = 2.0, G1-G24, phase error = 0.

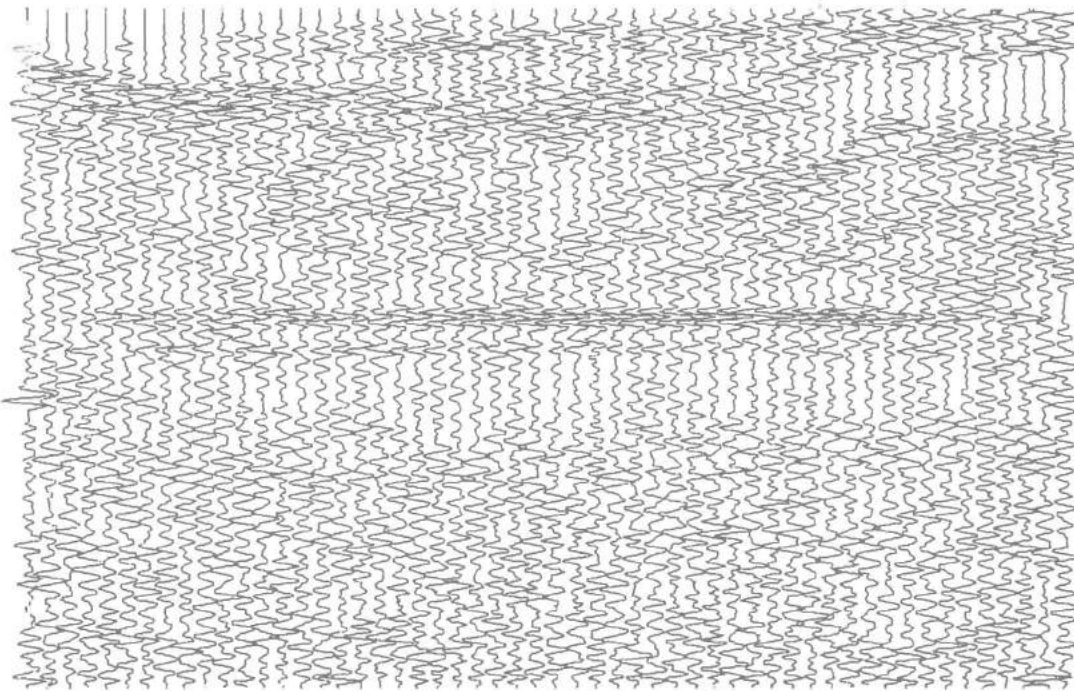


Fig. 5.38 Reflector depth = 150 ms, pulse amp. = 5.0, G1-G24, phase error = 0.

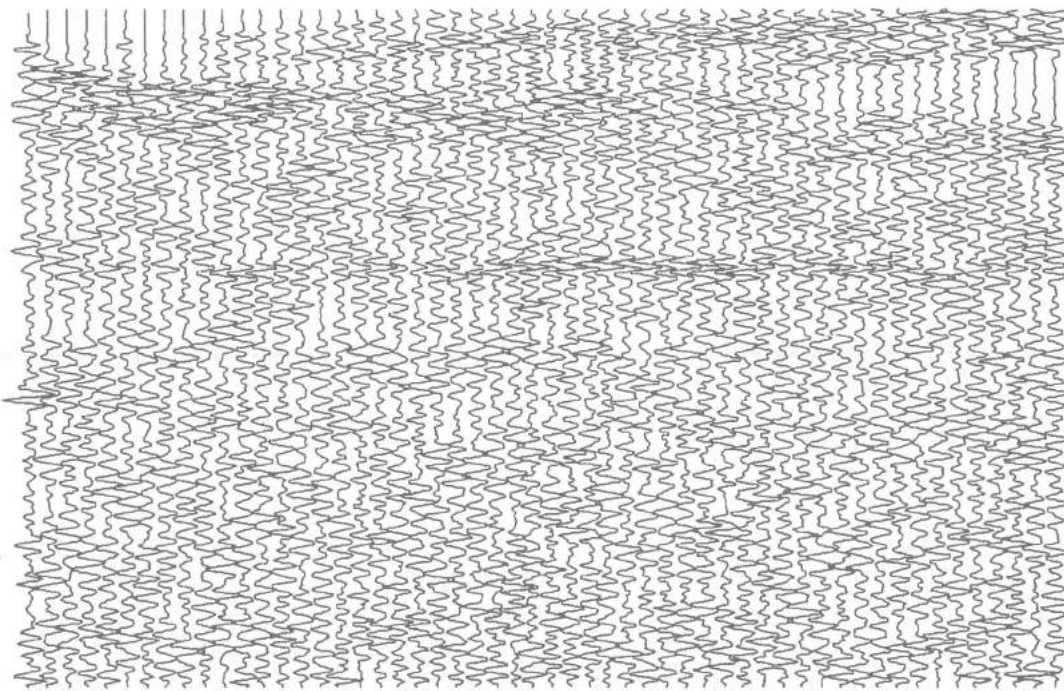


Fig. 5.39 Reflector depth, 125 ms, pulse amp. = 5.0, G1-G24, phase error = 0.

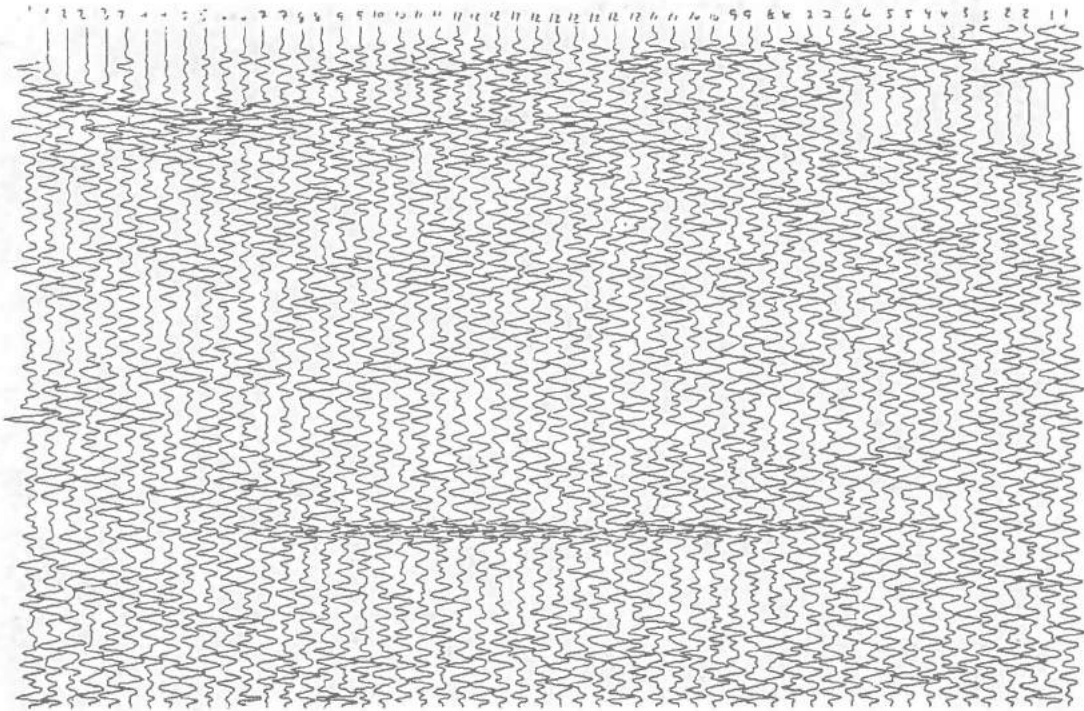


Fig. 5.40 Reflector depth = 250 ms, pulse amp. 0.5, G1-G24, phase error = 0.

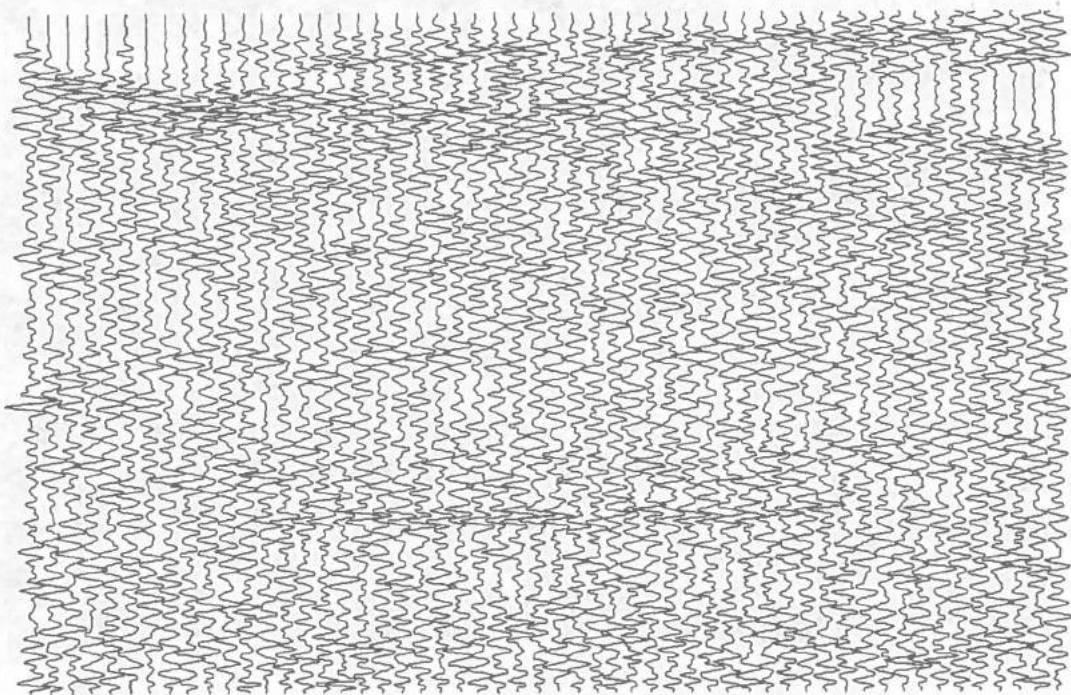


Fig. 5.41 Reflector depth 250 ms, pulse amp. = 0.3, G1-G24, phase error = 0.

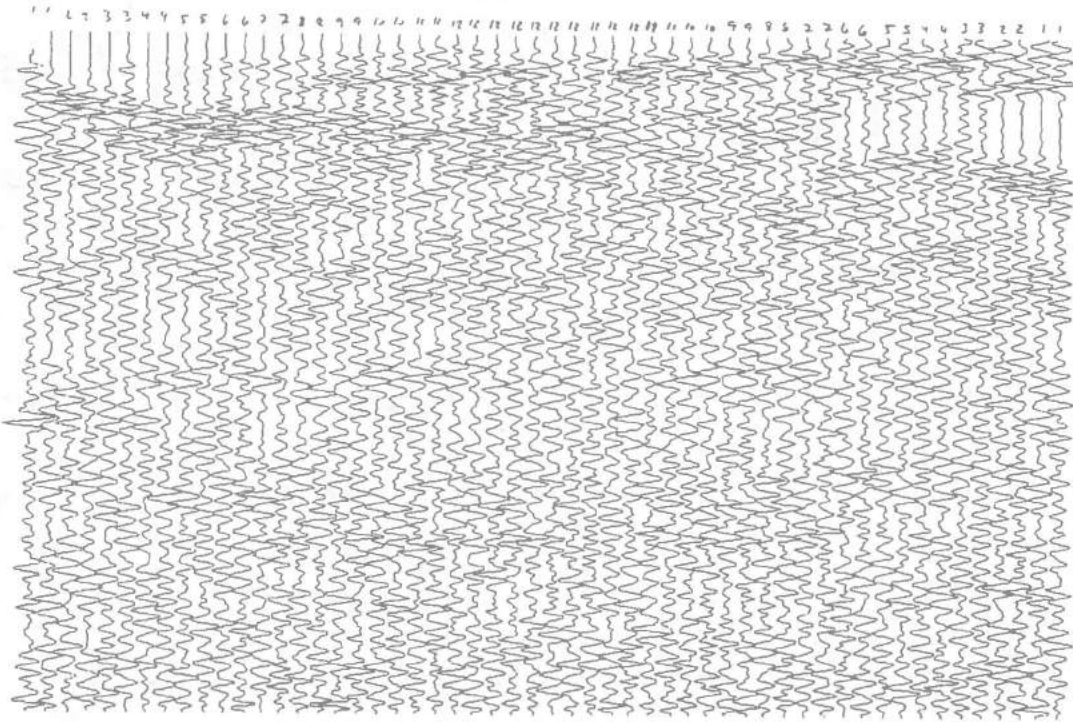


Fig. 5.42 Reflector depth=250 ms, pulse amp. = 0.2, G1-G24, phase error = 0.

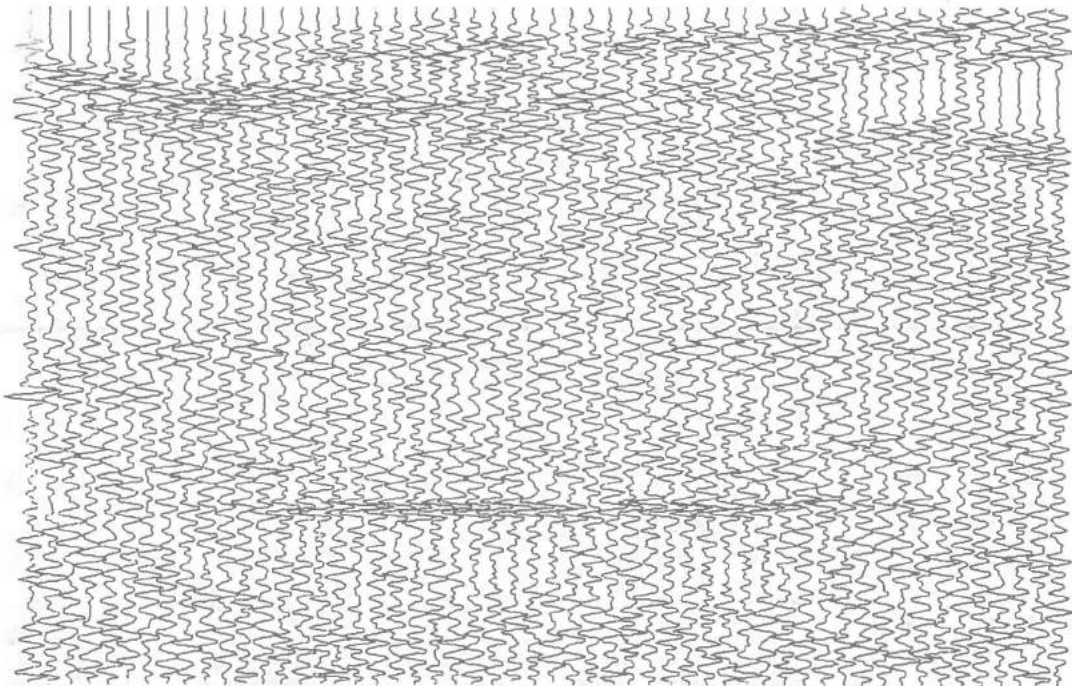


Fig. 5.43 Reflector depth = 250 ms, pulse amp. = 0.5, G1-G24, phase error = 1.

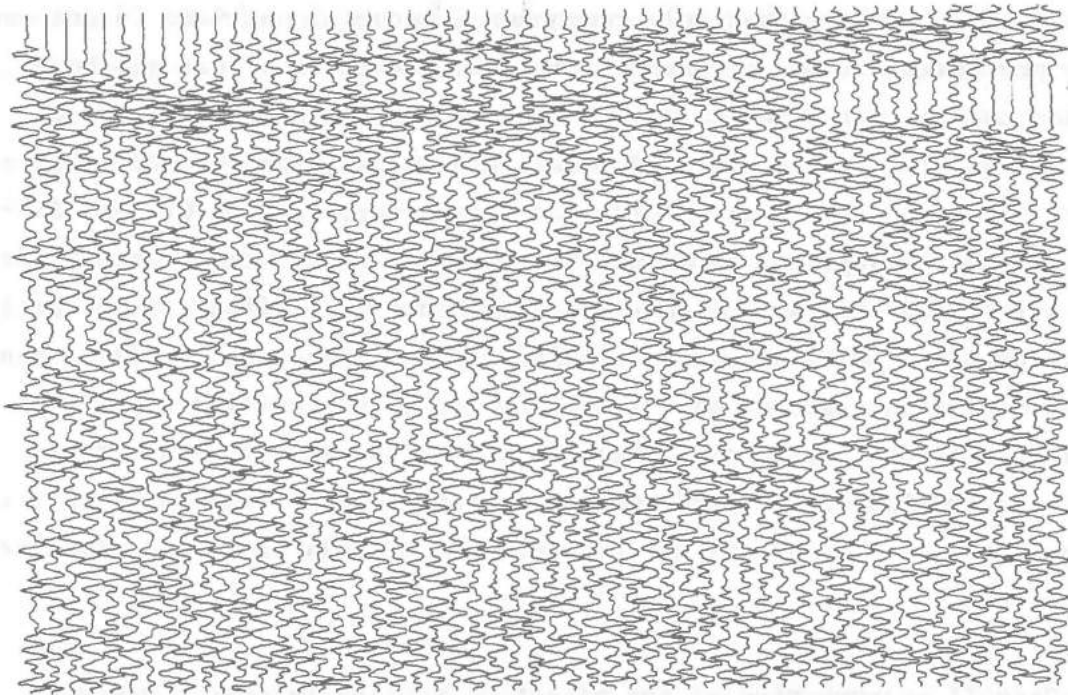


Fig. 5.44 Reflector depth = 250 ms, pulse amp. = 0.5, G1-G24, phase error = 2.

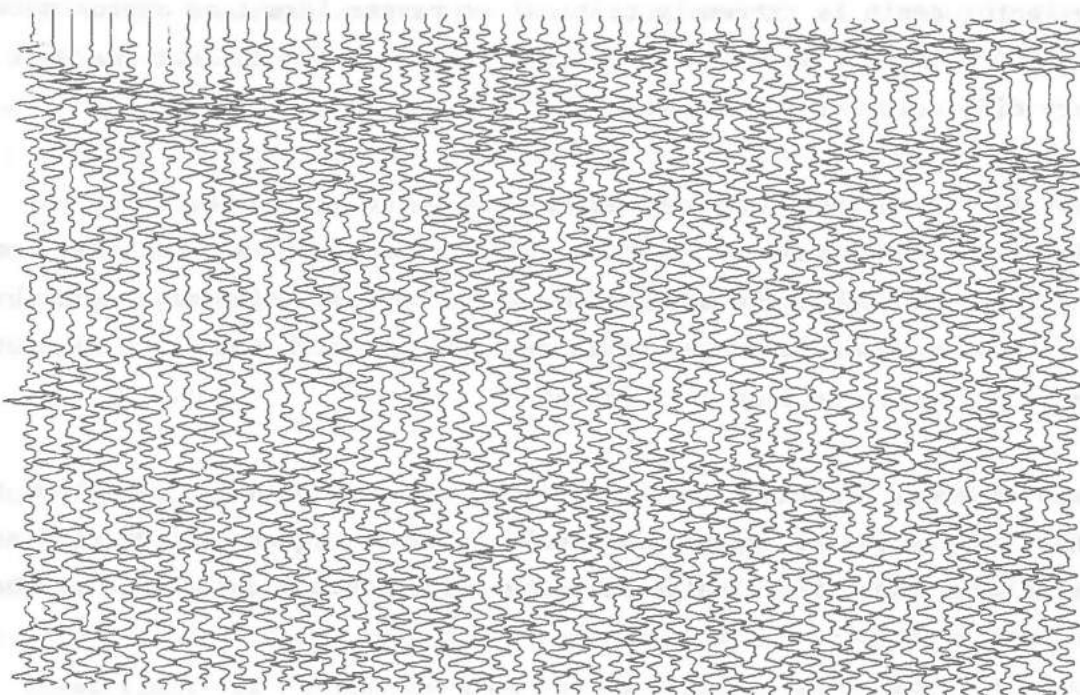


Fig. 5.45 Reflector depth = 250 ms, pulse amp. = 0.5, G1-G24, phase error = 4.

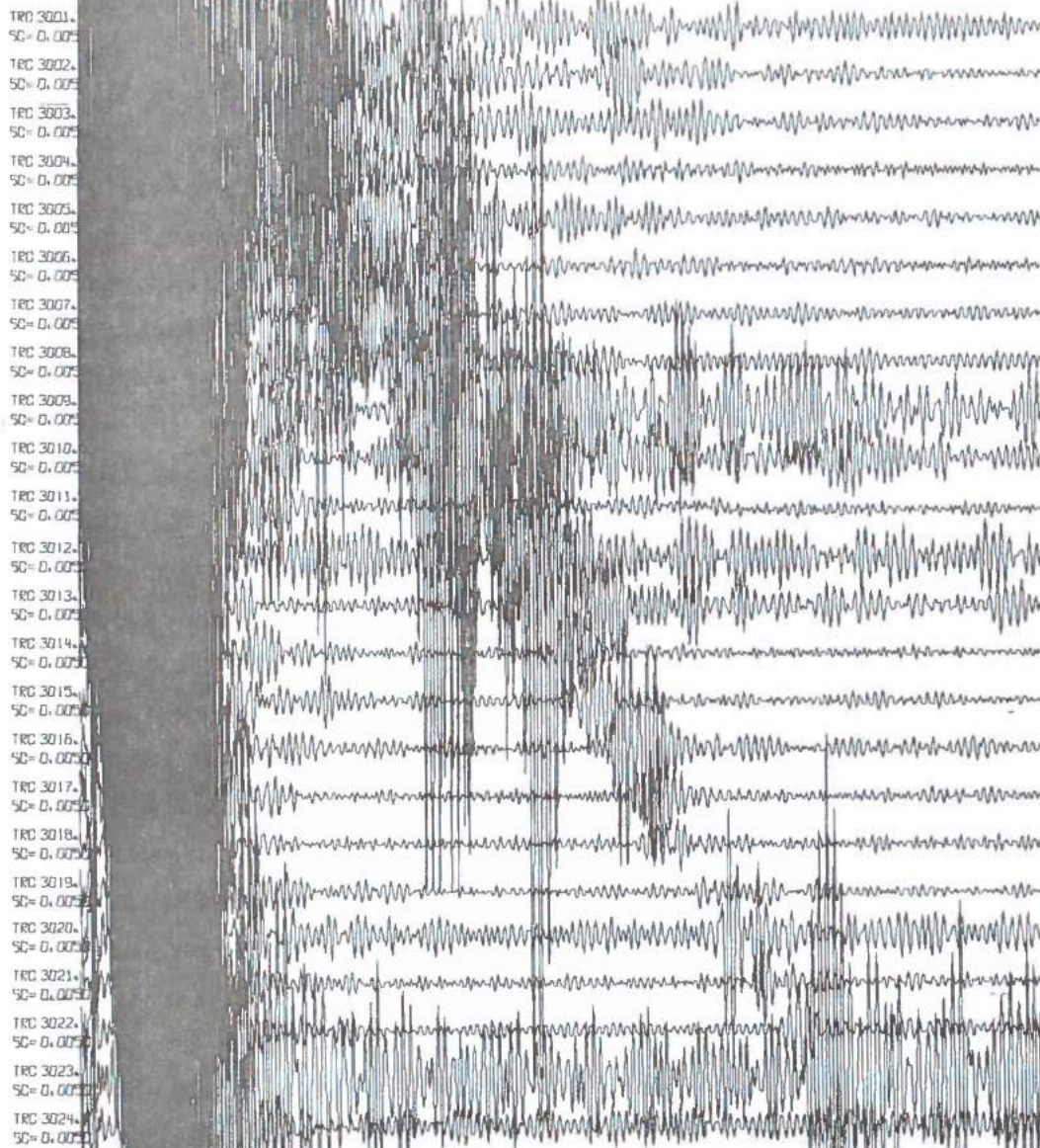


Fig. 5.46 Typical record from the Sulitjelma 1978 profile, recorded with a DFS V. Clipping level has been set relatively high. Total trace length is 500 ms.

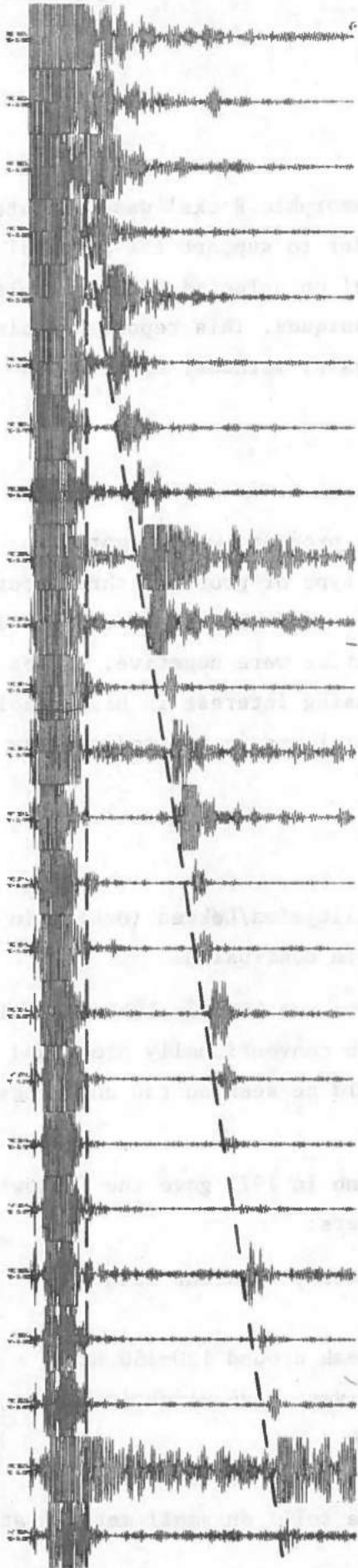


Fig. 5.47 Same data as in Fig. 5,46, plotted with a lower clipping level. Total trace length is 500 ms.



## 6. SUMMARY - CONCLUSIONS

### 6.1 Background

The NORSAR project 'Seismic Methods in Metamorphic Rocks' was initiated in May/June 1978. It was established in order to support the original Sulitjelma project 'Seismic Ore Prospecting' on selected problems related to signal processing and field lay-out techniques. This report contains a description of data collected, data analysis, methods, and results obtained on the NORSAR project.

### 6.2 Pre-project

In the initial planning stage of the NORSAR project, we attempted to check on on-going research efforts on this type of problems throughout the world in order to assess the current state of the art in the field. Although most of the responses to our inquiries were negative, we got certain indications that there is an increasing interest in high resolution seismic reflection methods and their potential use in non-sedimentary rock.

### 6.3 Scrutiny of earlier work

A scrutiny of relevant data collected in Sulitjelma/Løkken (Orkla) in the time interval 1976-77 gave the following main conclusions:

- A profiling experiment over a well-known ore body in Løkken (Orkla) 1976 seemed to give reflected energy on conventionally processed seismic sections, although nothing could be seen on the unprocessed records.
- Pulse tests performed in the Løkken mine in 1977 gave the following values of some important field parameters:
  - 1) P-velocities  $\sim$  5900 m/s, approximately constant down to 1000 m depth
  - 2) Main frequency range 50-200 Hz, peak around 120-150 Hz
  - 3) Energy source C4 (military explosives) gave slightly higher frequencies than ordinary dynamite
  - 4) Favorable geophone mounting, solid rock: on steel bolt
  - 5) Favorable geophone mounting, loose soil: on small metal plate.

#### 6.4 Theoretical estimates of the expected strength of reflected pulses

An attempt at estimating the attenuation characteristics in the Løkken granitic rock gave a value of the seismic quality factor (Q) of 0.42, corresponding to 0.6 dB/wavelength. Inserting this value into a theoretical signal model gave expected values of the signal-to-noise ratio of a reflected pulse of the order 0.2-0.3 on single records at 700-800 m reflector depth. Here is assumed a charge of 100 g, a reflection coefficient of 0.2 and the total absence of source-generated noise (most ideal case).

It was first concluded that these estimates were too low to expect the seismic reflection method to work in practice. The results were obtained on the basis of data recorded with the DHR 1632 digital instrument, which had been used (and was planned to be used) in past and future profiling work. However, due to a malfunctioning of the DHR 1632, some of the 1977 pulse tests were performed with a Texas Instruments DFS V, which is a considerably more advanced instrument. A very simple analysis showed that the signal-to-noise ratio of this instrument was at least 10 times larger than the value obtained with the DHR 1632, and that the prospects for the future suddenly turned out to be quite good. Unfortunately, this very simple fact was not discovered during the analysis of these pulse test data back in 1977.

#### 6.5 The effect of shot depth on source-generated noise

In order to study the effect of shot depth on source-generated noise, an experiment was carried out at Hadeland in December 1978. Shots were fired at different levels of a 60 m deep borehole and receivers were located at the surface. Unfortunately, the data from this experiment did not have the proper quality for surface noise analysis; the reason for this was that strong non-seismic waveforms were superimposed on the recordings (instrument cross-feed problems). However, it could be concluded from this experiment that shooting in a deep, water-filled borehole introduces a 'water-pulse' effect, that is, the water column above the shot level is lifted and generates a new seismic pulse when returning to its original position. The arrival time of this pulse will depend on factors such as charge size, shot depth, borehole diameter, etc., and may thus represent a considerable source of noise in time intervals where reflections are expected to arrive.

### 6.6 Source-generated noise

In order to analyze source-generated surface noise and corresponding possibilities of optimum signal enhancement, an experiment was carried out in the Løkken mine 1978. By simultaneous firing of charges deep in the mine tunnels and at the surface, reflected pulses could be simulated under realistic source-generated noise conditions. The experiments were performed with a number of different shot/receiver geometries.

The data were analyzed during fall/winter 1978/79 and the main results of this experiment were to state the fact that the DHR 1632 had a quite unsatisfactory instrument noise level in the interesting time window (say, 150-500 ms). The main reason for this was that the constant, pre-selectable gain of the DHR 1632 - according to the operator - had to be set in such a way that the very strong early surface waves (0-150 ms) passed unclipped through the amplifiers to avoid system saturation and corresponding trace distortion. In consequence, the strong direct waves 'consumed' the whole dynamic range of the system, leaving the later low-level part of the seismic wave field totally masked by the instrument noise.

A reanalysis of the 1976 DHR profiling data showed exactly the same effect. The final conclusion was that the DHR 1632 instrument was inappropriate for this work and that a more advanced instrument should be applied - that is, an instrument having a so-called automatic gain control (floating point recording).

### 6.7 Criteria for optimum design of shot/receiver lay-out

A simulation experiment was performed with profiling data from Sulitjelma 1978 (DFS V instrument) in order to obtain criteria for optimum design of shot/receiver lay-out. Reflectors were simulated at different depths by superimposing seismic pulses on the individual traces. The data were then processed by conventional CDP stacking methods, using various subsets of geophones, selected according to shot/receiver effects.

These simulations gave very interesting results as to which lay-outs should be consequently avoided in the field. Very simple criteria could be set up in the form of a 'triangle' in the time-distance plane determining

the minimum shot/geophone offset recommended, and in addition, a minimum reflector depth (of the order 4-500 m) below which reflections cannot be expected to be detected. By these results, we have obtained very useful general criteria for shot/geophone lay-out.

## 7. DISCUSSION - RECOMMENDATIONS FOR FUTURE RESEARCH

### 7.1 Status of the Project - August 1979

After slightly more than a year of NORSAR engagement in the seismic ore prospecting project, we had to admit that a great many of the results obtained turned out to be rather discouraging, as a number of data analyses simply reduced to studies of instrument-generated noise. Although this at first sight must be rated a rather negative conclusion, it is a very important one - the regrettable thing of course being that it was not obtained earlier. Nevertheless, the conclusion in itself is far more fruitful than any discussion of whether or not these facts should have been discovered at an earlier stage. In short, the relevant data/results may be summarized as follows:

- Advantageous geophone couplings are steel bolt (hard rock) and small metal plate (loose soil).
- The military explosives (C4) give satisfactory frequency content of the deep-penetrating seismic pulses (120-160 Hz at about 1000 m travel distance).
- Seismic pulse tests from the Løkken mine area are leading to fairly reliable estimates of attenuation factors and expected amplitudes of reflections. Even for the DHR data, the signal-to-noise ratio is good enough to give reliable results.
- These results show that a reflector at 700-800 m depth will have a good chance to be detected even on the single traces when using a DFS V instrumentation.
- Profiling data from Sulitjelma (DFS V, 1978) have given important general criteria for shot/geophone layout (simulation experiment).

### 7.2 Re-profiling of the Known Løkken Ore Body

As it turned out that the 1976 profiling data was subject to a number of serious defects (see Section 5), and in addition, was collected with a layout directly in conflict with the general criteria referred to above, we recommended a re-profiling of the known Løkken ore body using the DFS V instrumentation. In order to be able to study the various effects of source-generated noise in the actual reflection time windows (which we were not able to do earlier due to the lack of dynamic range in the data), it was decided to use densely spaced geophones (5 m) and to perform a considerable repeated shooting (a number of shots in each hole).

As mentioned, this re-profiling work was suggested by NORSAR on the basis of the results obtained from earlier data. In May/June 1979, Orkla Industrier A/S decided to carry out this experiment, and the work was scheduled to July/August. However, due to the fact that no proper instrumentation is available for land work, the experiment was not performed until October. Strictly speaking, this experiment is beyond the scope of this report, and should actually be considered as a continuation of the original NORSAR project. However, since the data have now been collected and the results turn out to be very promising, we shall include a small example of records. Fig. 7.1 shows records from a single shot, filtered with a bandpass filter 160-360 Hz, and Fig. 7.2 shows a direct stack of 4 different shots, each located 10 m apart. The records show prominent reflections from the ore body at 260 ms, exactly the time expected. For comparison, Fig. 7.3 shows a record from the same profile, recorded in 1976 (see Section 5). It should be stressed that these data are just filtered raw data, and that no advanced processing has been applied. In our opinion, these data represent a really good basis for a fruitful development of the reflection seismic methods in metamorphic rocks.

### 7.3 Recommendations for Further Developments

The re-profiling data from Løkken can, as mentioned, be considered as kind of status of the project at the time of completion of the original NORSAR engagement. We now feel that we are entering into a new phase of the project, that is, a work aimed at optimizing field layout and processing techniques to be used in future prospecting.

We would like to conclude with a brief summary of our major recommendations for the further developments of the project. They are as follows:

- Additional field experiments based on the general criteria obtained (see section 5) and on further analysis of the recent Løkken data.

These experiments are aimed at studying background noise as compared to shot-generated noise, the effect of repeated shooting (same hole), the design of shot arrays, the effect of charge size under various background

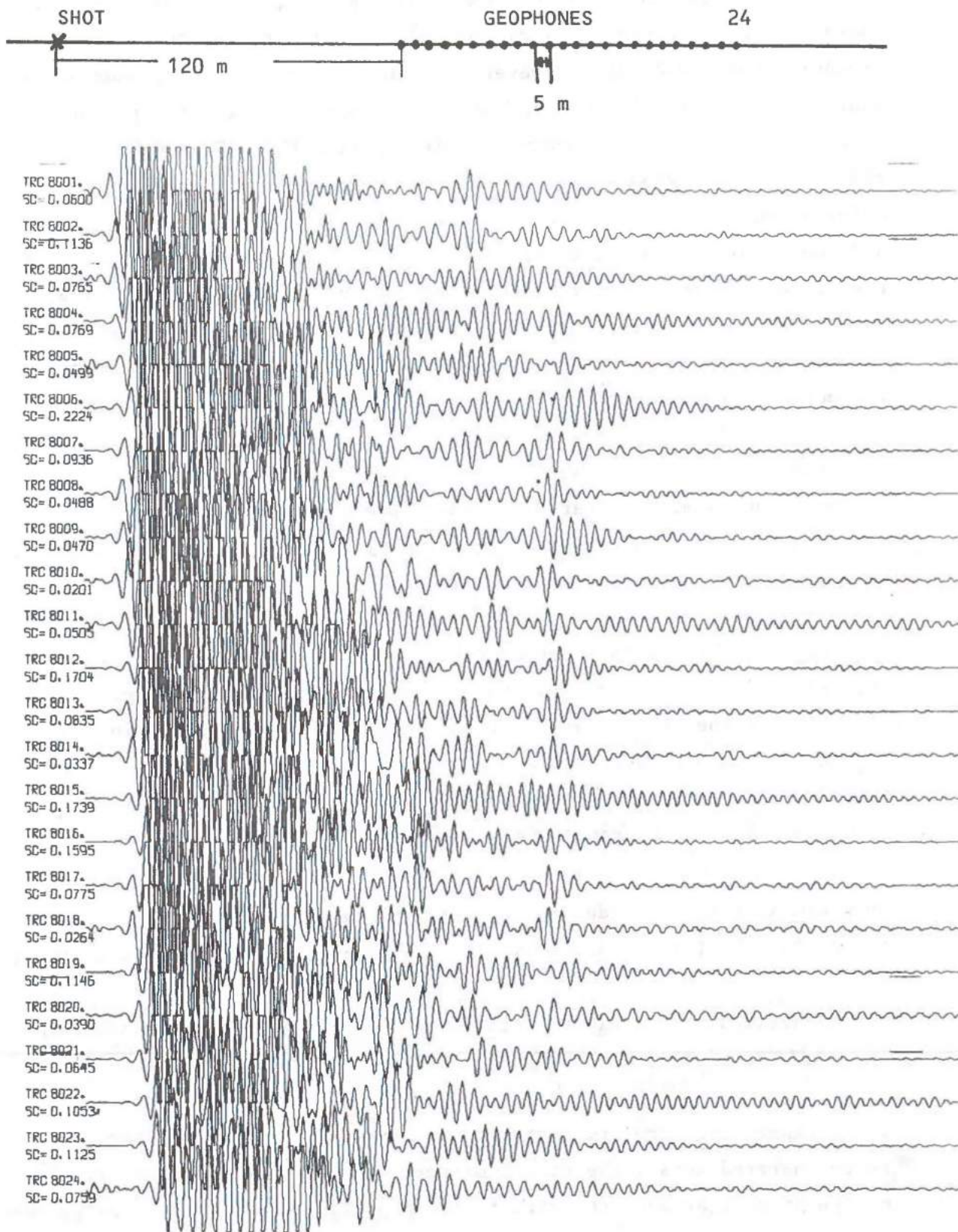


Fig. 7.1 Single shot records from the 1979 profile over the known Løkken ore body, filtered with a bandpass filter 160-360 Hz. Shot/receiver configuration is also shown. Total trace length is 500 ms.

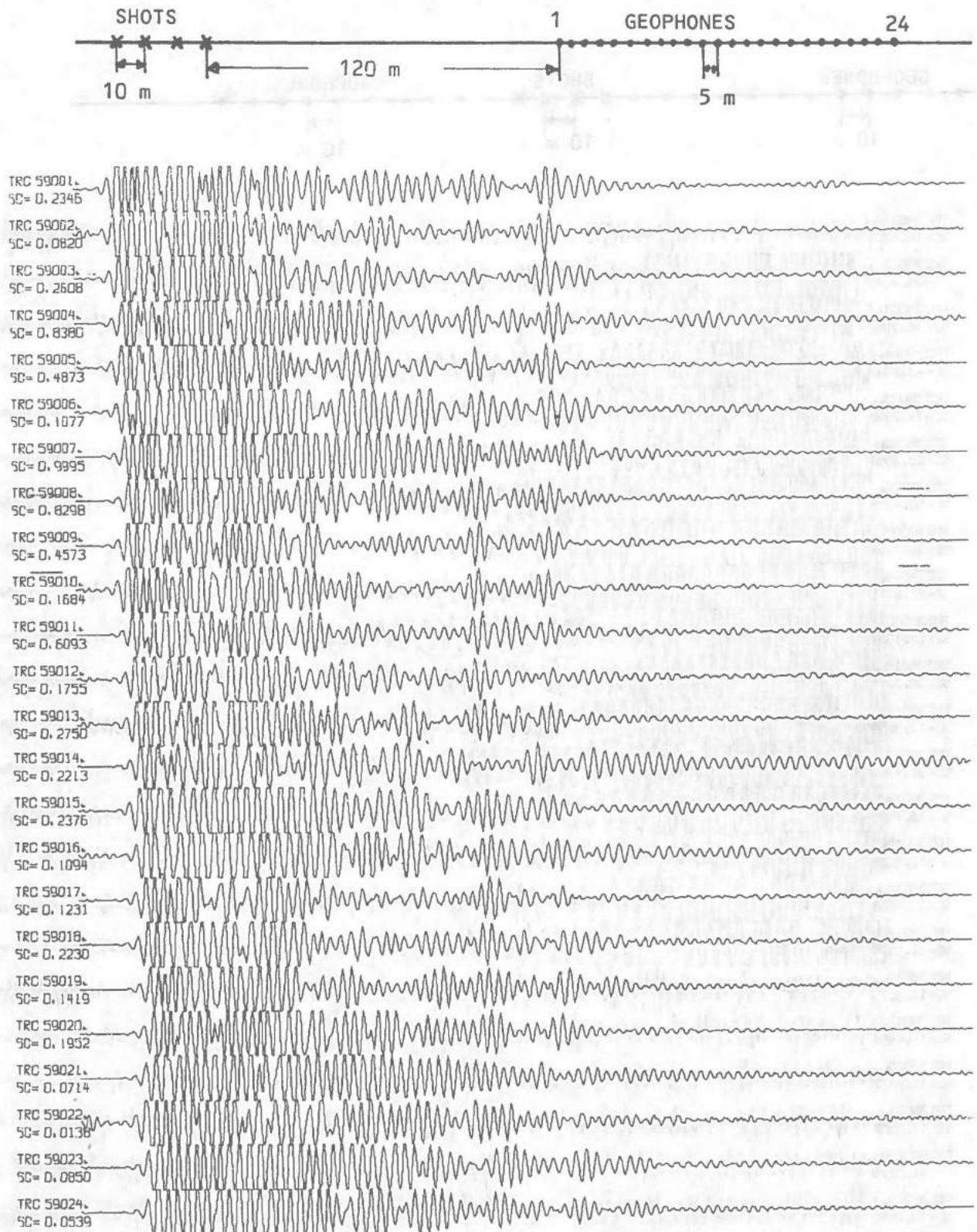


Fig. 7.2 4-shot vertical stack (same geophones) of records from the 1979 profile over the known Løkken ore body. Filter 160-360 Hz. Total trace length is 500 ms.



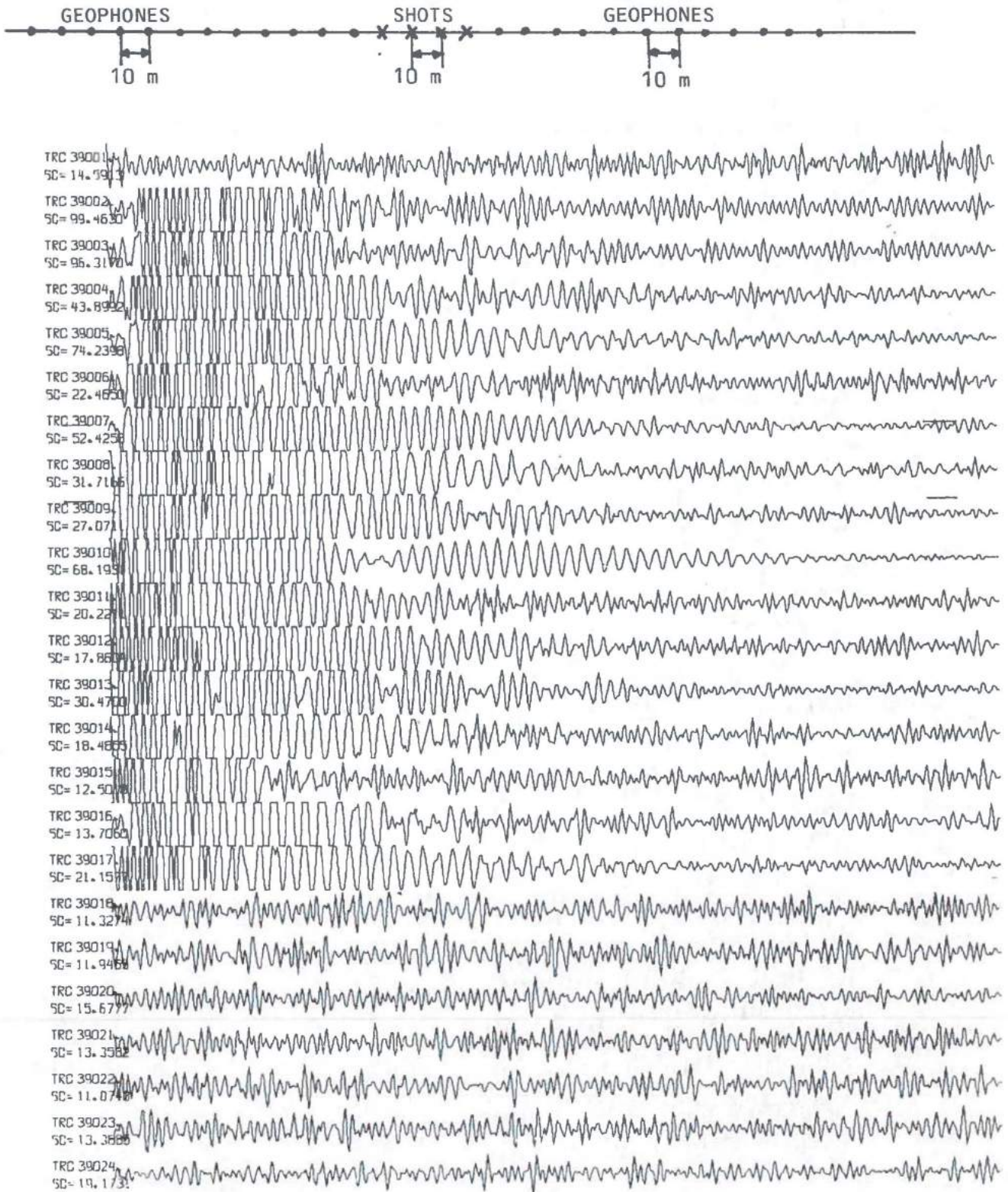


Fig. 7.3 4-shot vertical stack from the 1976 Løkken profile. The shot locations are nearly the same as in Fig. 7.2, however, the receiver configuration is different. Filter 160-360 Hz. Total trace length is 500 ms.

noise conditions, etc. We consider the results of such experiments to be of ultimate need for the design of optimal field techniques. For the first time, we have the possibility of carrying out a real optimization procedure, simply because we have got what we may call the basis of this kind of methods: namely, a well-defined optimization criterion. This criterion is as simple as it is necessary: To maximize the signal-to-noise ratio of the reflected waves. However, for this to be a fruitful criterion, the reflections must necessarily be detectable.

- The development of a new flexible processing package for land seismic data.

In this processing package, we would like to include techniques that significantly differ from the standard methods used in marine processing. Especially, the processing of algorithms should be flexible enough to handle any shot/receiver configuration, and should not necessarily be based on the standard CDP multifold stacking philosophy.

- The development of basically new field routines for long duration seismic profiling.

Today's field work suffers from the lack of possibilities of performing a satisfactory quality control of the data during the field operation. In addition, when covering large prospecting areas, very much time and effort may be saved if the field work could be supported by a continuous feed-back from data processing. This would ensure an excellent data control, and in addition a possibility to change, f.ex., the shot/geophone layout during the field operation (see Fig. 7.4).

- Implementation of 2-dimensional shot/receiver configurations.

In marine seismic prospecting the 2-dimensional methods in most cases work very well, due to the simple fact that marine sediments are often close to a 2-dimensional situation. However ore prospecting in metamorphic rocks presents a real, 3-dimensional world, and consequently, 2-dimensional layouts should be seriously considered. In fact, 3-dimensional methods have been developed today which involve little extra effort related to the field operation, but of course involves new kinds of processing techniques which significantly differ from the common 2-dimensional ones.

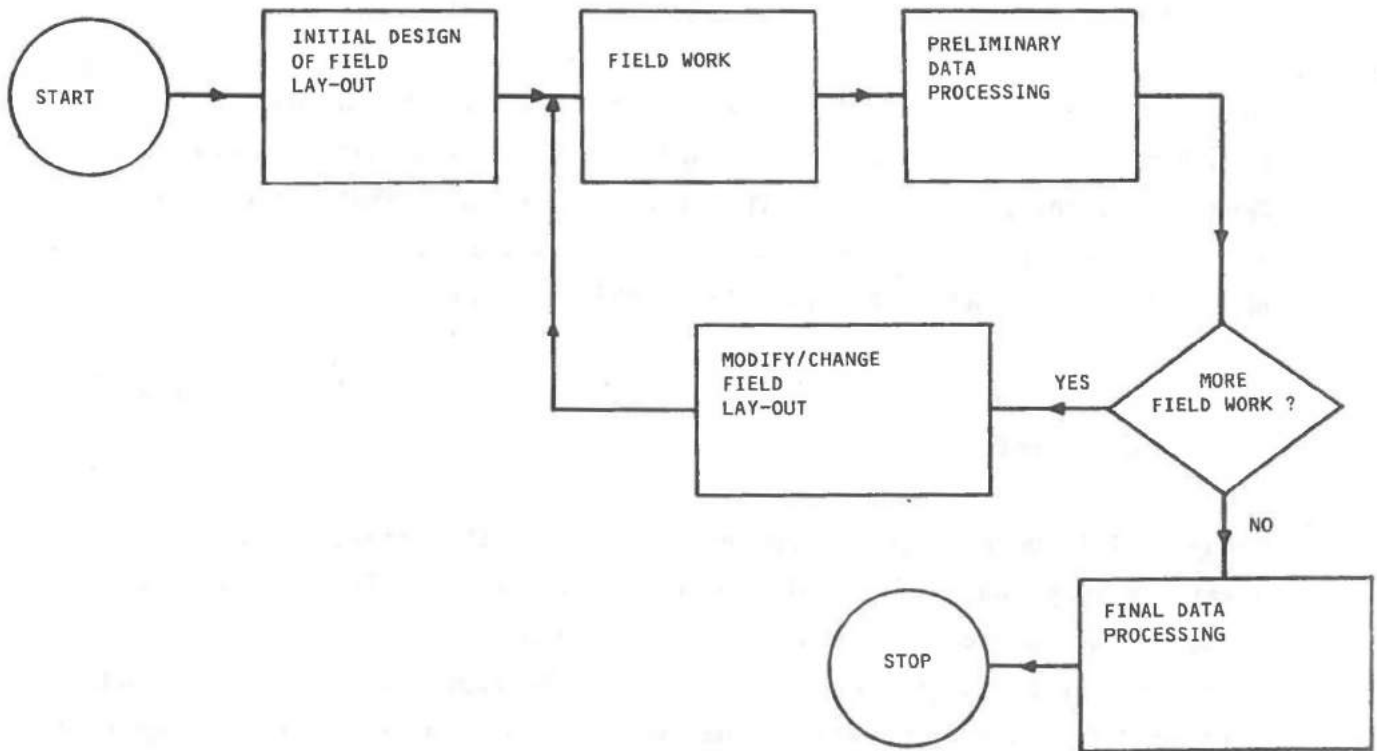


Fig. 7.4 Schematic illustration of an integrated field work/data analysis procedure.

REFERENCES

- Dobrin, M.B., 1976: Introduction to Geophysical Prospecting, McGraw-Hill Inc., New York.
- Geoteam, 1972: Seismiske målinger ved Mons Petter Gruve for A/S Sulitjelma Gruber, Rapport 3358.01, Geoteam, Stabekk, 27 juni 1972.
- Geoteam, 1974: Seismiske undersøkelser ved Sagmo Gruve for A/S Sulitjelma Gruber, Rapport 3358.02, Geoteam, Stabekk, 10. juli 1974.
- Geoteam, 1976: Refleksjonsseismiske målinger på Løkken for Orkla Industrier A/S, Rapport 4034.03, Geoteam, Stabekk, 9. desember 1976.
- Geoteam, 1978: Seismiske undersøkelser i Løkken Grube 1977 for Orkla Industrier A/S, Rapport 4034.04, Geoteam, Stabekk, 4. april 1978.
- Grammeltvedt, G., 1978: Refleksjonsseismiske målinger på Løkken 1976/77, Rapport, Orkla Industrier A/S.
- Hansen, T.S., 1978: Sammendrag av seismiske arbeider i regi av A/S Sulitjelma Gruber, Rapport, A/S Sulitjelma Gruber, 27. sept. 1978.
- Jaeger, J.C., and N.G.W. Cook, 1976: Fundamentals og Rock Mechanics, Chapman and Hall, John Wiley & Sons, New York.
- King, D., and M. Falvey, 1977: A Seismic Survey in the Cooper Basin in Queensland, APEA Journal.
- King, D., 1979: Mini-SOSIE Seismic Profiling for Coal in the Gloucester Basin of N.S.W., Bull. Aust. Soc. Explor. Geophys., Vol. 10, No. 2.
- Noponen, I.T., P.J. Heikkinen and P.J. Järvinmäki, 1978: A Seismic Reflection Survey on Exposed Precambrian Rock, Report S-2, Institute of Seismology University of Helsinki.
- Noponen, I.T., p. Heikkinen and S. Mehrotra, 1979: Applicability of Seismic Reflection Sounding in Regions of Precambrian Geology, Geoexploration, 17, pp 1-9.
- Nunn, K.R., and M. Boztas, 1977: Shallow seismic reflection profiling on land using a controlled source, Geoexploration, 15, pp. 87-97.
- Parasnis, D.S., 1972: Principles of Applied Geophysics, Chapman and Hall, Ltd., London.
- Ward, S.H., R.E. Campbell, J.D. Corbett, G.W. Hoffmann, C.K. Moss and P.M. Wright, 1978: Report: The Frontiers of Mining Geophysics, Geophysics, Vol. 42, pp. 878-886.
- Waters, K.H., 1978: Reflection Seismology. A Tool for Energy Resource Exploration, John Wiley & Sons, New York.
- Widess, M.B., 1973: How thin is a thin bed?, Geophysics, Vol. 38, p. 1176.
- Ziolkowski, A., and W.E. Lerwill, 1979: A Simple Approach to High Resolution Seismic Profiling for Coal, Geophysical Prospecting, Vol. 27, pp. 360-393.

